CHARACTERIZATION OF POST-TRANSLATIONALLY MODIFIED PEPTIDES AND PROTEINS USING LANTHANIDE-BASED LABELING STRATEGIES

By

Randi Lee Gant-Branum

Dissertation

Submitted to the Faculty of the

Graduate School of Vanderbilt University

in partial fulfillment of the requirements for the degree of

DOCTOR OF PHILOSOPHY

in

Chemistry

August 2011

Nashville, Tennessee

Approved:

Professor John A. McLean

Professor Donna J. Webb

Professor Eva M. Harth

Professor David E. Cliffel

Dedicated to my family,

Josh and Gradie Branum, who are my source of complete peace and joy

and to my parents,

Randall and Carrie Gant, who have been my lifelong source of inspiration and encouragement.

ACKNOWLEDGEMENTS

I would first like to profoundly thank my advisor, Dr. John McLean, for all of his guidance, support, and mentorship throughout this graduate journey. Graduate school has been an experience of both personal and professional growth, and he played a critical role in shaping both aspects of the person I am today. Working in his lab, I have built lasting friendships with Larissa Fenn, Michal Kliman, Josh Kerr, Jeff Enders, Cody Goodwin, Jody May, Sevu Sundarapandian, Kelly Hines, Jay Forsythe, and Seth Byers. I hope for the chance to continue our very engaging conversations in our professional lives and I wish them all the best in what life after Vanderbilt brings.

My research has also been guided by three other fantastic professors - Dr. David Cliffel, Dr. Eva Harth, and Dr. Donna Webb. Their support and insightful questions and suggestions have improved my critical thinking and strengthened my research. The Mass Spectrometry Research Core helped me process numerous samples, and Drs. Amy Ham, Hayes McDonald, and David Friedman provided me with invaluable guidance on how to interpret and validate tandem spectra.

Generous grants from Vanderbilt University, the Vanderbilt Institute for Chemical Biology, and the American Society for Mass spectrometry funded my research projects.

In the times after coursework and research were finished for the day, I greatly enjoyed the company of Heather McMillen, Rachel Snider, Jennifer McKenzie, Leslie Hiatt, Jessica Sammons, Danielle Kimmel, and Laura Engerer. We formed a tight-knit group on the first day of student orientation, and their friendship made my days at Vanderbilt all the better.

I wouldn't have realized my love of Chemistry without the inspiration and enthusiasm of the wonderful professors at the University of Tennessee at Chattanooga. Drs. Gail Meyer, Thomas Waddell, Douglas Kutz, Thomas Rybolt, Gregory Grant, Gretchen Potts, Stephen Symes, and John Lynch made the subject simple and elegant. Each professor brought their own unique flavor and excitement to the subject, and I continue to carry their lessons with me. My undergraduate mentor, Dr. Manuel Santiago, inspired me to try harder and reach higher to master the subject. His continued friendship and helpful advice long after my UTC graduation have been a great source of support.

But at the end of the day, no one is more responsible for the completion of this degree than my family. My parents' love and encouragement gave me the self-esteem to believe that anything was possible. My husband, Joshua Branum, supported me through every tough day and celebrated every victory with me. He is my rock of strength and I am proud to be married to him. Finally, I'd like to thank the most important person in my life - my daughter, Gradie Lynne Branum. Gradie, I have never loved anyone more. You fill me with more joy and happiness than I ever knew I could feel, and you, most of all, are my reason for reaching for the stars.

TABLE OF CONTENTS

Page

LIST OF TABLES

LIST OF FIGURES

Figure Page

CHAPTER 1

INTRODUCTION

1.1 Post-translational modifications in biological systems

Post-translational modifications (PTMs) on proteins are known to play a substantial role in the complexity and diversity of biological systems. This chapter discusses two key PTMs- protein phosphorylation and glycosylation – including their biological roles, associated diseases, significance in relation to each other, and how they are currently characterized. A number of challenges exist in characterizing each type of PTM, such as lability of the modification during MS fragmentation, substoichiometry, and difficulty in separation of the modified protein or peptide from complex mixtures. New methodologies that circumvent many of these challenges using lanthanide-based labeling and two mass spectrometry (MS) platforms - MALDI-TOFMS and ion mobility-mass spectrometry (IM-MS) - are proposed. An outline of objectives and research goals is highlighted.

1.1.1 The relevance of protein phosphorylation and glycosylation

The majority of cellular processes, particularly cell to cell interaction, cell differentiation, proliferation, mobility, division, and apoptosis, are governed by protein expression and post-translational modifications (PTMs) on proteins, which commonly take the form of phosphorylation, glycosylation, acetylation, methylation, etc. O-linked protein phosphorylation and glycosylation are

considered two of the most common PTMs and often compete for the same positions during a number of cellular functions. It has been shown that regulation of phosphorylation vs. glycosylation stoichiometries govern many cellular processes, outlined below. For this reason, phosphoproteomics and glycomics have moved to evaluate the direct role of these PTMs in regulating proteins responsible for the progression of Alzheimer's disease,[1-4] cancer proliferation,[5, 6] inflammatory diseases,[7, 8] and the onset of developmental neurological diseases.[9]

1.1.1.2 Protein phosphorylation

Phosphorylation of serine (Ser), threonine (Thr), and tyrosine (Tyr) residues (O-phosphorylation) occur with the assistance of kinases, which account for approximately 2% of the human genome.[10] It has been estimated that 50% of all proteins in a typical eukaryotic cell are phosphorylated.[11, 12] Protein phosphorylation is reported to play a critical role in the regulation of cell proliferation,[11] differentiation,[13] migration,[14-18] signalling,[11] survival,[11, 19] and apoptosis[20] Moreover, varying the stoichiometry of protein phosphorylation has been shown to regulate signaling cascades and rates of turnover of cell migration proteins, which are known to play a significant role in neurological disorders, pro-inflammatory disorders (*e.g.,* psoriasis and rheumatoid arthritis) and cellular behaviors associated with cancer cell proliferation.[10, 21, 22]

Protein phosphorylation is challenging to characterize due to the dynamic nature of the modification. There exist significant differences in the occurrence of pSer, pThr, and pTyr residues, in that these residues are typically observed in a ratio of 1800:200:1, respectively.[23] Adding to the complexity, the degree of phosphorylation changes according to the temporal cellular response. Moreover,

phosphorylated serine and threonine residues are labile in basic conditions encountered in common buffers and also during tandem MS fragmentation. Phosphates have been reported to rearrange in collision cells of MS instruments, resulting in increased noise, false positives, and reduction of signal corresponding to the original site of modification.[24, 25] These factors often result in substoichiometric levels of phosphorylated proteins available for analysis, which compound the challenges in phosphoproteomic characterization.

1.1.1.3 Protein glycosylation

Protein glycosylation is a common and complex form of post-translational modification which regulates the structure, stability, and function of proteins within the cell. Glycosylation is ubiquitous among all eukaryotes, and it is estimated that glycosylation occurs on 50% of all eukaryotic proteins.[26] It is reported to play a key role in functions on the cell membrane such as hormone uptake,[27] recognition of toxins or pathogens,[28, 29] and signaling to other cells.[30] It also plays a further role in cellular processes such as organization[31] and division.[6] Furthermore, glycosylation is required for the biological function of certain proteins, such as the Fc-effector function of immunoglobulin G (IgG).[7, 32-35] Moreover, glycosylation has been linked to reproduction,[36] embryonic stem cell development,[37] and the development of Alzheimer's disease,[3] arthritis,[8] and diabetes.[38] O-linked glycosylation exists on serine, threonine, and tyrosine residues, and occurs most frequently on serine. Proteins bearing O-linked N-Acetyl Glucoseamine (O-GlcNAc) have been implicated in AIDS-related lymphomas and viral and parasitic proteins.[31]

Characterization of protein glycosylation is challenging for a number of reasons, including substoichiometry and difficulty in determining the glycan structure. For example, O-GlcNAc (O-linked N-acetylglucosamine) is highly dynamic and deglycosylation is a rapid step for regulatory functions, resulting in substoichiometric amounts. Glycan branching is often complex and positional isomers are difficult to separate using traditional online separation methods for MS. Building blocks for the glycan comprise a large number of carbohydrates, and the functionality of the glycan is dependent upon its branching structure and terminal saccharides. Furthermore, glycosylation may be interchangeable with phosphorylation in some regulatory systems. Moreover, glycans are difficult to separate from complex biological mixtures, and often require a number of laborious chromatography steps to generate a pure mixture for analysis.

1.2 Current characterization strategies for PTMs

1.2.1 Characterization of phosphorylated proteins

Characterization of a phosphoprotein involves determination of the site of phosphorylation and determination of stoichiometry between different states. Traditionally, these two analyses are performed in separate experiments, as *a priori* knowledge of the sites of phosphorylation greatly facilitate targeted quantitative approaches. Moreover, site identification typically requires enrichment, as sequence coverage detected may be suppressed by more abundant concomitant species.

Classical phosphoproteomic enrichment includes separation and purification by 2-D gels, immunoprecipitation, immobilized metal affinity columns (IMAC), reversed-phase liquid chromatography (RPLC), or the use of selective enrichment via phospho-specific antibodies and 2-D gel separation. Each method offers advantages and disadvantages. A brief overview of separation methodologies and quantitative methodologies discussed below is provided in Table 1.

Classical phosphoproteomic quantitative and site elucidation methodologies include the use of ^{32}P radiolabels.[39] In this method, protein mixtures are typically separated by 2-D gel electrophoresis and subsequently imaged. Varying samples may quantitated by the relative amounts of radiation emitted, and site elucidation is performed by Edman degradation. This method is still in common use because of demonstrated dynamic range, but is restricted by three important limitations. First, this method requires the use of 2-D gels, which limit applicability to soluble and relatively abundant proteins. In many cases, protein phosphorylation occurs rapidly and is frequently observed in low abundance. Second, phosphoaminoacid analysis suffers from poor site specificity, and a significant amount of *a priori* knowledge is required about the sequence and potential sites of phosphorylation. Third, this method is labor-intensive, time consuming, and requires the use of radioactive labeling. Typical labeling experiments take between 3-7 days and

Table 1. Purification and Quantitation Methods for Phosphoproteomics

Method	Principle	Pros	Cons
Purification method			
2-D gel electrophoresis (2DIGE)[11, 40]	Separation of proteins by isoelectric point and size.	Can be done *in vivo* or *in vitro*, large dynamic range.	Limited to soluble proteins, spot overlap requires additional purification
Antibody enrichment	Generalized enrichment of phosphoproteins by binding to phosphorylation-specific antibodies.	Selective for phosphorylated tyrosine antibodies.	Not selective for phosphoserine and phosphotyrosine.
Immobilized metal-affinity chromatography (IMAC)[41, 42]	Enrichment of phosphoproteins and phospho-peptides *via* affinity toward positively charged metal ions (Fe^{3+}, Al^{3+}, Ga^{3+}, or Co^{2+}) chelated to a solid support.	Generalized phosphorylation enrichment without need for antibodies or radioactive materials.	Non-specific interactions require additional cleanup for phospho-proteomic characterization
Reversed-phase liquid chromatography (RPLC)[43]	Separation of phosphoproteins and phospho-peptides non-selectively by elution based on polarity and interaction with C-4 or C-18 column.	Standardized protocol, readily reproducible and commonly reported. High abundance phosphorylation sites are readily identified.	Does not enrich for phosphorylated peptides and proteins, all peaks from chromatogram must be fragmented for identification.
Immunoprecipitation [11, 44, 45]	Enrich specific phosphorylated proteins of interest *via* selective antibodies for the target protein (does not necessarily target phosphorylation domain).	Selective for targeted phosphorylated peptide or protein.	Significant *a priori* knowledge of the phosphorylation site required, not for phosphopeptide discovery. Custom antibody generation is costly.

Table 1 (cont'd). Purification and Quantitation Methods for Phosphoproteomics.

Quantitation method			
^{32}P radiolabels[39]	Labeling of phosphoproteins or phosphopeptides *in vivo* or *in vitro* with ^{32}P or ^{33}P. Detection using Edman degradation and autoradiography.	May be done in vivo, established method in the biological sciences.	Radioactive phosphorus requires special handling and special disposal.
Enzymatic stable isotope labeling[9, 46-48]	Stable isotope introduction to phosphoproteins or phosphopeptides *in vitro* via enzymatic digestion in $H_2{}^{18}O$.	Each peptide may be labeled via $^{18}O/^{16}O$ incorporation by trypsin. Trypsin reaction is highly versatile and may be performed in a number of conditions and varying pH. Method is relatively cheap.	Variable incorporation of 1 or 2 ^{18}O due to pH dependence. Missed cleavages must be accounted for and may confound quantitation.
Metabolic stable isotope labeling[9, 49]	Stable isotope introduction to phosphoproteins or phospho-peptides *via* incorporation of isotopically "heavy" or "light" amino acids containing ^{14}N or ^{15}N, ^{12}C or ^{13}C, etc.	Reduces error due to sample handling, nearly all peptides may be labeled.	Requires in-vivo labeling and subsequent purification prior to analysis. May not be done on in-vitro samples that are isolated from separate, non-quantitative experiments, labeling time dependent on cell culture time, limitation of available amino acids
Chemical modification stable isotope labeling[50-58]	Stable isotope introduction to phosphoproteins or phospho-peptides *via* chemical modification of isotopically "light" and "heavy" labels.	Selective for intended functionalities, available with additional built-in advantages such as reporter ion tags, biotin affinity, or ICP ionization.	Limited mass shifts (2-8 Da) limit analysis to small (<2500 Da) peptides or use of high resolution (FT-ICR-MS) instrumentation.

require extensive prior purification using affinity purification and treatment before analysis.

Many of these challenges can be addressed using mass spectrometry (MS) techniques. To circumvent the time intensive requirements of affinity chromatography methods, data-dependent scanning (tandem MS/MS experiments, typically on triple quadrupole instruments) followed by bioinformatic analysis is often used for PTM site localization. Although these methods are sufficiently sensitive to the substoichiometric amounts of phosphorylated sequences, they make inefficient use of chromatography time and require tandem spectra acquisition for each peak in the chromatogram regardless of whether the peak corresponds to the modifications of interest. Moreover, a substantial amount of manual validation is required, as phosphorylation site rearrangement has been noted.[24]

Quantitation is routinely performed using mass spectrometry. Current methods for MS-based quantitation include stable isotope and metal labeling techniques that take advantage of nearly identical labeled structures, differing only by the incorporation of a limited number of heavy isotopes. Contemporary stable isotope labeling was first introduced by three independent labs in the late 1990's and is now implemented enzymatically (*e.g.* O^{18} labeling),[46-48] metabolically (*e.g.* SILAC),[49, 56] or by chemical modification.[53, 59-61] Typically, these labeling strategies provide relative quantitation through incorporation of different stable isotopes for comparing relative protein expression profiles. Relative quantitation information can be expected, because the labeled peptides are isotopologues and hence their ionization efficiencies are assumed to be

identical. Protein expression is then elucidated by comparing the relative peak areas of each differentially labeled peptide (Figure 1).

The most prevalent method for enzymatic introduction of stable isotope labels is proteolytic ^{18}O-labeling first reported by Desiderio *et al.*[46] in 1983 and later improved by Mirgorodskaya et al. in 2000.[47] In this experiment, proteolytic enzymes are reacted with the protein of interest in $H_2{}^{18}O$, resulting in incorporation of an ^{18}O atom at the carboxyl terminus of each enzymatically cleaved peptide. This method suffers from variable incorporation of the isotope (one or two atoms can be incorporated, depending on pH and time scale of digestion), resulting in reduced signal intensity and moderate convolution of peak intensity comparisons.[9]

The most prevalent method for metabolic introduction of stable isotope labels is the stable isotope labeling by amino acids in cell culture (SILAC) method reported by Ong et al.[49] In this method, differentially expressed cells are grown in separate medium containing either native arginine and lysine or isotope labeled $^{13}C_6$-arginine and $^{13}C_6$-lysine that is taken into the cell and incorporated into the proteome. This ensures that all tryptic peptides carry at least one labeled residue corresponding to its unlabeled counterpart. An advantage of this method is that differentially labeled peptides may be combined at the culture level, eliminating errors typical of late-stage combination quantification techniques. It suffers, however, from high cost, insufficient selectivity, and relatively high time requirements for total isotope incorporation and preparation. Additionally, in

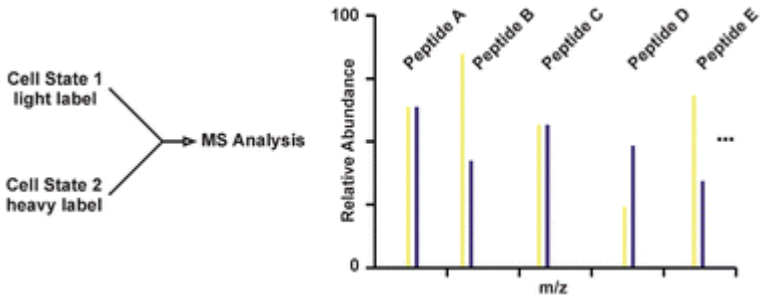

Figure 1. In a typical relative quantitation experiment, differentially expressed samples are encoded with isotopically “light” or “heavy” labels enzymatically, metabolically, or by chemical modification that generates mass shifts of 2-8 Da. Relative peak areas provide relative quantitation information. Adapted from reference.[9]

order for the method to be useful in phosphoproteomic determination, additional purification steps are also required to improve detection.

Chemical modification of phosphorylation sites has been achieved using several different methods. Aebersold and colleagues reported a tagging method in which a cysteamine linker is covalently bound to the phosphate group via an N,N'-dimethylaminopropyl ethyl carbodiimide (EDC) coupling reaction.[62] Smith and colleagues reported a method for relative quantitation of phosphorylated peptides and proteins (*i.e.* Phosphoprotein Isotope-Coded Affinity Tags, or PhIAT)[52] analogous to a protein quantitation method previously described by Gygi and colleagues termed isotope-coded affinity tags, or ICAT, which labels at cysteine residues. In the PhIAT method, phosphorylation at serine and threonine is converted to a cysteine-like moiety containing a free thiol via beta-elimination to yield dehydrobetaalanine or dehydroaminobutyric acid, respectively. Subsequent thiol Michael addition of an isotopically labeled dithiol linker provides the isotopologues and chemical reactivity for a covalent attachment to biotin. The labeled phosphorylated peptides are then digested, purified by affinity chromatography, and analyzed by LC-MS/MS. Relative quantitation information is gained by comparing relative peak areas for the isotopically "light" and "heavy" labeled peptides.[52, 57]

PhIAT provides versatile, selective relative quantitation information for phosphorylated peptides. However, all of these strategies limit the peptide mass that can be quantitated by a limited range of isotopic mass differences. For example, peptide mass is limited by the 2-8 Dalton mass shift afforded by the isotopically enriched linker portion of the label. At higher masses, (greater than

ca. 2500 Da), the natural isotopic envelopes of the isotopologues begin to overlap resulting in poorer relative quantitation accuracy.[9]

1.2.2 Characterization of glycosylated proteins

Characterization of a glycoprotein is occasionally required to fully explore the biological significance of protein phosphorylation. In this context, the sequence position and stoichiometry of the modification are desirable to probe any dynamic phosphorylation/glycosylation switching. Further glycomic characterization includes determination of the glycan structure. Glycan site determination is frequently accomplished using a combination of proteases, glycosidases, affinity chromatography, and LC-tandem mass spectrometry (Figure 2).[63, 64] Identifying the site of modification is challenging due to the temporal nature of glycosylation and the lability of the modification in basic pH and tandem MS. This characterization of the glycan is also complicated by noise from branch fragmentation, labile terminal saccharides, and fragments that are isobaric with concomitant species.[63, 64] These challenges in characterization compound when a protein has multiple glycosylation sites. Thus, classic glycomic methodologies require extensive separation and purification strategies to simplify analysis. Identification of the site of modification is accomplished with the use of endoproteases to cleave the protein into peptides and isolate each modification site onto individual peptides. High-performance liquid chromatography is then required to separate each peptide and tandem MS analysis is performed to determine the site of modification.

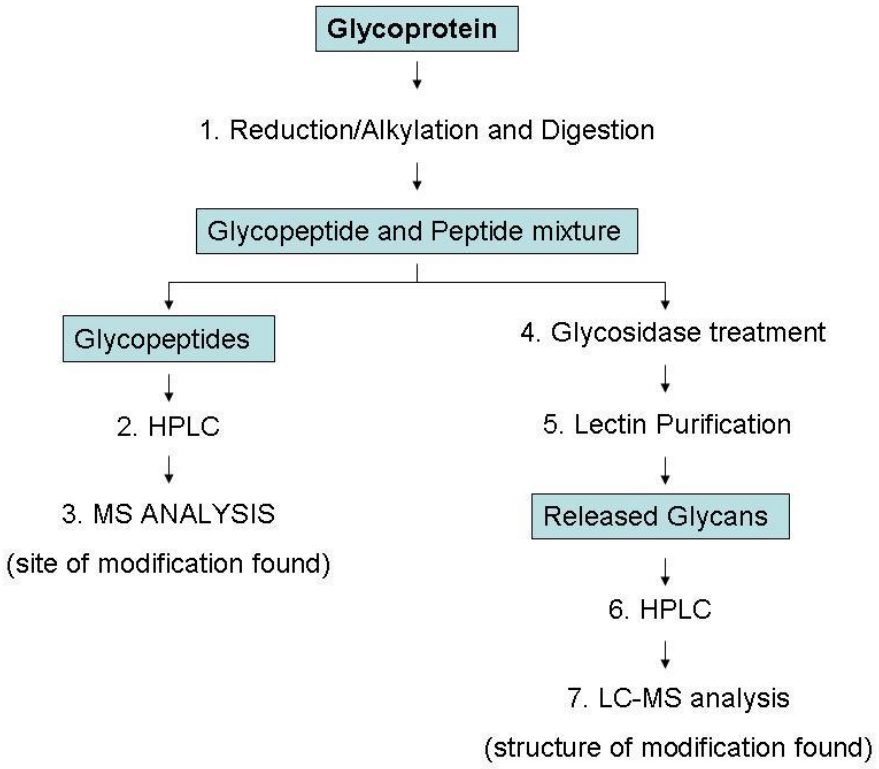

Figure 2. Traditional protocol for full glycoprotein characterization by MS. Stoichiometric information is typically not obtained.

Structural characterization of the attached glycan is then accomplished through the use of glycosidases, which cleave the attached glycan from the protein. Lectin chromatography is used to separate glycans from peptides, and high-performance liquid chromatography is used prior to tandem MS analysis. Although these separation methods can resolve glycans and facilitate characterization, similar polarities and size of the carbohydrate limits complete separation. Furthermore, offline chromatographic and affinity separations are known to be laborious and time consuming, requiring hours to days to complete.

1.3 Mobility shift labeling using ion mobility-mass spectrometry

Typical time intensive separation strategies for PTM analysis are circumvented using mobility shift labels and ion mobility-mass spectrometry. Ion mobility spectrometry is a well-developed gas-phase separation technique whereby ions are rapidly (μs to ms) separated based on their apparent surface area or collision cross section (CCS). Ions undergo elastic collisions with an inert buffer gas at pressures of 0.5-10 Torr as they move through the drift cell under the influence of either a traveling wave or a weak electrostatic field (Figure 3a). In traveling wave ion mobility, ions traverse the mobility cell under the influences of a transient DC voltage and an alternating RF voltage that acts as a potential barrier. Ions with larger apparent surface area will have slower drift times due to more ion-neutral collisions than ions with smaller surface areas. An illustration of this concept is provided in Figure 3b.

When coupled with mass spectrometry (Figure 3c), IM-MS can differentiate ions of interest from analyte ions having the same mass but different

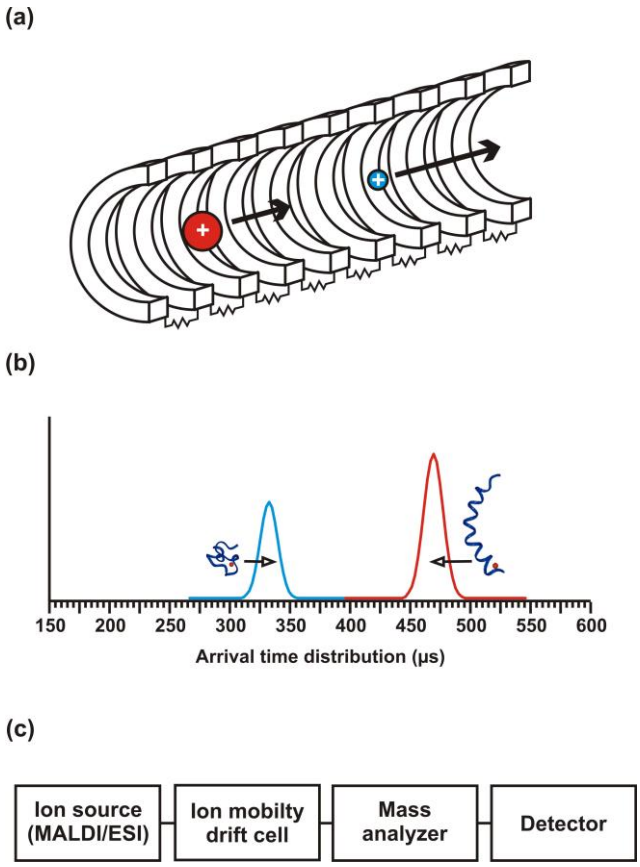

Figure 3. a) Ion mobility separates on the basis of collisions with a neutral buffer gas under the influence of a weak electrostatic field, resulting in differing arrival time distributions for conformers of a peptide. b) An example of two conformations of example peptide $[Ac\text{-}Y(AEAAKA)_5F\text{-}NH_2+Na]^+$. The folded version (blue, also indicated above in blue), exhibits a faster arrival time than the extended version (red, also indicated above in red) due to a reduction in apparent surface area for collisions in the mobility cell. Structures shown are two representative conformers obtained through molecular dynamics calculations and represent local maxima. c) Ion mobility may be coupled to mass spectrometry using a number of platforms, but the general arrangement is presented in this schematic.

structures (*i.e.,* isobaric species). An instrument schematic of this combination is provided in Figure 4. IM separations are slow relative to mass analysis (ms vs ns), and many mass spectra are acquired over the elution profile of the ions from the drift cell. The resultant IM-MS data is 3-dimensional, typically shown with arrival time distribution (IM drift time) on the y-axis, m/z on the x-axis, and relative abundance on the z-axis. Such 3D data is typically projected in two dimensions with false coloring for relative abundance as illustrated in Figure 5.

For a particular molecular class of given density, ion mobility scales as length squared, while mass scales as length cubed. Because mobility separations are not completely orthogonal to mass detection, molecular classes exhibit correlation lines in IM-MS 2-D conformation space. For example, a sample of approximately 600 singly-charged peptide signals occupied a narrow band of arrival time distribution vs. *m/z* with greater than 99% of the peptides having less than a 7% deviation from the mean.[65] Lipids, carbohydrates, and nucleotides were also reported to reside in their own correlation lines in the 2D conformation space.[66] Differences in the relative gas-phase packing efficiencies of each type of biomolecule (nucleotides> carbohydrates> peptides> lipids) can be exploited to separate each biomolecular class, illustrated in Figure 6. Structural separation of all four types of biomolecules was demonstrated in our group using IM-MS.[66]

This is an advantage to a number of "omics" strategies,[66] including lipidomics,[67] proteomics,[68] phosphoproteomics,[69] and glycomics.[70] IM-MS has also been demonstrated on complex samples such as whole-cell lysates,[71] non-covalent complexes,[72] and thin tissue sections[73] as a more rapid separation and detection method than traditional LC-MS analysis.

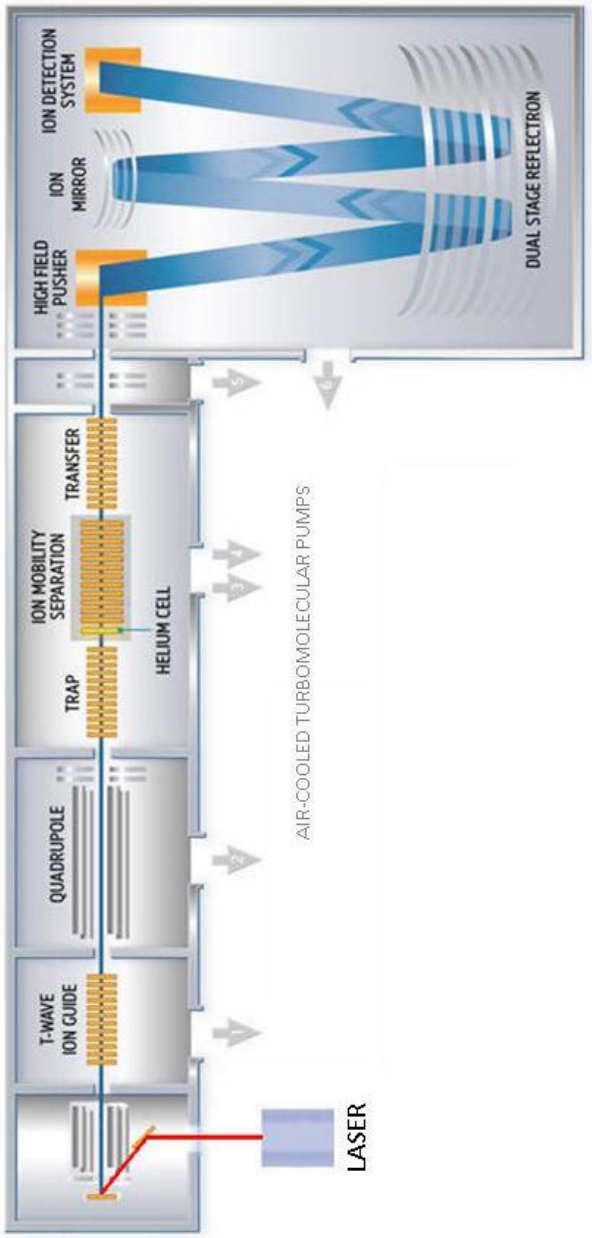

Figure 4. Schematic diagram of the MALDI-TWIM-TOFMS Instrument (Synapt HDMS G2, Waters Corp., Manchester, UK).

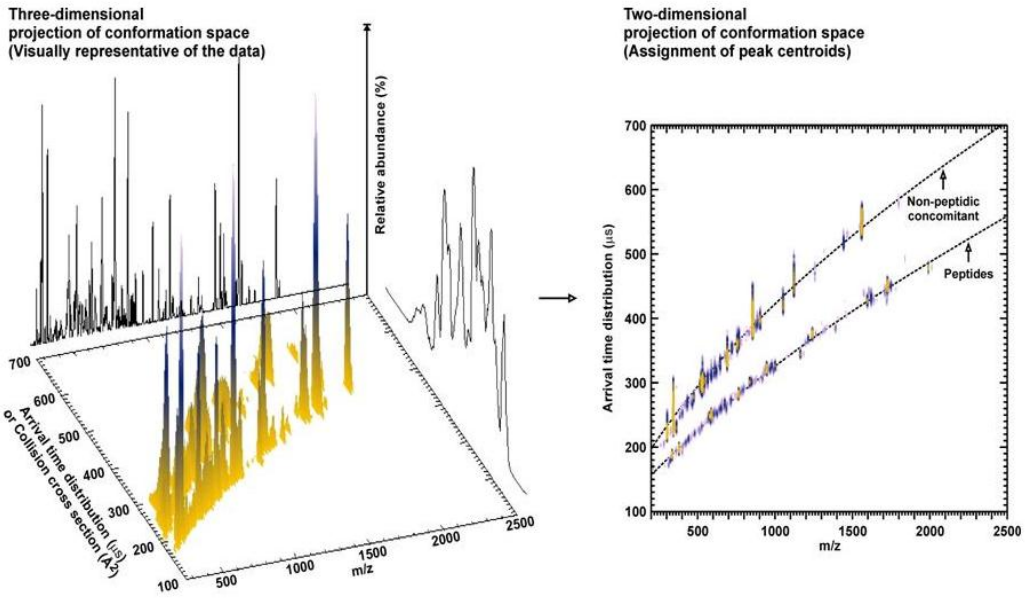

Figure 5. Data projection from three-dimensional (arrival time distribution vs. m/z vs. relative abundance) to two dimensional (arrival time distribution vs. m/z), with false coloring representing relative abundance.

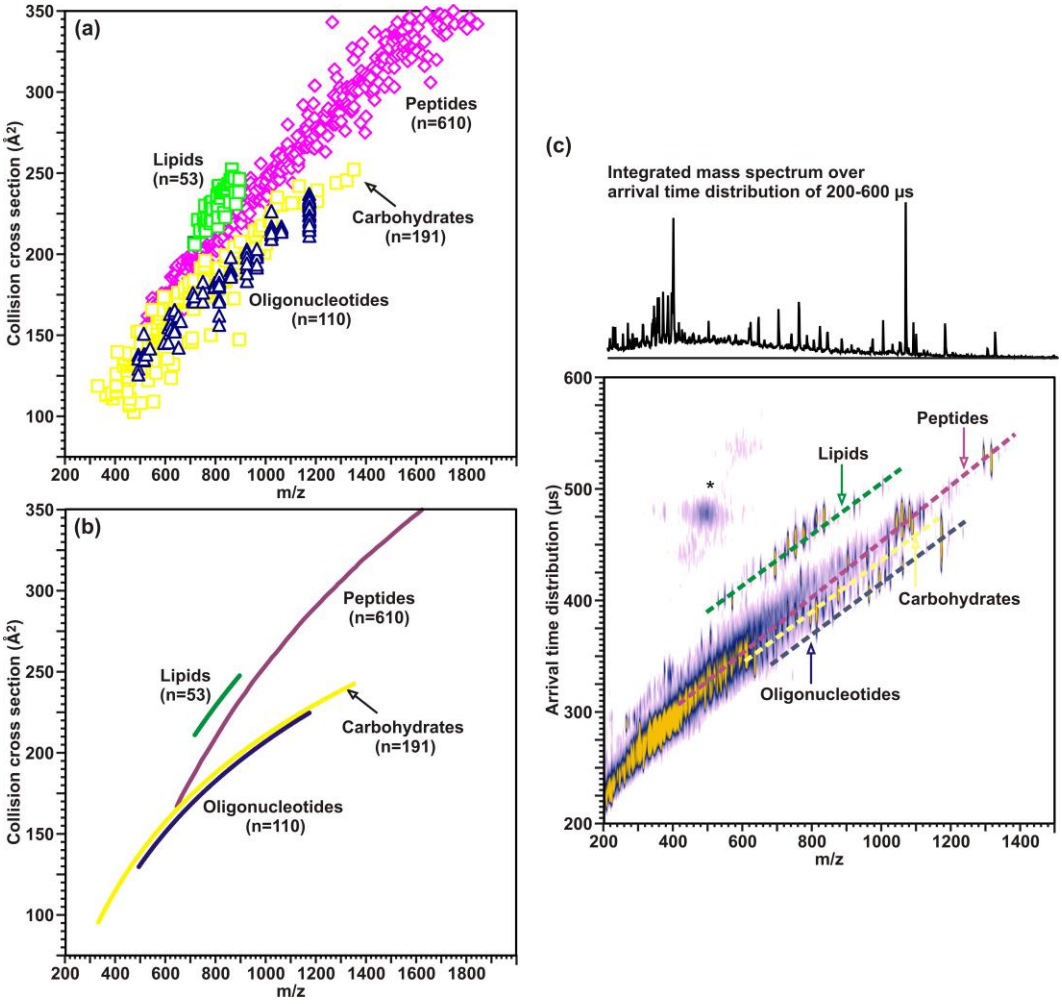

Figure 6. Differences in the relative gas-phase packing efficiencies of each type of biomolecule (nucleotides> carbohydrates> peptides> lipids) are shown. a) Ion surface areas vs. *m/z* from a pool of 53 lipids, 610 peptides, 191 carbohydrates, and 110 oligonucleotides. b) Mean correlation lines ion surface area vs. *m/z* for each biomolecular class. c) Separation of biomolecular class in real time (as acquired from the Synapt HDMS IM-MS instrument). Adapted from reference 66.

It should be noted, however, that minor modifications (*e.g.,* phosphorylation sites) within each biomolecular class were not significantly resolved (0-6% deviation) from unmodified molecules.[69]

1.3.1 Mobility shift strategies

One of the central aims of this project is to resolve post-translationally modified peptides and proteins from their unmodified counterparts in IM-MS using mobility shift strategies for further characterization. Mobility shift strategies have been previously described.[72, 74] In these strategies, labeled functionalities are shifted to an area outside of the IM-MS correlation band where signals are not predicted to occur in the absence of labeling. Due to the curvature of the correlation band, two mobility shift strategies are possible – shift reagents of either low or high density (Figure 7) whereby labeled signals are shifted to an area above or below the peptide correlation band, respectively. Lanthanide-based chelating label are selected as covalent high density IM-MS shift reagents since the lanthanide metal imparts a larger increase in mass to the labeled peptide than apparent surface area.

1.3.1.1 Lanthanide-based labeling strategies

Most commonly, lanthanide-based (Ln-based) labeling strategies utilize a trivalent lanthanide metal (Ln(III)) specific tag (Figure 8) that contains a linker portion and a functionally reactive portion. Because the ionic radii of all Ln(III) are nearly invariant, the chelating moiety is insensitive to which lanthanide is incorporated. Thus, any lanthanide metal may be

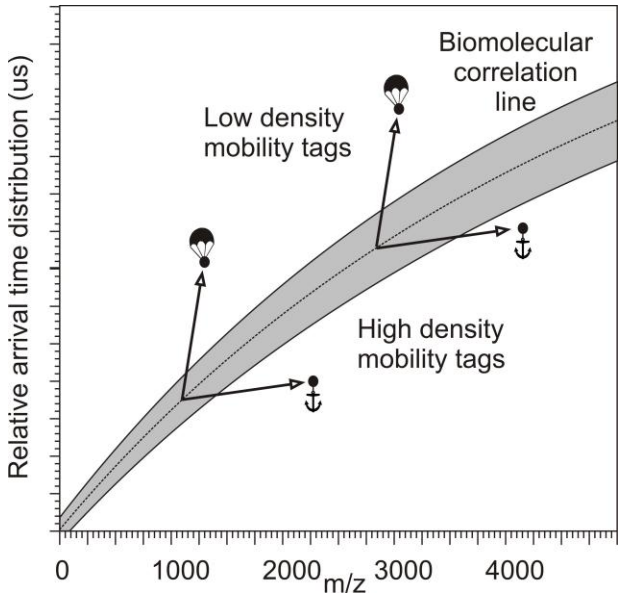

Figure 7. Conceptually, an ion mobility shift reagent either increases surface area with a small increase in mass, or increases mass with a small increase in surface area, respectively. These two possibilities are indicated by filled-circles (●) coupled to parachutes and anchors. Note that owing to the curvature of the peptide correlation, increasing surface area provides greater deviations from the fit at higher mass, while increasing mass (or density) provides greater deviations from the fit at lower mass.

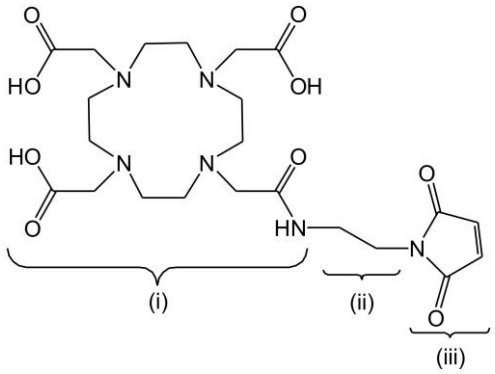

Figure 8. An illustration of the structure of lanthanide-based relative quantitation reagents. The tag consists of a (i) metal chelation region, (ii) a linker region, and a (iii) region chemically selective for cysteine.

selected to encode a particular quantitative sample for up to 15 multiplexed analyses. The subsequent mass shift between differentially labeled samples can then be tuned by selection of the Ln(III), (*e.g*. La/Lu result in a mass difference of 36 Da), which are sufficiently large to circumvent limitations for quantitation of larger peptides using isotopologue quantitation strategies. Ionization efficiency of different lanthanide metals can be expected to be nearly identical. Another advantage to using DOTA-Ln complexes is that it may be bound to a natural antibody (*i.e.*, antibody 2d12.5) with no known analogues for selective purification of Ln-labeled peptides.[75]

Two common strategies using lanthanide-based labeling are termed element-coded affinity tagging (ECAT)[58] and metal-coded affinity tagging (MeCAT).[50] Note that in principle both strategies are specific to labeling at the sulfhydryl group of cysteine. Labeling for primary amines has been reported,[55] however Ln-labeling strategies have been reported for PTMs have not been reported to date.

Here, the potential for lanthanide-based labeling strategies as mobility shift reagents for ion mobility-mass spectrometry is explored. It is hypothesized that addition of Ln-chelated labels will shift labeled peptides out of IM-MS regions where signals are predicted to occur and that this approach will provide a rapid means for identifying a separated modified peptide for subsequent analysis. This approach will reduce extensive online separations prior to analysis and will circumvent processing of hundreds of thousands of spectra as is typical in LC-MS analysis. Furthermore, incorporation of different metals provides both a shift in IM and the potential for relative quantitation information. This is significant, because in contrast with MS-only measurements, shifting signals away from

endogenous chemical noise improves the accuracy in peak area analysis for relative quantitation of protein expression profiles.

In this work, I explore the potential for lanthanide-based labeling as an an alternative to isotopologue-based quantitation labels and as IM-MS mobility shift reagents for protein phosphorylation and glycosylation. Phosphorylated and glycosylated peptides and proteins may be modified by beta-elimination/Michael addition (BEMA) chemistry that converts the labile phosphorylation site to a functionality that is readily labeled.[76-81] In the proposed strategy, phosphorylated and glycosylated peptides are converted into free thiols using BEMA chemistry and subsequently lanthanide-encoded via maleimide chemistry (Figure 9). Samples are then identified and quantitated. The potential use of this method to quantitate between glycosylation and phosphorylation is discussed in Chapter 6.

1.4 Summary and Objectives

For my dissertation research, I aimed to simplify phosphoproteomic characterization by achieving simultaneous site identification and quantitation using lanthanide-based tagging. Characterization of this modification is often accomplished in separate experiments and involves determination of the site of modification, the stoichiometry, and in some cases, the elucidation of glycan stoichiometry when it temporally replaces phosphorylation. I explored the potential for lanthanide-based labeling to overcome challenges associated with quantitative labeling, and the potential for these labels to serve as mobility shift labels to facilitate the characterization for post-translationally modified peptides in ion mobility-mass spectrometry biomolecular conformation space. It was

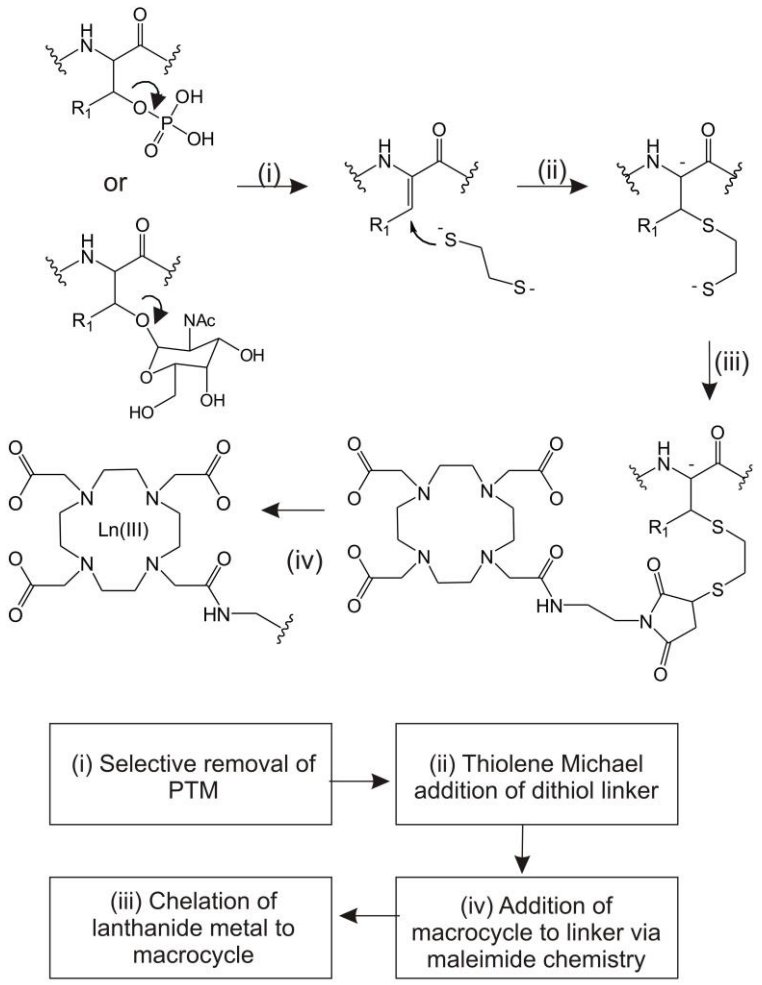

Figure 9. Beta-elimination/Michael addition strategy for labeling phosphorylated and glycosylated peptides and proteins. i) The site of modification is beta-eliminated in basic conditions, resulting in dehydroalanine or dehydroamino-butyric acid for modified serine and threonine residues, respectively. ii) A dithiol linker is added by Michael addition chemistry. iii) A bifunctional ligand containing a lanthanide-chelating moiety and a thiol-selective moiety is added via maleimide chemistry. iv) Finally, the samples are encoded with lanthanide metals via chelation to the Ln-chelation region.

hypothesized that, when used as mobility shift reagents, lanthanide-based labels would provide enhanced separation of selected PTMs from the peptide correlation line in IM-MS, facilitating additional analysis such as quantitation and site identification. Furthermore, I also evaluated the utility of these labels in profiling glycan stoichiometry. The objectives, which are addressed in the following chapters, are outlined below:

1. What are the advantages and challenges in performing traditional data-dependent analysis for phosphorylation characterization when analyzing a previously uncharacterized, non-model phosphorylated protein? What areas of these routine analyses can be improved? Evaluation of this question is addressed in the work detailing phosphorylation site analysis on the cell migration signaling protein APPL1 in Chapter 2: Identification of phosphorylation sites within the signaling adaptor APPL1 by mass spectrometry.

2. Can lanthanide-based labeling strategies be used to circumvent challenges associated with the quantitation and site identification of phosphorylated peptides and proteins? These questions are explored in Chapter 3: Simultaneous relative quantitation and site identification of phosphorylated peptides and proteins using lanthanide-based labeling for MALDI-TOFMS analysis.

3. Can lanthanide-based labels effectively be used as mobility shift labels to separate phosphorylated peptides and proteins from their unphosphorylated counterparts in IM-MS conformation space? What advantages does this separation method provide over traditional phosphoproteomic characterization by

data-dependent MS analysis? This is discussed in Chapter 4: Rapid separation, identification, and quantitation of phosphorylated peptides and proteins using lanthanide-based labels as ion mobility-mass spectrometry mobility shift labels.

4. Can lanthanide-based mobility shift labeling be applied to probe the stoichiometry of phosphorylation vs. glycosylation? This is addressed in Chapter 5: Enhanced separation and characterization of glycosylated peptides using lanthanide-based labeling and ion mobility-mass spectrometry.

Completion of these experiments revealed that lanthanide-based labels have great utility in circumventing challenges associated with phoshoproteomic and glycomic characterization by reducing separation steps and reducing analysis time while provided the added advantages of more versatile quantitation. Overall, the strategies described in the following chapters present simplify phosphoproteomic and glycoproteomic analysis by providing simultaneous modification site identification and stoichiometric information while facilitating rapid separation when used as a mobility shift label in IM-MS conformation space.

CHAPTER 2

IDENTIFICATION OF PHOSPHORYLATION SITES WITHIN THE SIGNALLING ADAPTOR APPL1 BY MASS SPECTROMETRY

2.1 Introduction

In this chapter, phosphopeptide site identification, one segment of full phosphoproteomic characterization, is performed using established data-dependent tandem MS methods to evaluate the robustness and to identify the challenges associated with phosphoproteomics using data-dependent methodologies and the subsequent bioinformatics processing. Site identification is accomplished for the uncharacterized protein Adaptor protein containing a PH domain, PTB domain and Leucine zipper motif (APPL1), speculated to play a role in the signaling cascade that governs cell migration. APPL1 is a 709 amino acid membrane associated protein that has been reported to play a key role in the regulation of apoptosis, cell proliferation, cell survival, and vesicular trafficking.[82, 83] APPL1 is widely expressed and found in high levels in the heart, brain, ovary, pancreas, and skeletal muscle.[82] Although a significant amount of interest has been generated in the interactions and function of APPL1, the complete phosphorylation profile of this protein has not been described. To date, phosphorylation of three residues, threonine 399, and serines 401 and 691, which were identified from global profiling studies,[19, 84-87] are reported in protein databases, including Phosphosite, Proteinpedia/Human Protein Reference Database, and Expasy-SwissProt.

APPL1 mediates its function through a series of domains, including an N-terminal Bin-Amphiphysin-Rvs (BAR), a central Pleckstrin homology (PH), and a

C-terminal phospho-tyrosine binding domain (PTB).[82, 88] Both the BAR and PH domains are involved in binding to cell membranes. The BAR domain is a dimerization motif associated with the sensing and/or induction of membrane curvature, while the PH domain binds to phosphoinositol lipids.[89, 90] The BAR domain has also been shown to be critical in the ability of APPL1 to localize to endosomal structures.[91] In APPL1, the BAR and PH domains are thought to act together as a functional unit forming an integrated, crescent-shaped, symmetrical dimer that mediates membrane interactions.[92, 93] Moreover, the BAR and PH domains function together to create the binding sites for Rab5, which is a small GTPase involved in endosomal trafficking.[93, 94] The C-terminal PTB domain of APPL1 has been shown to be critical in the ability of APPL1 to bind to several signaling molecules, including the serine/threonine kinase Akt, the neurotrophin receptor TrkA, the adiponectin receptors AdipoR1 and AdipoR2, Human Follicle-Stimulating Hormone (FSHR), and the tumor suppressor DCC (deleted in colorectal cancer).[82, 95-98]

In this study, phosphorylation sites were identified on APPL1 using both contemporary mass spectrometry (MS)-based methods, namely, by liquid chromatography (LC)-coupled to data-dependent tandem MS on both an LTQMS and LTQ-Orbitrap-MS. The bioinformatic algorithm SEQUEST was used to process the MS/MS data obtained in these phosphorylation mapping experiments. However, spectral assignments required manual validation of all identified phosphorylation site spectra. To obtain near-complete coverage of APPL1, multiple proteases were used in parallel phosphorylation site mapping experiments in the contemporary approaches. Proteolytic digestion with Glu C, trypsin, and chymotrypsin yielded sequence coverages of 44.6%, 88.3%, and 81.1%, respectively, with a combined sequence coverage of APPL1 of greater

than 99%. A total of 13 phosphorylation sites were detected and four of these sites were found within APPL1 interacting domains, suggesting a potential regulatory role in APPL1 function.

2.2 Experimental

2.2.1 Reagents and plasmids

FLAG M2-agarose affinity gel, FLAG peptide (DYKDDDDK), and mouse IgG agarose were purchased from Sigma (St. Louis, MO). Calyculin A was purchased from Calbiochem (San Diego, CA). Sodium vanadate was obtained from Fischer Scientific (Fairlawn, NJ). Peroxovanadate was prepared as previously described.[99] FLAG-GFP plasmid was prepared by inserting the FLAG epitope sequence into pcDNA3 (Invitrogen, Carlsbad, CA) and cloning EGFP C1 (Clonetech) into the vector at *Kpn*I and *Bam*HI sites. Human APPL1 (accession number GI: 124494248) was then cloned into the FLAG-GFP plasmid at *Eco*RI and the insertion, as well as orientation, of APPL1 was confirmed by sequencing. Proteases were purchased from Promega Corp. (Madison, WI), and all additional buffers were purchased in solid form from Sigma and prepared as stated.

2.2.2 Protein expression

Protein expression was performed in collaboration with Donna J. Webb and colleagues. Human embryonic kidney 293 (HEK-293) cells were maintained in Dulbecco's Modified Eagle's Medium (DMEM) (Invitrogen) supplemented with 10% fetal bovine serum (FBS) (Hyclone) and penicillin/streptomycin (Invitrogen). HEK-293 cells were transfected with FLAG-GFP-APPL1 (12 μg per 150 mm dish) using Lipofectamine 2000 (Invitrogen). After 36 h, cells were incubated with 1

mM peroxovanadate and 50 nM calyculin A in DMEM with 10% FBS for 30 min and extracted with 25 mM Tris, 100 mM NaCl, and 0.1% NP-40 (pH 7.4). The lysates were precleared twice with mouse IgG-agarose for 1 h at 4 °C, and immunoprecipitated with FLAG-agarose (Sigma, St. Louis, MO) for 2 h at 4 °C. Samples were washed three times with 25 mM Tris and 100 mM NaCl, pH 7.4, and FLAG tagged APPL1 was eluted by incubation of the beads with 0.2 mg/mL FLAG peptide in 25 mM Tris, pH 7.4, for 1 h at 4 °C. Purified APPL1 protein was subjected to sodium dodecyl sulfate−polyacrylamide gel electrophoresis (SDS-PAGE) followed by Coomassie blue staining. The concentration of APPL1 was quantified with a LI-COR Biosciences ODYSSEY Infrared Imaging System using bovine serum albumin (BSA) as a standard.

2.2.3 Proteolytic digestion

For MS analyses, APPL1 was separated into three equal aliquots and proteolytically digested by trypsin, chymotrypsin, and Glu C proteases, respectively. Briefly, proteolysis was performed by taking 2.6 µg of APPL1 (20 µL) and diluting to 25 µL with 25 mM ammonium bicarbonate. Cysteine sulfhydryl groups were reduced by the addition of 1.5 µL of 45 mM dithiothreitol (DTT) for 30 min at 55 °C followed by alkylation with 2.5 µL of 100 mM iodoacetamide for 30 min at room temperature in the dark. Digestion was performed using 100 ng (1:40 enzyme/substrate, w/w) of trypsin gold (Promega, Madison, WI), chymotrypsin (Princeton Separations, Freehold, NJ), or endoproteinase Glu C (Calbiochem EMD Biosciences, Gibbstown, NJ) at 37 °C for 16, 4, or 6 h, respectively. Proteolysis was quenched by adding 1 µL of 88% formic acid. Subsequently, the digest was lyophilized and then reconstituted in 25 µL of 0.1% formic acid.

2.2.4 Western blot analysis

Western blot analysis was performed in collaboration with Donna J. Webb and colleagues. Briefly, purified APPL1 protein was subjected to SDS-PAGE, and then transferred to a nitrocellulose membrane. The membrane was incubated with primary antibody against GFP (Invitrogen) or 4G10 (a kind gift from Steve Hanks, Vanderbilt University) at a dilution of 1 µg/mL. The membrane was then incubated with IR Dye 800 Conjugated Affinity Purified anti-Rabbit IgG or anti-Mouse IgG (Rockland) at a dilution of 0.1 µg/mL, and visualized using a LI-COR Biosciences ODYSSEY Infrared Imaging System.

2.2.5 Linear ion trap and LTQ-Orbitrap MS

LC-MS/MS analyses of APPL1 digests were performed using a linear ion trap mass spectrometer (LTQ, Thermo Electron, San Jose, CA) equipped with an autosampler (MicroAS, Thermo) and an HPLC pump (Surveyor, Thermo), and Xcalibur 2.0 SR2 instrument control. Ionization was performed by using nanospray in the positive ion mode. Spectra were obtained using data-dependent scanning tandem mass spectrometry in which one full MS scan, using a mass range of 400−2000 amu, was followed by up to 5 MS/MS scans of the most intense peaks at each time point in the HPLC separation. Incorporated into the method was data-dependent scanning for the neutral loss of phosphoric acid or phosphate (−98 *m*/*z*, −80 *m*/*z*), for which MS^3 was performed. Dynamic exclusion was enabled to minimize redundant spectral acquisitions. High resolution data was collected using a similar strategy on a LTQ-Orbitrap mass spectrometer with the exception that the full MS scan was performed in the Orbitrap at 30,000 m/z

resolution, rather than at unit mass resolution on the LTQMS. Further instrumental details are available in the supplementary information.

2.2.6 Bioinformatic analysis

Tandem MS/MS spectra acquired in LTQMS and LTQ-Orbitrap-MS experiments were identified using SEQUEST (University of Washington). MS/MS spectra were extracted from the raw data files into .dta format with spectra containing fewer than 25 peaks being excluded. Files labeled as singly charged were created if 90% of the total ion current occurred below the precursor ion, and all other spectra were processed as both doubly- and triply charged ions. Proteins were identified using the TurboSEQUEST version 27 (rev. 12) algorithm (Thermo Electron) and the IPI Human database version 3.33 (67837) sequences. Search parameters are outlined in the supplementary information. Manual verification was performed on all phosphorylation assignments having an Xcorr value above 1, 2, and 2.5 for charges +1, +2, and +3, respectively. Validation was performed as previously described.[100] All spectra are hosted online at the address listed in the Appendices according to MIAPE standards.[101]

2.3 Results and Discussion

2.3.1 Comprehensive phosphorylation map of human APPL1 by LTQ- and Orbitrap-MS

In this study, a comprehensive phosphorylation profile of APPL1 is described for the first time. To accomplish this, FLAG-GFP-APPL1 was expressed in HEK-293 cells by the Webb group and subsequently

immunoprecipitated for MS analysis according to the purification scheme outlined in Figure 10 a. A major band corresponding to the molecular mass of APPL1 was observed when the immunoprecipitate was subjected to SDS-PAGE and stained with Coomassie blue (Figure 10 b). The band was confirmed to be APPL1 by Western blot analysis (Figure 10 c). A total of 15 µg was expressed for this characterization and divided between multiple protease digests and instrumental platforms. Before subjecting APPL1 to MS analysis, we examined the phosphorylation state of this protein using 4G10 phosphotyrosine antibody. APPL1 was phosphorylated on tyrosine residues as determined by Western blot analysis with 4G10 (Figure 10 c). Several other minor bands were detected in the immunoprecipated samples, which could correspond to endogenous APPL1 or APPL1 binding proteins. However, insufficient peptide signal from MS analyses precluded positive protein identification of these additional minor bands.

At least 13 (as discussed below) phosphorylation sites with 99.6% total amino acid sequence coverage were identified using multiple proteases, including trypsin, chymotrypsin, and Glu C, followed by LC-MS analyses using both an LTQMS instrument and an LTQ-Orbitrap instrument. Of these reported phosphorylation sites, three could not be located to a single amino acid (i.e., phosphorylation was determined to exist within a range of potential sites within a peptide). Table 2 shows each confirmed phosphorylation site assignment by sequence position using the LTQMS instrument. In total, 10 phosphorylation sites were identified by combining the data obtained for trypsin, chymotrypsin, and Glu C digests to obtain a sequence coverage of 95.3%. Of these 10 sites, only two

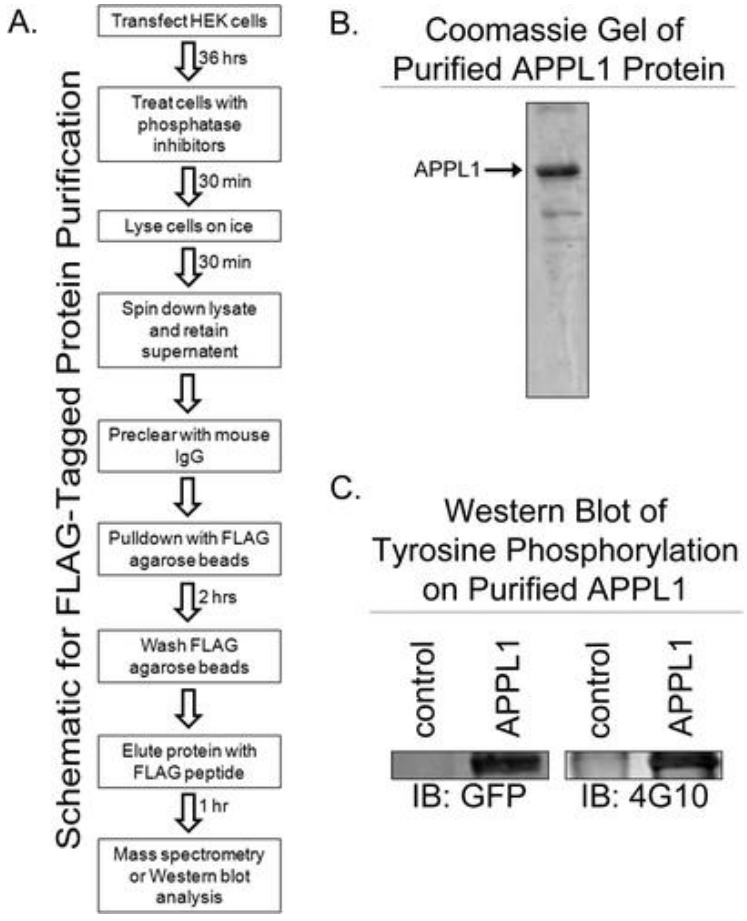

Figure 10. a) Schematic showing the generalized protocol used for purifying FLAG-tagged proteins. b) SDS-PAGE gel of immunoprecipiated FLAG-GFP-APPL1 stained with Coomassie blue. Arrow points to purified FLAG-GFP-APPL1. c) Western blot with GFP-specific antibody (left panel) or phospho-tyrosine antibody (right panel). Left panel shows the purified protein is FLAG-GFP-APPL1 (IB: GFP) and right panel shows that APPL1 is phosphorylated on tyrosine residues (IB: 4G10).

Table 2. Phosphorylation Sites within APPL1 Identified by LTQMS

peptides	position	Protease	$[M + H]^+$ (*m*/*z*)
^{92}VIDEL**SS**CHAVLSTQLADAMMFPITQFK^{119}	‡	Trp	3175.53
^{376}Q**pY**LSENPEETAAR^{389}	378Y	Trp	1700.75
^{390}VNQSALEAVTP**SPS**FQQR^{407}	‡	Trp	2038.99
^{456}DII**pS**PVC*EDQPGQAKAF^{472}	459S	Chymo	1954.93
^{479}TNPFGESGGSTK**pS**ETEDSILHQLFIVR^{505}	491S	Trp	3029.46
^{595}SESNLSSVC**pY**IFESNNEGEK^{614}	604Y	Trp	2315.94
^{669}LIAASSRPNQASSEGQFVVL**pS**SSQSEE SDLGEGGK^{703}	689S	Trp	3631.71
^{683}GQFVVLSS**pS**QSEESDLGEGGKKRE^{706}	691S	Glu C	2633.24
^{683}GQFVVLSSSQ**pS**EE**pS**DLGEGGKKRE^{706}	693S, 696S	Glu C	2713.24

a. The “p” denotes pa. “p*X*” and/or boldface denotes phosphorylation; asterisk, “*” denotes carboxyamidomethylation.
b. The symbol “‡” denotes sequence regions where single residue is known to be phosphorylated between the residues underlined. Phosphorylation on a specific residue on those regions cannot be confirmed.
c. Represents digestion by multiple proteases. Trp, Chymo and Glu C correspond to the proteases, trypsin, chymotrypsin, and Glu C, respectively.

could not be located to a specific residue, that is, phosphorylation was confirmed to exist between amino acids 97−98 (SS) and 401−403 (SPS). Table 3 shows the confirmed phosphorylation sites using the LTQ-Orbitrap instrument. By combining the data obtained for Glu C, trypsin, and chymotrypsin digests, nine phosphorylation sites were identified with sequence coverage of 99.6%. Several of these phosphorylation sites were detected in multiple peptides derived from proteolytic miscleavages corresponding to the same site of phosphorylation. Of these nine sites, two could not be located to a specific residue, but were confirmed to exist between amino acids 401−403 (SPS) and 689−691 (SSS). Moreover, a number of potential phosphorylation sites were eliminated from consideration, as phosphorylation site rearrangement prevented a confident assignment. A comparison of the phosphorylation sites identified using the LTQMS and LTQ-Orbitrap yielded four unique sites by the former and three unique sites by the latter. We detected five phosphorylation sites, including serines 401/403, 459, 691, 693, and 696 by both methods. Interestingly, most of the phosphorylation sites we detected in human APPL1 are conserved in rat and mouse APPL1 (Table 4), raising the possibility that these sites serve a functional role.

Two of the previously identified phosphorylation sites in APPL1, 401S and 691S, were detected in our analysis while one additional site, 399T, was not definitively assigned. Phosphorylation of 401S was initially identified in epithelial carcinoma (HeLa) cells as part of a large-scale characterization of nuclear

Table 3. Phosphorylation Sites Identified within APPL1 by LTQ-Orbitrap-MS

Peptide	position	protease	$[M+H]^+$ (*m/z*)	Mass error (ppm)
^{367}IC*TINNI**pS**KQIYLSENPEETAARVNQSAL^{395}	374S	Chymo	3356.66	3.30
^{390}VNQSALEAVTP**SPS**FQQR^{407}	‡	Trp	2038.96	−2.45
^{415}AGQSRPPTARTS**pS**SGSLGSESTNL^{438}	427S	Chymo	2428.11	−0.62
^{418}SRPPTARTS**pS**SG**pS**LGSESTNL^{438}	427S, 430S	Chymo	2251.96	0.93
^{418}SRPPTARTS**pS**SGSLGSESTNL^{438}	427S	Chymo	2171.99	1.10
^{451}TPIQFDII**pS**PVC*EDQPGQAKAF^{472}	459S	Chymo	2541.17	0.08
^{456}DII**pS**PVC*EDQPGQAKAF^{472}	459S	Chymo	1954.91	−1.64
^{457}II**pS**PVC*EDQPGQAKAF^{472}	459S	Chymo	1839.86	0.33
^{669}LIAASSRPNQASSEGQFVVL**SSS**QSEES DLGEGGK^{703}	‡	Trp	3631.68	−3.71
^{683}GQFVVLSS**pS**QSEESDLGEGGKKRE^{706}	691S	Glu C	2633.21	−0.46
^{683}GQFVVLSSSQ**pS**EESDLGEGGKKRESE^{708}	693S	Glu C	2849.28	5.58
^{683}GQFVVLSSSQ**pS**EESDLGEGGKKRE^{706}	693S	Glu C	2633.21	−0.57
^{686}VVLSS**pS**QSEESDLGEGGKKRE^{706}	691S	Glu C	2301.06	0.13
^{686}VVLSSSQ**pS**EE**pS**DLGEGGKKRE^{706}	693S, 696S	Glu C	2381.03	−1.89

a. The “p” denotes phosphorylation; asterisk, “*” denotes carboxyamidomethylation.
b. The symbol “‡” denotes sequence regions where single residue is known to be phosphorylated between the residues underlined. Phosphorylation on specific residue cannot be confirmed.
c. Represents digestion by multiple proteases. Trp, Chymo and Glu C correspond to the proteases, trypsin, chymotrypsin, and Glu C, respectively.

Table 4. Comparison of Peptide Sequence Surrounding Identified Phosphorylation Sites in APPL1

Site	Position	Homologues	Peptide Sequence
‡ 97/98S	92-119	Human	VIDELSSCHAVLSTQLADAMMFPITQFK
		Rat	VIDELSSCHAVLSTQLADAMMFPISQFK
		Mouse	----------
374S, 378Y	367-395	Human	ICTINNISKQIYLSENPEETAARVNQSAL
		Rat	ICTINNISKQIYLSENPEETAARVNQSAL
		Mouse	ICTINNISKQIYLSENPEETAARVNQSAL
‡ 401/403S	390-407	Human	VNQSALEAVTPSPSFQQR
		Rat	VNQSALEAVTPSPSFQQR
		Mouse	VNQSALEAVTPSPSFQQR
427S, 430S	418-438	Human	SRPPTARTSSSGSLGSESTNL
		Rat	SRPPTARTSSSGSLGSESTNL
		Mouse	SRPPTARTSSSGSLGSESTNL
459S	451-472	Human	TPIQFDIISPVCEDQPGQAKAF
		Rat	TPIQFDIISPVCEDQPGQAKAF
		Mouse	TPIQFDIISPVCEDQPGQAKAF
491S	479-505	Human	TNPFGESGGSTKSETEDSILHQLFIVR
		Rat	TNPFGESGGSTKSETEDSILHQLFIVR
		Mouse	TNPFGESGGSTKSETEDSILHQLFIVR
604Y	595-614	Human	SESNLSSVCYIFESNNEGEK
		Rat	SESNLSSVCYIFESNNEGEK
		Mouse	SESNLSSVCYIFESNNEGEK
689S, 691S, 693S, 696S	669-703	Human	LIAASSRPNQASSEGQFVVLSSSQSEESDLGEGGK
		Rat	LIAASSRPSQSGSEGQ-LVLSSSQSEESDLGEEGK
		Mouse	LIAASSRPNQAGSEGQ-LVLSSSQSEESDLGEEGK
‡ 689/690/691S	669-703	Human	LIAASSRPNQASSEGQFVVLSSSQSEESDLGEGGK
		Rat	LIAASSRPSQSGSEGQ-LVLSSSQSEESDLGEEGK
		Mouse	LIAASSRPNQAGSEGQ-LVLSSSQSEESDLGEEGK

a. The symbol "‡" denotes sequence regions where single residue is known to be phosphorylated between the residues underlined. Phosphorylation on specific residue on those regions cannot be confirmed.

phosphoproteins and in an analysis of protein phosphorylation in developing mice brains.[86, 87] This site was subsequently shown to be phosphorylated in HeLa cells in two additional studies.[84, 85] Phosphorylation of 691S was detected in HEK-293 cells in response to DNA damage using ionizing radiation.[19] We also identified phosphorylation of this site in HEK 293 cells under physiological conditions. Phosphorylation at 399T was identified in a global profiling study,[84] but a positive identification could not be definitively made in our experiments. Our spectra potentially suggested phosphorylation at 399T, but in these spectra, this site was not the highest confidence assignment. Furthermore, the previous study examined protein phosphorylation during mitosis using HeLa cells arrested in the mitotic phase of the cell cycle while our analysis was performed in HEK-293 cells under conditions in which they were progressing through the cell cycle. Thus, it is possible that phosphorylation of this site is transient if it is regulated by cell cycle progression and difficult to detect.

2.3.2 Phosphorylation sites within APPL1 functional domains

The confirmed phosphorylation sites obtained on both instruments are shown in Figure 11a. Of the confirmed sites, four were found in APPL1 interacting domains. Namely, serines 97/98 were located in the BAR domain, raising the possibility that phosphorylation at these sites could disrupt APPL1 dimerization as well as endosomal localization. Interestingly, as shown in the crystal structure of the BAR and PH domains, serines 97/98 are located on the concave surface of the BAR domain, which is thought to interact with

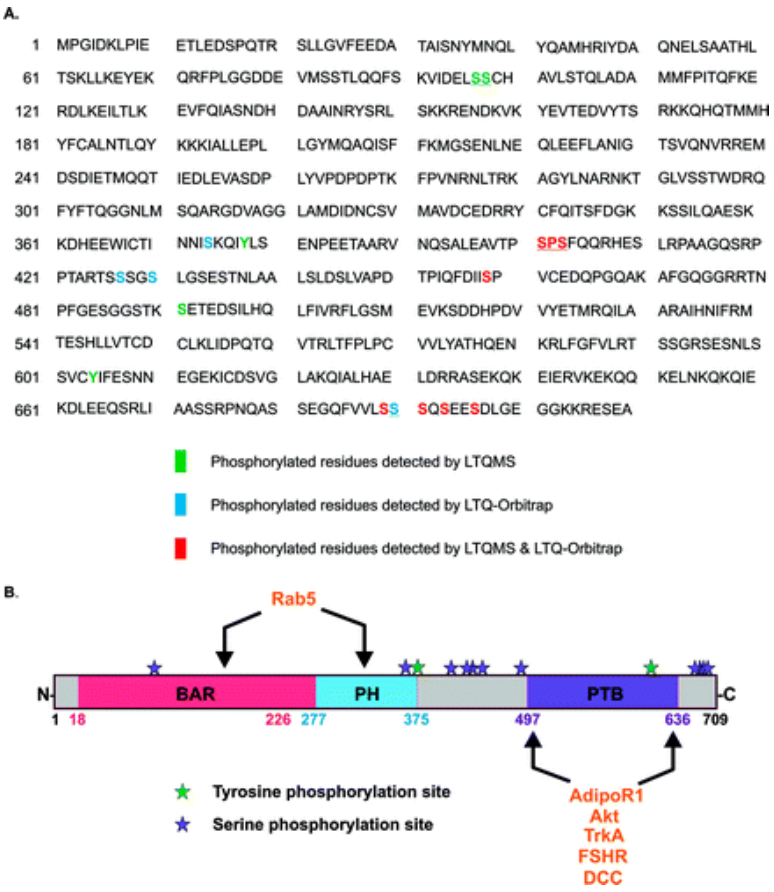

Figure 11. a) Phosphorylation sites identified in APPL1, using LTQMS and LTQ-Orbitrap MS. Underlined sites indicate that one phosphorylation is known to exist within the region. b) A schematic of APPL1 is shown with identified phosphorylation sites relative to the position of APPL1 domains. Interacting regions within APPL1 for several proteins and receptors are also indicated.

membranes (Figure 11b).[92, 102]

Therefore, phosphorylation at this site could potentially regulate membrane interactions. Serine 374 and tyrosine 378 are clustered near the edge of the PH domain (Figure 11b), suggesting a potential link to APPL1 localization. Collectively, these sites in the BAR and PH domains may contribute to altered APPL1 binding to Rab5, since together these domains are important for this interaction. Finally, tyrosine 604 was found in the PTB domain, which is typically involved in protein−protein interactions, and phosphorylation in this domain may regulate the ability of APPL1 to bind to its interacting protein partners. Interestingly, a significant number of identified phosphorylation sites are found outside of known domains. Even though these sites are outside described domains, it does not imply a lack of functional significance. These sites may have importance in regulating the structure and molecular interactions of APPL1.

2.3.3 Advantages and challenges to contemporary phosphoproteomic methodologies

Figures 12 and 13 demonstrate the necessity of manual verification and challenges associated with site identification using bioinformatics analyses. For example, the peptide in Figure 12, GQFVVLSSSQpSEESDLGEGGKKRE, was identified correctly, but because the incorrect peak was used as the monoisotopic peak, the mass error of the precursor ion (−381 ppm) was outside of the acceptable range (−5 to 5 ppm). Conversely, an example of an erroneous SEQUEST assignment is shown in Figure 13. Although b and y ion coverage bracketing the phosphorylation site is sufficient for a high X-corr value and high

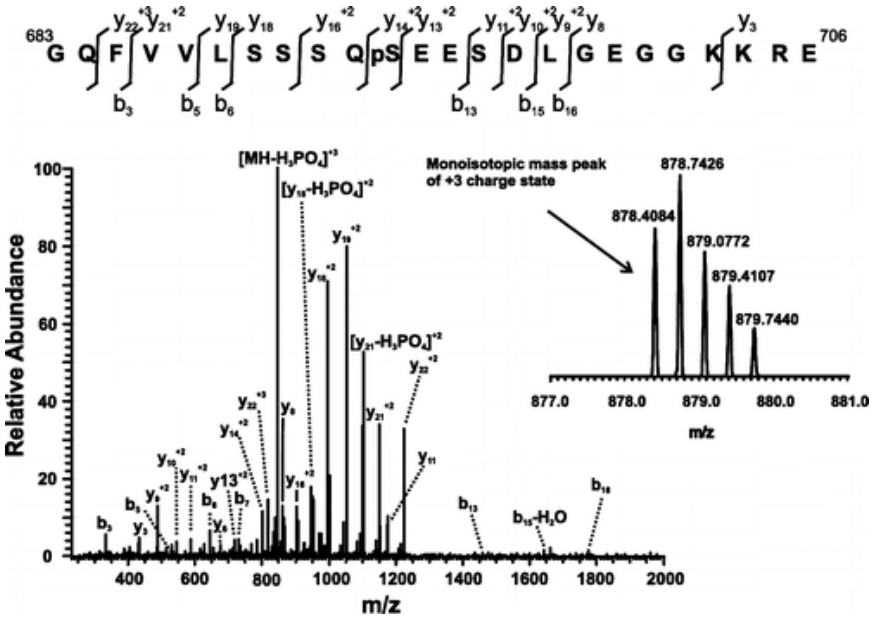

Figure 12. Tandem MS/MS spectrum acquired using an LTQ-Orbitrap illustrates peak validation for accurate SEQUEST assignments. Inset illustrates a situation whereby the instrument selected the peak at 878.7426 as the monoisotopic peak resulting in erroneous mass accuracy (−381 ppm). Manual validation of the data correctly assigns the accurate monoisotopic peak at 878.4084 resulting in a mass accuracy for the parent species of 0.56 ppm.

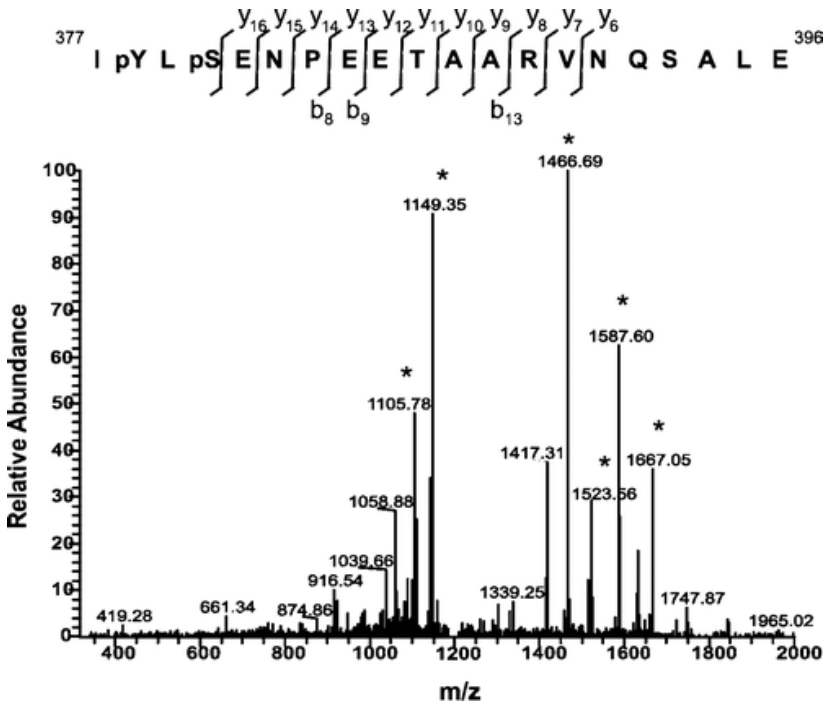

Figure 13. Tandem MS/MS spectrum of a phosphorylation site incorrectly assigned by SEQUEST having the highest Xcorr value of 2.19. SEQUEST assignments report 15% b-ion sequence coverage and 55% y-ion coverage from the y_5 ion to the y_{16} ion. Of the eight most abundant peaks in the spectrum, six ions, indicated by an asterisk, correspond to neither b nor y ions, or to characteristic neutral losses. Manual verification was performed to detect such errors in the bioinformatic assignments. Additionally, the b and y ion coverage fails to bracket the suggested sites of phosphorylation, namely, tyrosine 378 and serine 380.

sequence coverage confidence, high abundance peaks do not correspond to b and y ions or their respective neutral losses. Collectively, these examples and ambiguity arising from gas-phase rearrangement illustrate the continuing need to validate sequencing data in phosphorylation site mapping experiments.[24, 25]

Phosphorylation site validation is challenging for a number of reasons, including low stoichiometries and co-elution of these low abundant peptides with more abundant and easily ionized peptides. Furthermore, though the objective of phosphorylation site discovery was met for characterization of APPL1, significant laborious manual interpretation, validation, and confirmation were needed. Moreover, due to the challenges associated with site discovery, quantitative information is typically not gained in the same experiment, requiring additional time and resources to complete a full characterization. Thus the need for a more selective and rapid strategy for online separation of phosphorylated peptides to facilitate protein phosphorylation characterization is evident.

2.4 Conclusion

Emerging data indicate an important role for APPL1 in regulating various cellular processes, such as cell proliferation, apoptosis, and survival, which points to a need to gain insight in to the regulation of this protein. Since phosphorylation is an important regulatory mechanism, we generated a comprehensive map of phosphorylation sites within APPL1. We

detected 13 phosphorylation sites within APPL1, with four of these being identified in functional domains. These sites have potential implications in regulating APPL1 function and interactions, which represents an important avenue for future study. A number of challenges exist in determining the sites of modification for an uncharacterized protein, such as coelution, reversible phosphorylation, phosphorylation site rearrangement, and the impracticality of performing quantitation in the same experiment. Lanthanide-based phosphorylation-specific labeling is introduced in the following chapters, which circumvents many of the challenges encountered in traditional data-dependent protein phosphorylation characterization.

2.5 Acknowledgements

I would like to thank Donna J. Webb and Joshua A. Broussard for their work in expression and purification of APPL1, and for their assistance in interpretation of the results and their impact on our understanding of the interactions of APPL1. I would also like to thank Hayes McDonald, Amy Ham, and Salisha Hill of the Vanderbilt Proteomics Core for assistance and helpful discussions. This work was supported by the Vanderbilt University College of Arts and Sciences, the Vanderbilt Institute for Chemical Biology, the Vanderbilt Institute of Integrative Biosystems Research and Education, the American Society for Mass Spectrometry (Research Award to J.A.M.).

CHAPTER 3

SIMULTANEOUS RELATIVE QUANTITATION AND SITE IDENTIFICATION OF PHOSPHORYLATED PEPTIDES AND PROTEINS USING LANTHANIDE-BASED LABELING FOR MALDI-TOFMS ANALYSIS

3.1 Introduction

As outlined in Chapter 2, there is a demonstrated need for a comprehensive protein phosphorylation characterization strategy whereby phosphorylated peptides are selectively separated from their unphosphorylated counterparts and sites of phosphorylation are identified and quantitated in the same experiment. In this chapter, challenges associated with phosphopeptide quantitation and site identification are addressed.

Current mass spectrometry based strategies for quantifying sites of protein phosphorylation include stable isotope techniques that take advantage of mass shifts provided by isotopologues. Challenges associated with isotopologue quantitative labeling include isotopic overlap of modified peptides of higher mass. Lanthanide-based labeling strategies allow for greater mass separation than current isotope-based strategies due to incorporation of lanthanide metals of greater mass differences (2-36 Da), but have not been previously demonstrated for selective phosphopeptide quantitation. In this chapter, we demonstrate a strategy for site identification and relative quantitation of phosphorylated peptides and proteins using a phosphorylation-specific lanthanide-based labeling strategy. Because the chemistry is specific for phosphorylation, we term this labeling strategy Phosphopeptide-Element Coded Affinity Tagging, or PhECAT. In this benchmarking report, phosphorylated peptides are selectively modified at the

phosphorylation site via beta-elimination/anionic thiol Michael addition chemistry. In this manner, phosphorylated peptides are converted to cysteine-like residues, which then readily react with cysteine-specific labels. This lanthanide-chelating label is added via maleimide chemistry and selected lanthanide metals are subsequently chelated to a macrocycle moiety. Because these labels replace a labile phosphate with a covalent moiety, phosphorylation site rearrangement can be avoided and phosphorylation site identification is less challenging. To demonstrate this technique, model phosphorylated peptides and those derived through proteolytic digestion of a model phosphorylated protein are quantitated in 1:5, 1:1, and 5:1 molar ratios with comparable sensitivity and relative error (~10%) to current isotopologue-based relative quantitation strategies. Moreover, the site of phosphorylation for bovine beta-casein fragment 48-63 was identified without any site rearrangement of the label evident.

3.2 Experimental

3.2.1 Materials and preparation

Model phosphorylated peptides and proteins were investigated for proof-of-concept experiments. Phosphorylated peptide samples having the sequence WAGGDApSGE (m/z 928.8) were purchased from American Peptide Company (Sunnyvale, CA) and used without further purification. Phosphorylated peptide samples having the sequence KKKKKRFpSFKKpSFKLSGFpSFKKNKK was purchased from Anaspec (Freemont, CA). Phosphorylated protein bovine β-casein was purchased from Sigma-Aldrich (St. Louis, MO). Trypsin was purchased from Promega Corp. (Madison, WI). C-18 spin columns were purchased from Pierce (Rockford, IL). 1,4,7,10-Tetraazacyclododecane- 1,4,7-

tris- acetic acid-1-maleimidoethylacetamide, or Maleimido-mono-amide-DOTA was purchased from Macrocyclics (Dallas, TX) and dissolved in DMSO. 1,2-ethanedithiol (EDT) was purchased from Fluka (St. Gallen, Switzerland). 2,5-dihydroxybenzoic acid (DHB) was purchased from Sigma and dissolved in 50% methanol to a final concentration of 30 mg/mL. Lanthanide metals were purchased from Strem Chemicals (Newburyport, MA) and dissolved in distilled deionized water (18 MΩ cm^{-1}) to a final concentration of 25 mg/mL. Dimethylsulfoxide, acetonitrile, and ethanol were purchased from Sigma.

3.2.2 Digestion of phosphorylated proteins

Proteins were dissolved in ammonium bicarbonate buffer (pH 8.0) and thermally denatured at 90˚C for 20 minutes and quenched at -20˚C.[34] Cysteine-cysteine bonds and free cysteines were reduced with dithiothreitol (final molarity of 4 mM) and alkylated with iodoacetamide (final molarity of 20 mM). Proteins were subsequently digested with trypsin in a 1:40 weight to weight ratio for 16-20 hours at room temperature and purified by C-18 spin columns (Pierce, Rockford, IL) prior to derivatization.

3.2.3 Selective derivatization of phosphorylated peptides and proteins

Model and tryptic peptides were subjected to a beta-elimination (Figure 14(i)) and anionic thiol Michael addition reaction (Figure 14(ii)) resulting in the selective elimination of phosphoric acid followed by addition of ethanedithiol. In this reaction, each sample was derivatized in a reaction mixture containing 2.5 mM EDTA, 0.2 M ethanedithiol, 0.5 M NaOH, 1.5 M acetonitrile, 1.5 M ethanol, 5 M DMSO, and water for 1-2 hrs under nitrogen at 55ºC in a manner similar to

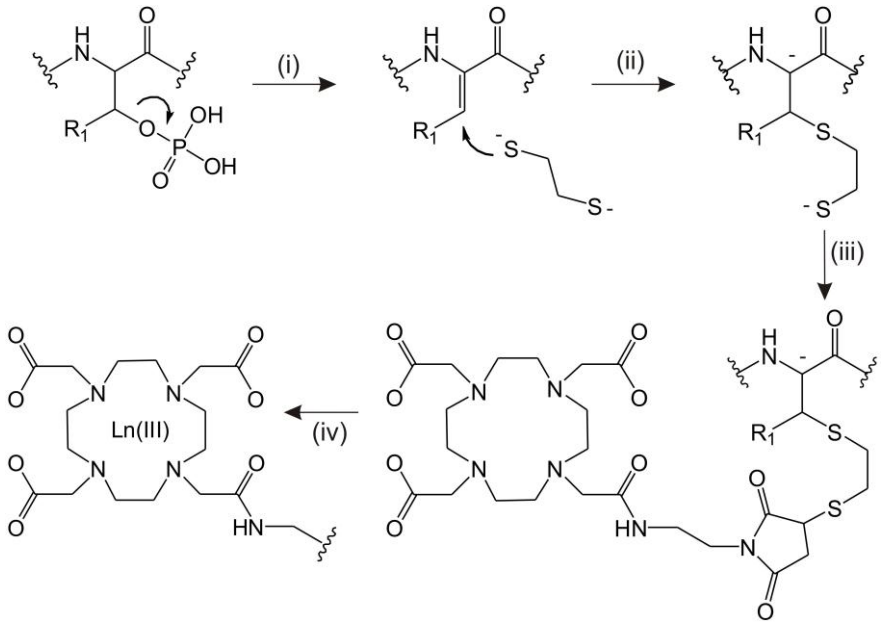

Figure 14. Reaction scheme for PhECAT (i) Phosphoric acid is removed via Beta-elimination in basic conditions (ii) Ethanedithiol is subsequently added to the conjugated diene via anionic thiol Michael addition (iii) The remaining free thiol is attached to the macrocylic via maleimide chemistry (iv)Finally, lanthanides are chelated to the macrocyclic portion of the tag.

reaction conditions described previously.[79, 103, 104] This resulted in conversion of phosphorylated serine and threonine into dehydroalanine or dehydroaminobutyric acid, respectively. The samples were then neutralized and purified by gel filtration (Sephadex G-10, Sigma) and reaction completion was confirmed by MALDI-TOFMS. Subsequently, the thiolated peptides were labeled with a 10-fold excess of maleimido-DOTA (Figure 14(iii)) in a mixture containing acetate buffer (pH 5.5) and DMSO in 1:1 ratio (v/v), resulting in a covalent bond between the free sulfhydryl group and the maleimide portion of the lanthanide-based tag. Finally, selected lanthanide metals were chelated to the maleimide portion of the tag by adding a 100-fold molar excess of metal to peptide and heating to 80ºC for 45 minutes (Figure 14(iv)). Differentially labeled samples were then combined and purified by C-18 spin columns and analyzed using MALDI-TOFMS.

3.2.4 Instrumentation and data analysis

Spectra were obtained using a Voyager-DE STR (Applied Biosystems, Inc.) MALDI-TOFMS instrument in the delayed extraction (DE), positive, reflector mode. MALDI matrix preparation consisted of 2,5-dihydroxybenzoic acid (DHB) in 50% methanol. The samples were spotted using the dried-droplet method. Data analysis was performed using Data Explorer software version 4.3 (Applied Biosystems, Foster City, CA). At least 3 trials were analyzed for each relative quantitation experiment. Spectra were acquired by rastering the MALDI laser at random over the entire matrix spot. Relative molar amounts were calculated by dividing the relative peak area of the derivatized state 1 by the relative peak area of derivatized state 2.

Fragmentation of the labeled phosphorylated peptides and proteins were performed on a Waters Synapt© HDMS (Waters, Inc. Milford, MA) instrument

with MALDI as the ionization source. Data analysis was performed using MassLynx© software (Waters). Six Dalton doublets (the anticipated mass shift afforded by the Tb and Ho metals selected for labeling) were manually selected for fragmentation and analyzed for potential phosphorylation sites in order to assess the stability of the lanthanide label.

3.3 Results and Discussion

While methods for MS-based relative quantitation of peptides and proteins using chemical modification methodologies have been described in detail, there are few reports of label-based relative quantitation strategies that are selective for phosphorylation that provide sufficient mass shift for large peptides. The available methods have enormous utility in quantitation of phosphorylated peptides and proteins, but suffer from three important limitations – (i) they are limited to low mass peptides due to spectral congestion caused by an overlap of increasingly larger isotopic envelopes, (ii) they are limited in affinity purification to avidin/streptavidin, which can pull down non-specific peptides as well as labeled peptides, and (iii) the number of simultaneously analyzed peptides is limited (simultaneous quantitation of 2-8 samples are commonly reported).

Here, we report a multiplexed relative quantitation strategy that addresses these limitations with the added utility of site assignment using PhECAT. Subsequent to the reduction and alkylation of free thiol groups of cysteine, phosphoryl groups on serine and threonine are selectively removed in the form of phosphoric acid via beta-elimination chemistry perfomed under basic conditions, followed by an addition of ethanedithiol via anionic thiol Michael addition chemistry, resulting in a conversion of a phosphate moiety to a free thiol. Thiol-

selective chemistry is performed on the remaining free thiol to attach the PhECAT label to the modified phosphorylated peptide. When the relative phosphorylation concentrations of different cell states are compared, these labels can be chelated to any lanthanide metal, which provides the necessary mass shift for quantitative comparisons. Furthermore, the number of samples that may be quantitated is only limited by the number of available isotopically enriched lanthanide metals (simultaneous quantitation of 2-15 samples is possible). A schematic diagram of this strategy is illustrated in Figure 15. Moreover, antibodies selective for lanthanide-DOTA complexes with no natural analogs have been reported as an alternative to biotin/streptavidin purification.[75]

3.3.1 Relative quantitation of phosphorylated peptides and Proteins using PhECAT

Varying molar amounts of phosphorylated peptides and proteins were derivatized in this manner and quantitated in proof-of-concept experiments. An example of a typical relative quantitation experiment is illustrated in Figure 16. In this example, the peptide WAGGDApSGE was differentially tagged with Tb and Ho labels in a 1 to 5 molar mixture, respectively. The calculated peak area ratio was 0.199, exhibiting a 0.5% experimental error from the known relative molar amounts. Molar ratios of 1:5, 1:1, and 5:1 were demonstrated with Tb and Ho-chelated tags, purified, and spotted with matrix before being analyzed by MALDI-MS. Table 5 depicts the results from varying the molar ratios of the phosphorylated peptides.

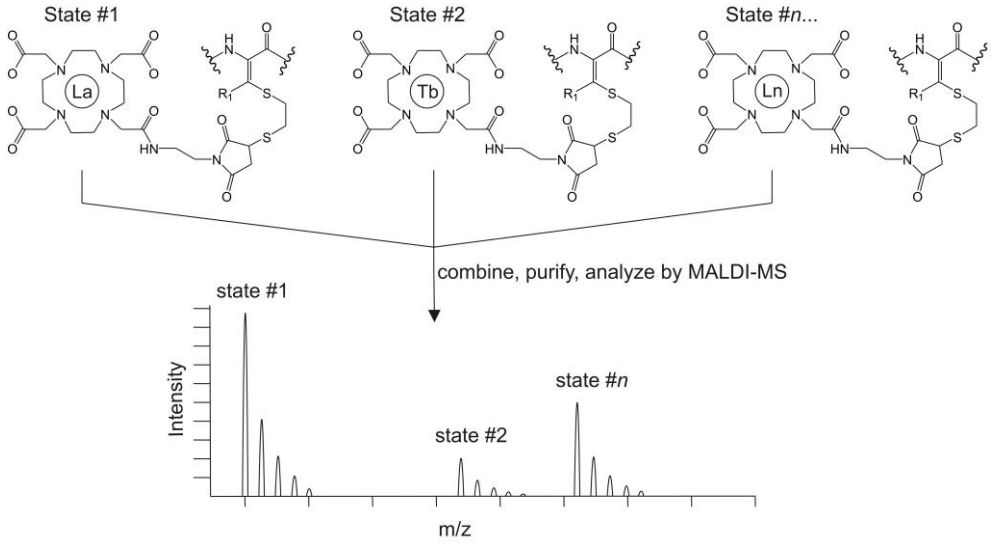

Figure 15. Labeling of multiple sample states with DOTA tags coordinated to different lanthanide metals. In this illustrative figure, a 5:1:2.5 may be differentially coded with different lanthanide metals. Thus, the number of simultaneous samples that can be combined for relative quantitation is limited only be the number of different metals (or metal isotopes) that are used.

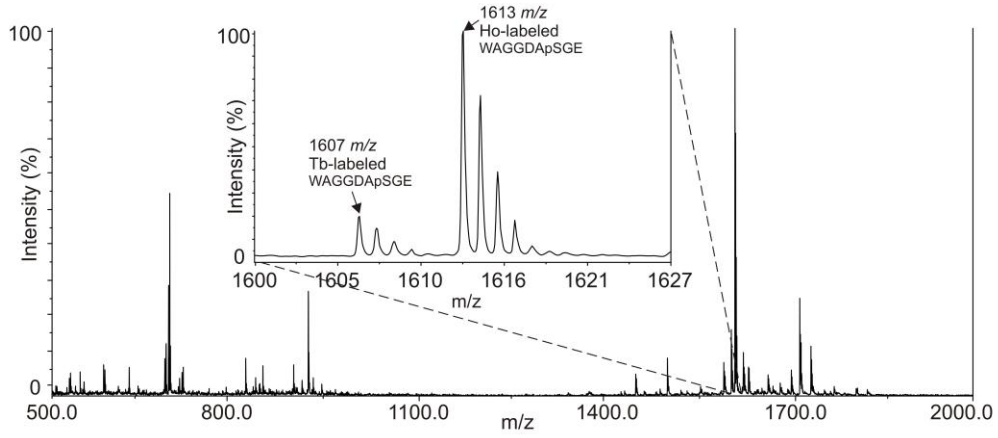

Figure 16. The phosphorylated peptide having the sequence WAGGDApSGE was derivatized in the manner previously described. The full scan m/z is shown. Although there are several minor peaks associated with excess labeling reagent, the labeled peptide is the dominant peak in this spectrum. (Inset) Relative quantitation between Tb and Ho labeled peptides having a molar ratio of 1:5, respectively. The measured peak areas were 1898.93 and 9529.45 for Tb and Ho, respectively, resulting in a calculated molar ratio of 0.199.

Table 5. Relative Quantitation of phosphorylated peptides and proteins using lanthanide-chelating tags in MALDI-TOFMS.

Peptide Sequence[a,b]	$[M+H]^{+}$ [c]	$[M^{*}+H]^{+}$ Tb, Ho[d]	Molar ratio of derivatized peptides	Measured molar ratio of peptides derivatized with Ho-tag and Tb-tag (average # of trials)	Relative Percent Error[e]
WAGGDA**pS**GE from delta sleep-inducing peptide	928.8	1607.2, 1613.2	5.0: 1.0 (Tb:Ho)	5.408 (3)	+8.2
WAGGDA**pS**GE from delta sleep-inducing peptide	928.8	1607.2, 1613.2	1.0: 1.0 (Tb:Ho)	1.029 (4)	+2.9
WAGGDA**pS**GE from delta sleep-inducing peptide	928.8	1607.2, 1613.2	1.0: 5.0 (Tb:Ho)	0.207 (5)	+3.5
^{48}FQ**pS**EEQQQTEDELQDK^{63} from bovine B-casein	2060.7	2739.1‡, 2745.1‡	1.0: 5.0 (Ho:Tb)	0.217 (3)	+8.4
^{48}FQ**pS**EEQQQTEDELQDK^{63} from bovine B-casein	2060.7	2739.1‡, 2745.1‡	1.0: 1.0 (Tb:Ho)	1.089 (3)	+8.9
^{48}FQ**pS**EEQQQTEDELQDK^{63} from bovine B-casein	2060.7	2739.1‡, 2745.1‡	1.0: 5.0 (Tb:Ho)	0.226 (3)	+12.8

a. "p" denotes phosphorylation, sequence positions bracket the sequence for tryptic peptides

b. Phosphorylated peptides purchased and used without additional purification.

c. Monoisotopic masses for unlabeled phosphorylated peptides.

d. Calculated monoisotopic peaks for labeled phosphorylated peptides. "*"denotes PhECAT labeling, "‡" denotes relative quantitation calculations where the peak having the highest relative abundance was selected for peak area quantitation rather than the monoisotopic peaks. This is primarily due to the fact that, here, the monoisotopic peak has the lowest intensity. In this case, the peaks of highest intensity (2741.1, 2747.1) were selected.

e. Percent errors are reported according to the following formula:

(Average Peak Area Ratio – Anticipated Peak Area Ratio) / Anticipated Peak Area Ratio

For the peptide WAGGDApSGE, the average error associated with three separate quantitation experiments (*i.e.*, the average of errors associated with three experiments profiling three separate molar ratios) was calculated to be 8.5%. For the protein bovine beta-casein the tryptic peptide FQpSEEQQQTEDELQDK was quantitated using the same range of molar ratios. A typical quantitation experiment is shown in Figure 17. In this example, beta-casein was derivatized in a 1 to 5 molar ratio with Tb- and Ho-chelated labels, respectively. The measured molar ratio of Tb-labeled sample to Ho-labeled sample was 0.203, which has a relative error of 1.67%. The average error associated with three separate quantitation experiments was calculated as 6.4%. These errors are comparable to current isotope coded affinity labels, with the added advantages larger shifts in mass doublets afford, i.e. 2-36 Da for single phosphorylation sites, allowing for quantitation of high- mass peptides without peak convolution from adjacent isotopes. For multiple phosphorylation sites, the mass difference scales with the number of the labels, providing even greater separation. These results also indicate that this method has error competitive to current quantitative phosphoproteomic methods and should have utility in relative quantitative studies of complex biological samples. The utility of lanthanide ions as luminescent chromophores in LC separations have been well described, and may increase confidence in phosphorylation site labeling at an additional stage of analysis.[41] Moreover, the addition of a macrocycle may shift LC elution times for phosphorylated peptides, which may assist in separation of closely spaced phosphorylated and non-phosphorylated species.

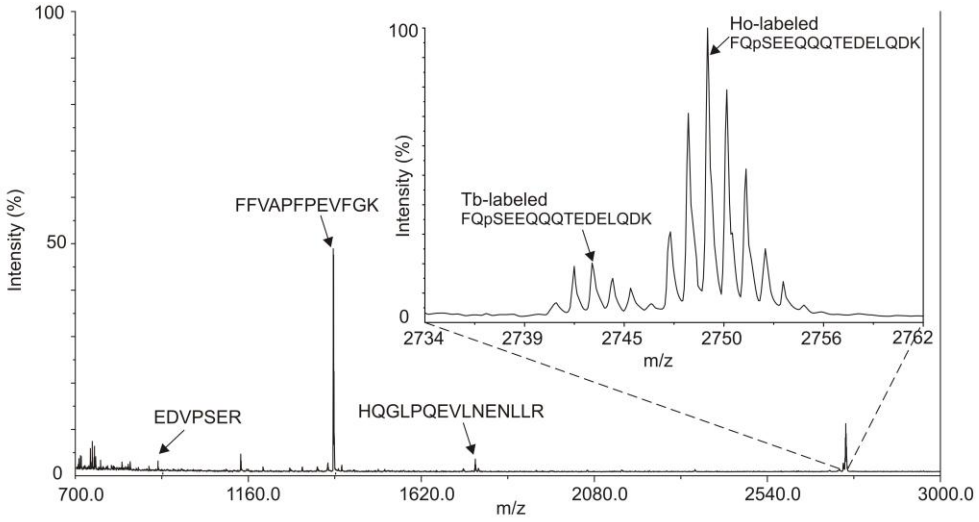

Figure 17. Bovine beta-casein was derivatized in the manner previously described. The full m/z is shown. In addition to standard digest peaks (tryptic beta-casein peptides), the labeled phosphorylated peptide having the sequence FQpSEEQQQTEDELQDK is observed, and is one of the dominant peaks in this spectrum. (Inset) Relative quantitation between a 1:5 molar mixture of Tb and Ho labeled beta-casein. The measured peak areas are 455.77 and 2241.51 for Tb and Ho, respectively, resulting in a calculated molar ratio of 0.2039.

3.3.2 Fragmentation and phosphorylation site identification

PhECAT labeled peptides were examined by tandem MS to evaluate the utility of these tags for phosphorylation site-identification. An example of a typical tandem spectrum is shown in Figure 18. The expected b/y series ions were observed, including full b ion coverage from the b_3 to the b_{15} ion, all labeled and several unlabeled y ions including y_9, y_{11}, and $y_{13\text{-}15}$, and several labeled water loss ions with little evidence for fragmentation of the label. It should be noted that all fragment ions covalently bound to the PhECAT label exhibit higher intensities than unlabeled fragment ions. The stability of this label enables predictable mass shifts of anticipated b and y ions which gives an indication of the site of modification previously phosphorylated. Furthermore, because this tag is not labile and does not show phosphorylation site rearrangement (as is the case with phosphoric acid and phosphate plus water loss), it has an added advantage of more confident phosphorylation site assignment.

3.3.3 Challenges in quantitation of phosphorylated threonine.

Beta-elimination/Michael addition of phosphorylated threonine has been reported to be more challenging due to steric hinderance caused by the methylated alpha carbon.[51] The PhECAT labeling strategy was applied toward two peptides containing phosphorylated threonine. The peptide containing the sequence KKALRRQEpTVDAL was incubated for 4 and 6 hours using the reaction conditions described above. Although beta-elimination reacted to completion, Michael addition was not achieved to completion. Figure 19 illustrates the minimal impact of increased incubation

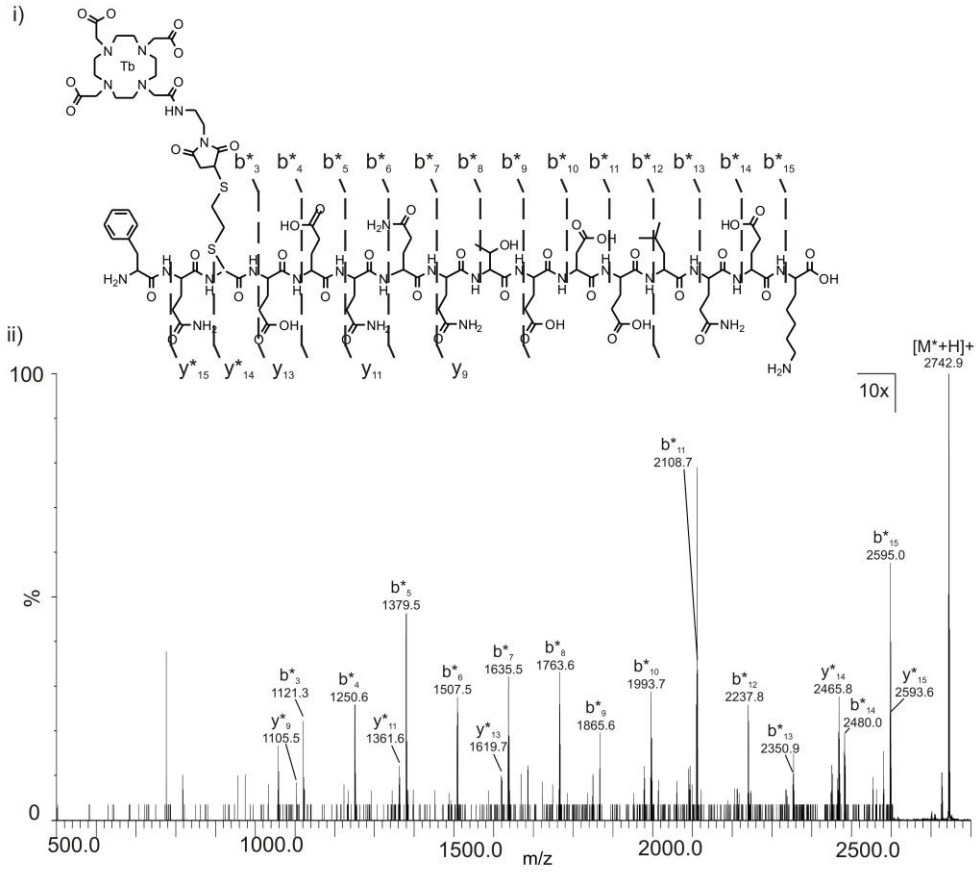

Figure 18. i) Structure of a terbium-labeled tryptic beta-casein phosphorylated peptide having the sequence FQpSEEQQQTEDELQDK. An asterisk indicates that the ion is covalently modified with the PhECAT. Observed fragmentation peaks are indicated on the peptide structure. Fragmentation coverage of 86.7% and 33.3% of the labeled peptide was observed for b and y ions, respectively. Five additional y ions were located, but were not reported due to inadequate S/N. Fragmentation coverage of b and y water loss ions is provided in the appendices. Importantly, all of the anticipated ions corresponding to labeled positions are observed, demonstrating the utility of this label for phosphopeptide site identification as well as relative quantitation. ii) Fragmentation spectrum of labeled FQpSEEQQQTEDELQDK. Fragment ions are labeled. It should also be noted that labeled fragment ion species exhibit greater intensity than non-labeled fragment ion species. Spectral peaks from 500 m/z to 2600 m/z were intensified 10x to increase visibility of b and y spectral assignments.

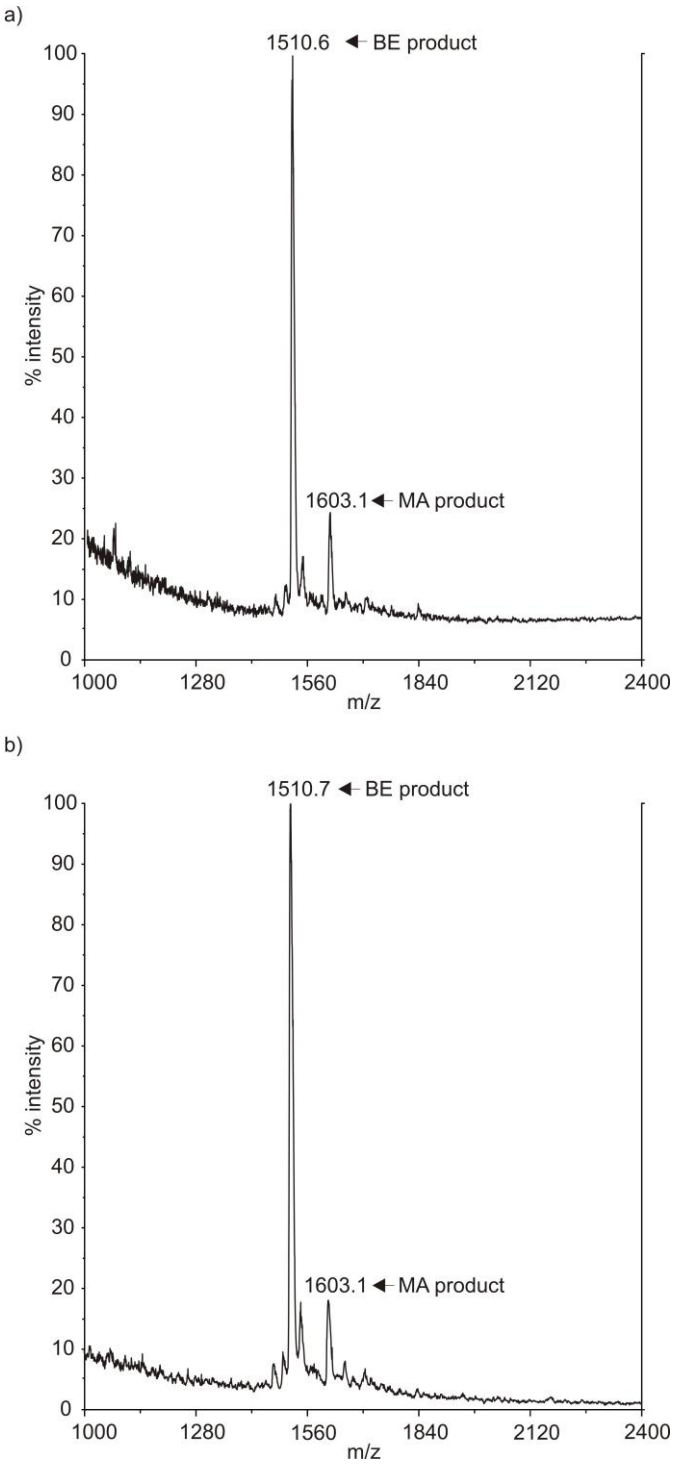

Figure 19. a) Completion of the beta-elimination/Michael addition reaction for KKALRRQEpTVDAL with a 4-hour incubation time at 50°C. b) Completion of the beta-elimination/Michael addition reaction for KKALRRQEpTVDAL after a 6-hour incubation time at 50°C. Incubation time does not increase the Michael addition product.

time on the Michael addition product. The peptide containing the sequence LKRApTLG was incubated for 24 hours, resulting in a marginal increase of Michael addition product (Figure 20). These results are consistent with a report from Gross and colleagues,[51] which describes minimal Michael addition product increase with respect to increased incubation time (in the Supplementary Material of Gross, *et al*). To circumvent this, Gross and colleagues included an additional separation step between beta-elimination and Michael addition, transforming the chemistry from a one-pot to a two-pot process. It can be reasoned that even though phosphorylated threonine generates a low yield of labeled product, the relative quantitation of phosphorylated threonine is still possible to within acceptable error (<10%), and percent yields are expected to remain consistent between samples with consistent labeling technique.

3.3.4 The role of arginine in phosphorylation site stabilization

Myristoylated Alanine-Rich C Kinase Substrate (MARCKS) peptide fragment 151-175 (KKKKKRFpSFKKpSFKLSGFpSFKKNKK) was derivatized in the manner above and beta-elimination/Michael addition was checked for completeness. Although this peptide contains three phosphorylated serine residues, beta-elimination/Michael addition was only observed for one phosphorylated residue (Figure 21). This is consistent with observations made by Woods and colleagues,[105-107] where observations of non-covalent complexes of phosphorylated residues and quarternary amines (*i.e.*, arginines) were reported. It is speculated that the two unlabeled phosphorylation sites form a strong complex with the excess of quarternary amines in the peptide. Woods, et al. suggests the addition of aromatic compounds (*e.g.*, hexachlorobenzene) to

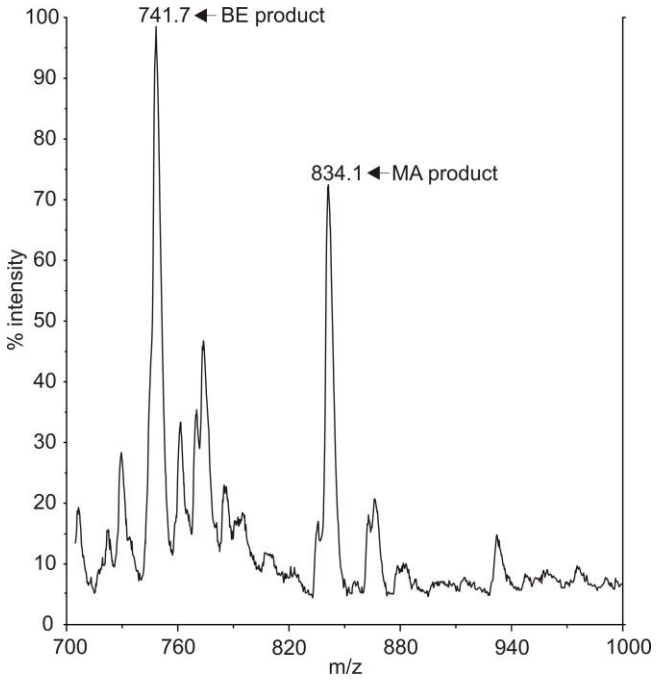

Figure 20. Completion of the beta-elimination/Michael addition reaction for LKRApTLG with a 24-hour incubation time at 50°C. Significant increases in incubation time do not affect the yield of the Michael addition product.

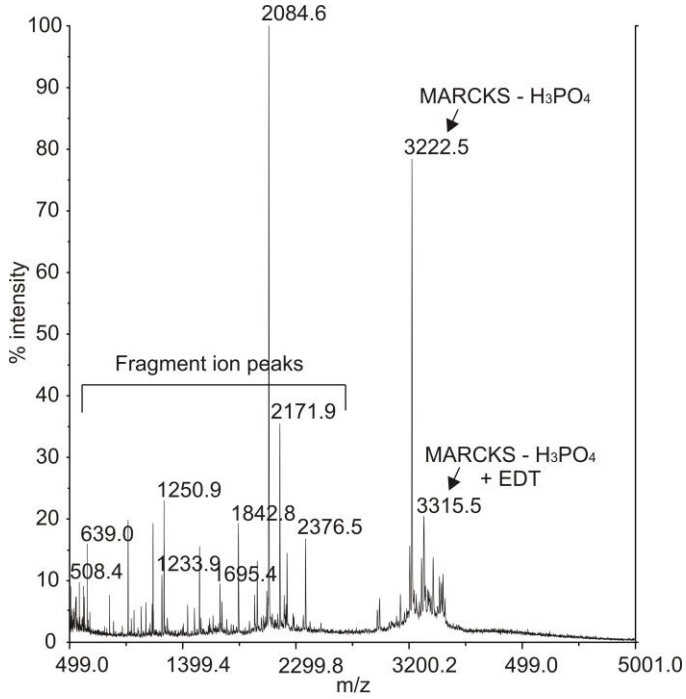

Figure 21. Spectra profiling the completion of the beta-elimination/Michael addition reaction for the triply phosphorylated MARCKS peptide. One phosphorylated residue is labeled, indicating a near-covalent cation pi-interaction of the phosphorylated residues and the guanidinium group of the arginine residues in the peptide sequence.[105, 106] Moreover, the Michael addition reaction is not quantitative, as indicated by the relative low abundance with respect to the beta-eliminated peptide. Additional fragmentation peaks corresponding to b and y ions from in-source fragmentation are indicated.

solution to compete with electrostatic interactions between arginines and phosphorylation sites. To circumvent unanticipated arginine-phosphorylation interactions of peptides, peptides that contain arginine should be treated with aromatic compounds prior to derivatization to ensure that the phosphorylation site is available for modification.

The solvent-accessible phosphorylated residue on MARCKS was quantitated using Tb- and Ho-chelated lanthanide labels. A typical quantitation experiment is shown in Figure 22. In this experiment, a 1 to 3 (Tb to Ho, respectively) molar mixture was quantitated. For peptides above 3000 Da, a 6-Da shift was not adequate to resolve the differentially labeled peaks, illustrating the need for labels to provide larger mass shifts and the utility of lanthanide- based labels to design quantitative strategies using mass shifts that support the mass of the peptides of interest.

3.4 Conclusions

Current methods of MS-based protein quantitation primarily focus on quantifying relative expression profiles through labeling non-post-translationally modified peptides. This offers a limited view of the biological activity of cells, because many biological functions are dependent on temporal protein modifications, specifically, protein phosphorylation. The available methods for phosphoprotein quantitation provide good specificity for the site of phosphorylation, however, they have limited applicability for peptides of increasing mass. In this work, we have demonstrated the utility of PhECAT for relative quantitation of phosphorylated peptides using

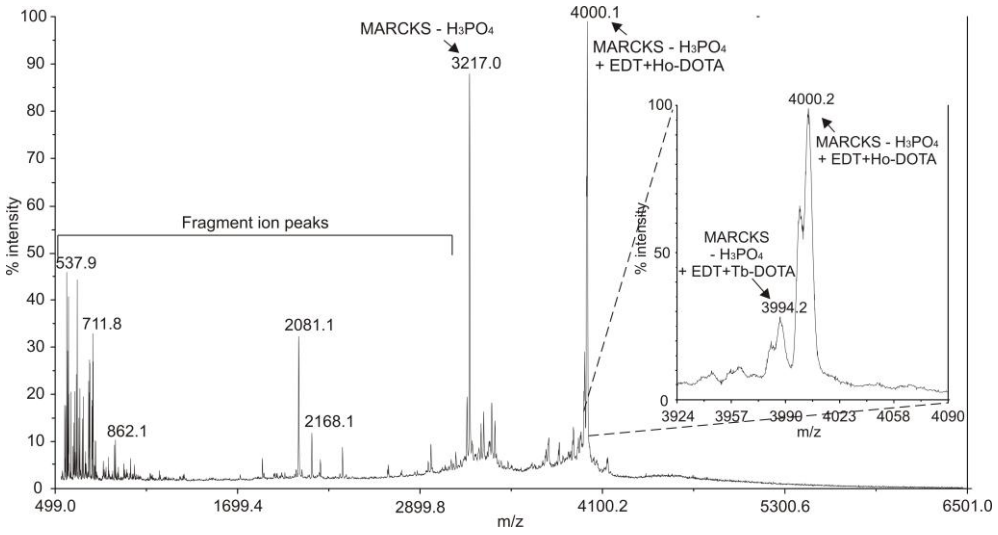

Figure 22. Spectra illustrating the lanthanide-based labeling (PhECAT strategy) of the uncomplexed phosphorylated residue in the MARCKS peptide. Note that the % intensity of the labeled species is significantly greater than the intensity of the Michael addition product in Figure 19, indicating that the lanthanide-based label improves ionization and detection, which is an added advantage in phosphoproteomic characterization. (inset) Relative quantitation between Tb-and Ho-labeled species aquired on a DE-Voyager MALDI-TOFMS. Here, a 6-Da mass shift was not sufficient to resolve labeled peptides of masses greater than 3000 m/z on a typical MALDI-TOFMS, illustrating the need for larger mass shifts provided by lanthanide encoded labeling.

MALDI-MS. We propose that this method may circumvent challenges encountered by label-free quantitation, such as gas-phase phosphorylation site rearrangement, and has potential utility in quantitating the relative expression of protein phosphorylation with the additional utility of providing a confident phosphorylation site assignment.

3.5 Acknowlegements

I would like to thank Dr. Thomas J. Kerr, Ms. Katie Dextraze (Georgia Institute of Technology), Dr. Larissa S. Fenn, Mr. Michal Kliman, and Dr. Brian Huffman for assistance in the initial stages of this work. Financial assistance for this work was provided by the Vanderbilt University College of Arts and Sciences, the Vanderbilt Institute for Chemical Biology (Pilot Project Grant), the Vanderbilt Institute for Integrative Biosystems Research and Education, and the American Society for Mass Spectrometry (Research Award to JAM).

CHAPTER 4

RAPID SEPARATION, IDENTIFICATION, AND QUANTITATION OF PHOSPHORYLATED PEPTIDES AND PROTEINS USING LANTHANIDE-BASED LABELS AS ION MOBILITY-MASS SPECTROMETRY MOBILITY SHIFT LABELS

4.1 Introduction

The stoichiometry of protein phosphorylation regulates numerous biological processes. As addressed in the previous chapter, current mass spectrometry-based strategies for quantifying sites of protein phosphorylation include isotopologue strategies that limit the size of the peptide quantitated and require high resolution MS instruments, which are less common and costly to operate. Lanthanide-based labeling strategies allow for greater mass separation than current isotope-based strategies due to incorporation of lanthanide metals of greater mass differences (2-36 Da), and may be used as mobility shift “anchors” for rapid visualization in ion mobility-mass spectrometry (IM-MS) analysis. Moreover, lanthanide-based labels may provide mobility shift and selective separation of the labeled phosphorylated peptides. This facilitates rapid identification and selection of labeled ions for further characterization.

In this chapter, we demonstrate lanthanide-based labeling for phosphorylated peptides, or Phosphopeptide Element-Coded Affinity Tagging (PhECAT), for rapid identification, relative quantitation, and phosphorylation site identification of phosphorylated peptides and proteins in complex mixtures using IM-MS as a separation platform. Briefly, in the PhECAT method, phosphorylated peptides are selectively modified at the phosphorylation site via beta-

elimination/anionic thiol Michael addition chemistry. In this manner, phosphorylated peptides are converted to cysteine-like residues, which then readily react with cysteine-specific labels. A lanthanide-chelating label is added via maleimide chemistry and selected lanthanide metals are subsequently chelated to a macrocycle moiety. Labeled phosphorylated peptides are then visually identified by a mobility shift from the anticipated peptide correlation line generated in IM-MS, quantitated, and fragmented in the transfer portion of the instrument to provide comprehensive phosphopeptide analysis. To demonstrate this technique, phosphorylated peptides and protein mixtures from proteolytic digestion are identified and quantitated in various molar ratios with comparable sensitivity and relative error to current isotopologue-based relative quantitation strategies. Moreover, site identification of the modified phosphorylation site is achieved, demonstrating that the label is covalent on the site of modification and more stable than b and y ions generated by cleaving peptide bonds. This strategy provides more confident site identification than that obtained in data-dependent LC-MS/MS strategies because this method circumvents phosphorylation-site rearrangement in the collision cell.

4.2 Experimental

4.2.1 Materials

Model phosphorylated peptides and proteins were investigated for proof-of-concept experiments. Phosphorylated protein bovine β-casein was purchased from Sigma-Aldrich (St. Louis, MO). Trypsin was purchased from Promega Corp. (Madison, WI). C-18 spin columns were purchased from Pierce (Rockford, IL). Maleimido-mono-amide-DOTA was purchased from Macrocyclics (Dallas, TX)

and dissolved in DMSO. 1,2-ethanedithiol (EDT) was purchased from Fluka (St. Gallen, Switzerland). 2,5-dihydroxybenzoic acid (DHB) was purchased from Sigma and dissolved in 50% methanol to a final concentration of 30 mg/mL. Lanthanide metals were purchased from Strem Chemicals (Newburyport, MA) in chloride salt form and dissolved in distilled deionized water (18 MΩ cm^{-1}) to a final concentration of 25 mg/mL. Dimethylsulfoxide, acetonitrile, and ethanol were purchased from Sigma.

4.2.2 Digestion of phosphorylated proteins

Proteins were dissolved in ammonium bicarbonate buffer (pH 8.0) and thermally denatured at 90˚C for 20 minutes and quenched at -20˚C.[34] Cysteine-cysteine bonds and free cysteines were reduced with dithiothreitol (final molarity of 4 mM) and alkylated with iodoacetamide (final molarity of 20 mM). Proteins were subsequently digested with trypsin in a 1:40 weight to weight ratio for 16-20 hours at room temperature and purified by C-18 spin columns (Pierce, Rockford, IL) prior to derivatization. Digestion was confirmed by MALDI-TOFMS (data not shown).

4.2.3 Selective derivatization of phosphorylated peptides and proteins

Tryptic peptides were subjected to a beta-elimination (Figure 23(i)) and anionic thiol Michael addition reaction (Figure 23(ii)) resulting in the selective elimination of phosphoric acid followed by addition of ethanedithiol. In the beta-elimination/Michael addition reaction, each sample was derivatized in a

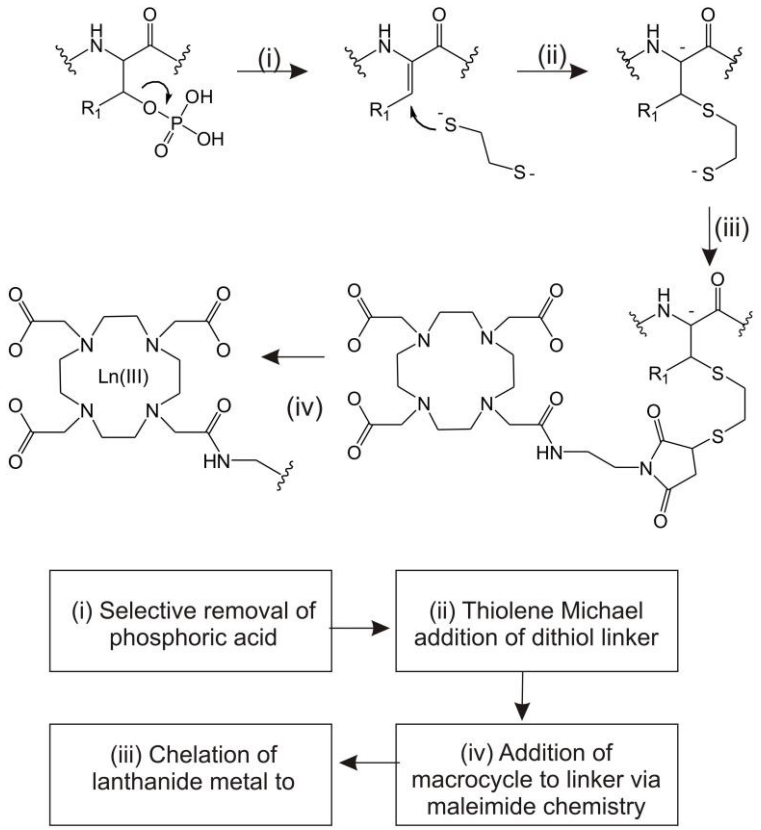

Figure 23. Reaction scheme for PhECAT (i) Phosphoric acid is selectively removed (ii) Ethanedithiol is subsequently added to the conjugated diene via anionic thiol Michael addition (iii) The remaining free thiol is attached to the macrocylic via maleimide chemistry (iv) Finally, lanthanides are chelated to the macrocyclic portion of the tag.

reaction mixture containing 2.5 mM EDTA, 0.2 M ethanedithiol, 0.5 M NaOH, 1.5 M acetonitrile, 1.5 M ethanol, 5 M DMSO, and water for 1-2 hrs under nitrogen at 55ºC. This resulted in conversion of phosphorylated serine or threonine into dehydroalanine or dehydroaminobutyric acid, respectively. The samples were then neutralized and purified by polyacrylamide gel (size range >1800 Da, Thermo) and reaction completion was confirmed by MALDI-TOFMS. Subsequently, the thiolated peptides were labeled with a 10- to 50-fold excess of maleimido-DOTA (Figure 23(iii)) in a mixture containing acetate buffer (pH 5.5) and DMSO in 1:1 ratio (v/v), resulting in a covalent bond between the free sulfhydryl group and the maleimide portion of the lanthanide-based tag. Finally, samples were encoded with lanthanide metals by chelation to the DOTA portion of the tag by adding a 100- to 500-fold molar excess of metal to peptide and heating to 80ºC to speed up chelation for 45 minutes (Figure 23(iv)). Differentially labeled samples were then combined and purified by C-18 spin columns and analyzed MALDI-IM-TOFMS.

4.2.4 Instrumentation and data analysis

Spectra were obtained using a Synapt HDMS (Waters Corp., Manchester, UK) MALDI-IM-TOFMS in positive, reflector mode. MALDI matrix preparation consisted of 2,5-dihydroxybenzoic acid (DHB) in 50% methanol. The samples were spotted using the dried-droplet method. Data analysis was performed using MassLynx (Waters Corp., for Synapt data) and DriftScope (Waters Corp., for Synapt data). At least 3 trials were analyzed for each relative quantitation experiment. Spectra were acquired by rastering the MALDI laser at random over the entire matrix spot.

Labeled peaks were identified by mobility shift (<3%) in MALDI-IM-TOFMS data and quantitated. Relative molar amounts were calculated by dividing the relative peak area of the derivatized state 1 by the relative peak area of derivatized state 2. Fragmentation of the labeled phosphorylated peptides and proteins were performed on a Waters Synapt HDMS (Figure 24a) in the transfer portion of the instrument, which was chosen because of the added advantage of having fragmentation spectra organized by mobility (Figure 24b).

Peaks shifted out of peptide correlation space were manually selected for fragmentation and analyzed for potential phosphorylation sites in order to assess the stability of the lanthanide label and confirm the site of phosphorylation. Fragmentation spectra were processed using MassLynx software using the Subtract, Smooth, and Center processing tools and subsequently sequenced *de novo* using an anticipated peak list generated from the ExPASy Peptide Mass © program.

4.3 Results and Discussion

While methods for MS-based relative quantitation of peptides and proteins using chemical modification methodologies have been described in detail, there are few reports of label-based relative quantitation strategies that are selective for phosphorylation. The available methods have great utility in quantitation of phosphorylated peptides and proteins, but three important challenges exist – (i) they are limited to low mass peptides due to spectral congestion caused by an overlap of increasingly larger isotopic envelopes, (ii) identification of labeled species is challenging in complex mixtures, and

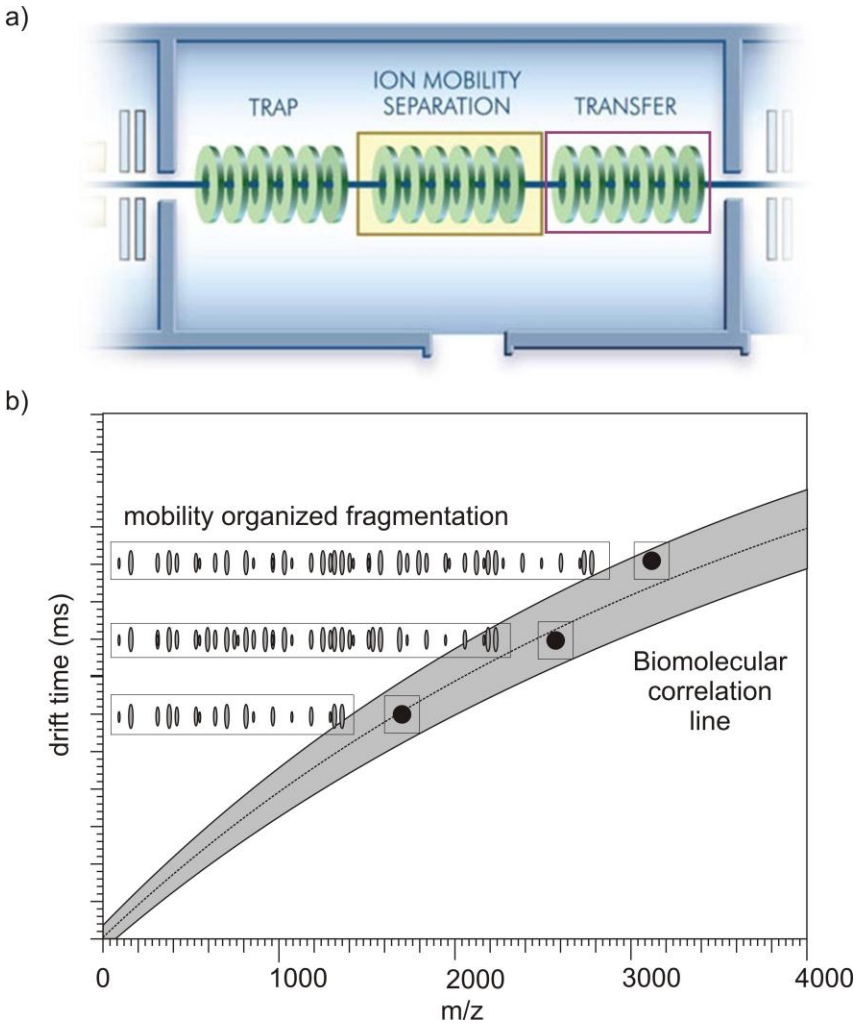

Figure 24. a) A schematic of the mobility cell portion of the Synapt HDMS G2. In these experiments, ions were separated in the mobility portion and subsequently fragmented in the transfer portion of the instrument. b) An advantage of this fragmentation strategy is that fragment ions are organized by mobility.

(iii) the number of simultaneously analyzed peptides is limited (simultaneous quantitation of 2-8 samples are commonly reported).

Here, we report a multiplexed relative quantitation strategy that addresses these limitations using lanthanide-based labels with MALDI-IM-MS in addition to the MALDI-TOFMS platform described in Chapter 3. A schematic diagram of this comprehensive phosphoproteomic strategy is illustrated in Figure 25. In this strategy, phosphorylated peptides and proteins are selectively labeled with a lanthanide-chelated tag. Quantitative information is obtained in both platforms by encoding each sample with a different lanthanide, which provides the necessary mass shift for quantitative comparisons (Figure 25, top and middle, right). The number of samples that may be quantitated is only limited by the number of available isotopically enriched lanthanide metals (simultaneous quantitation of 2-14 samples is possible, excluding radioactive Promethium). Used in the MALDI-TOFMS platform, these labels provide larger mass differences to avoid isotopic overlap while quantitating phosphorylated peptides of higher mass. Used in the MALDI-IM-TOFMS platform, these labels have added utility in converting the phosphorylation site into a high-density “anchor” (Figure 25, bottom left). This anchor shifts the labeled peptide below the peptide correlation line in IM-MS space. Shifting labeled peaks away from unlabeled peaks facilitates selection and identification in complex mixtures for further site localization. Site identification is achieved by fragmenting peptides with an observed shift in IM-MS conformation space and identifying b and y ions exhibiting the additional mass of the covalent label (Figure 25, bottom right).

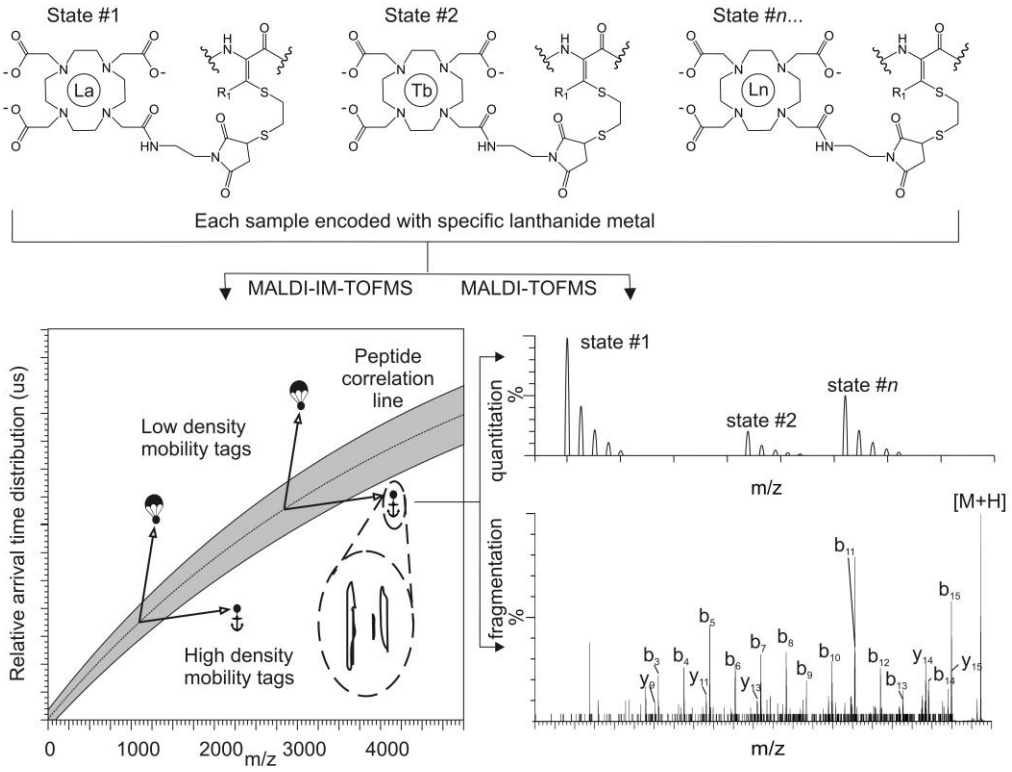

Figure 25. Labeling of multiple sample states with DOTA tags coordinated to different lanthanide metals. In this illustrative figure, a 5:1:2.5 may be encoded with different lanthanide metals and quantitated using either MALDI-IM-TOFMS or MALDI-TOFMS platforms. Thus, the number of simultaneous samples that can be combined for relative quantitation is limited only be the number of different metals (or metal isotopes) that are used. An added advantage to using this strategy and the MALDI-IM-TOFMS platform is rapid visual identification of labeled species for subsequent tandem MS analysis of the phosphorylation site.

4.3.1 Relative quantitation of phosphorylated peptides and proteins using PhECAT.

Varying molar amounts of phosphorylated peptides and proteins were derivatized and quantitated in proof-of-concept experiments. The results of these quantitation experiments are provided in Table 6. An example of a typical relative quantitation experiment using the MALDI-IM-MS platform is illustrated in Figure 26. In this experiment, labeled phosphorylated peptides are visually identified by their shift away from the peptide correlation line. A mass spectrum is extracted from the 2D plot using MassLynx Chromatogram software and relative peak area information is obtained (Figure 26, inset). In this example, a 1:5 molar ratio of Tb- and Ho-labeled FQpSEEQQQTEDELQDK is shown. In conjunction with fragmentation data, PhECAT strategies in IM-MS provide rapid identification and relative quantitation of the labeled peptide for characterization of phosphorylated peptides. Relative quantitation data and spectra for PhECAT strategies using MALDI-IM-TOFMS is provided in the Appendices of this work.

The reported error for this strategy is comparable to current isotope coded affinity labels, with the added advantages of larger shifts in mass doublets (*i.e*. 2-36 Da for single phosphorylation sites), allowing for quantitation of high-mass peptides without peak convolution from adjacent isotopes. For multiple phosphorylation sites, the mass difference scales with the number of the labels, which provides even greater separation. These results also indicate that this method has error competitive to current quantitative phosphoproteomic methods and should have utility in relative quantitative studies of complex biological samples. The utility of lanthanide ions as luminescent chromophores in

Table 6. Relative Quantitation of phosphorylated peptides and proteins using lanthanide-chelating tags in MALDI-IM-TOFMS.

Peptide Sequence[a,b]	$[M+H]^{+}$ [c]	$[M^{*}+H]^{+}$ Tb, Ho[d]	Molar ratio of derivatized peptides	Measured molar ratio of peptides derivatized with Ho-tag and Tb-tag (average # of trials) [e]	Relative Percent Error[f]
[48] FQ**pS**EEQQQTEDELQDK [63] from bovine B-casein	2060.7	2739.1‡, 2745.1‡	1.0: 5.0 (Ho:Tb)	0.172 (3)	+14.0
[48] FQ**pS**EEQQQTEDELQDK [63] from bovine B-casein	2060.7	2739.1‡, 2745.1‡	1.0: 1.0 (Tb:Ho)	1.159 (3)	+15.9
[48] FQ**pS**EEQQQTEDELQDK [63] from bovine B-casein	2060.7	2739.1‡, 2745.1‡	1.0: 5.0 (Tb:Ho)	0.293 (3)	+46.6
[48] FQ**pS**EEQQQTEDELQDK [63] from bovine B-casein	2060.7	2739.1‡, 2745.1‡	3.0: 1.0 (Ho:Tb)	2.341 (3)	-17.1
[48] FQ**pS**EEQQQTEDELQDK [63] from bovine B-casein	2060.7	2721.1‡, 2739.1‡, 2745.1‡	1.0: 1.0: 5.0 (Pr:Tb:Ho)	0.140, 0.130 (3)	-30.0,-35.0

a. "p" denotes phosphorylation, sequence positions bracket the sequence for tryptic peptides

b. Phosphorylated proteins purchased and used without additional purification.

c. Monoisotopic masses for unlabeled phosphorylated peptides.

d. Calculated monoisotopic peaks for labeled phosphorylated peptides. "*"denotes PhECAT labeling, "‡" denotes relative quantitation calculations where the peak having the highest relative abundance was selected for peak area quantitation rather than the monoisotopic peaks. This is primarily due to the fact that, here, the monoisotopic peak has the lowest intensity. In this case, the peaks of highest intensity (2741.1, 2747.1) were selected. $[M^{*}+H]^{+}$ of Pr, Tb, Ho where applicable.

e. 1.0: 1.0: 5.0 (Pr:Tb:Ho) relative ratios expressed as Pr:Ho and Tb:Ho, respectively.

f. 1.0: 1.0: 5.0 (Pr:Tb:Ho) relative ratios expressed as Pr:Ho and Tb:Ho, respectively. Percent errors are reported according to the following formula:

(Average Peak Area Ratio – Anticipated Peak Area Ratio) / Anticipated Peak Area Ratio

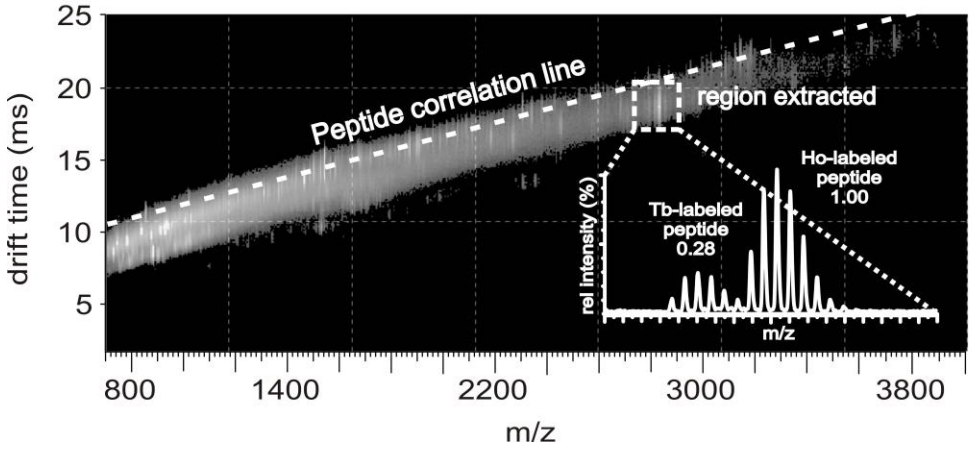

Figure 26. 2D IM-MS plot of derivatized tryptic beta-casein. The peptide mixture was first proteolytically digested with trypsin followed by selective labeling according to scheme 1. Unlabeled tryptic peaks establish the peptide correlation line, indicated by the dashed line. The phosphorylated peptide having the sequence FQpSEEQQQTEDELQDK was derivatized with Tb- and Ho-chelated labels in a 1:5 mixture and exhibit a structural shift below the peptide correlation line. (inset) Upon identification of labeled species, extraction of the relative peak areas of the labeled species provides quantitative information.

LC separations have been well described, and may increase confidence in phosphorylation site labeling at an additional stage of analysis. Moreover, the addition of a macrocycle may shift LC elution times for phosphorylated peptides, which may assist in separation of closely spaced phosphorylated and non-phosphorylated species.

4.3.2 Selection, fragmentation, and identification of the site of phosphorylation

PhECAT experiments performed using only MALDI-TOFMS as the analysis platform utilize anticipated mass shifts (*i.e.*, labeling with known lanthanides generates predictable mass multiplets which can be identified with quantitation software) to identify labeled quantitated species (data not shown). PhECAT experiments performed using MALDI-IM-TOFMS as the analytical platform take advantage of the high density of the PhECAT labels which result in a shift of labeled phosphorylated peptides away from the anticipated peptide correlation line, facilitating selection of phosphopeptides for fragmentation. PhECAT selection and fragmentation using MALDI-IM-TOFMS is demonstrated in Figure 27. Labeled peptides were first visually identified by their shift from peptide correlation space (Figure 27(i)) and selected for fragmentation in the transfer portion of the Synapt instrument. An example of a typical tandem spectrum is shown in Figure 27(ii). The expected b/y series ions were observed, including full b ion coverage from the b_3 to the b_{15} ion, all labeled and several unlabeled y ions including $y_{8\text{-}12}$, several labeled water loss ions, and the intact label with little evidence for fragmentation of the label. It should be noted that all fragment ions

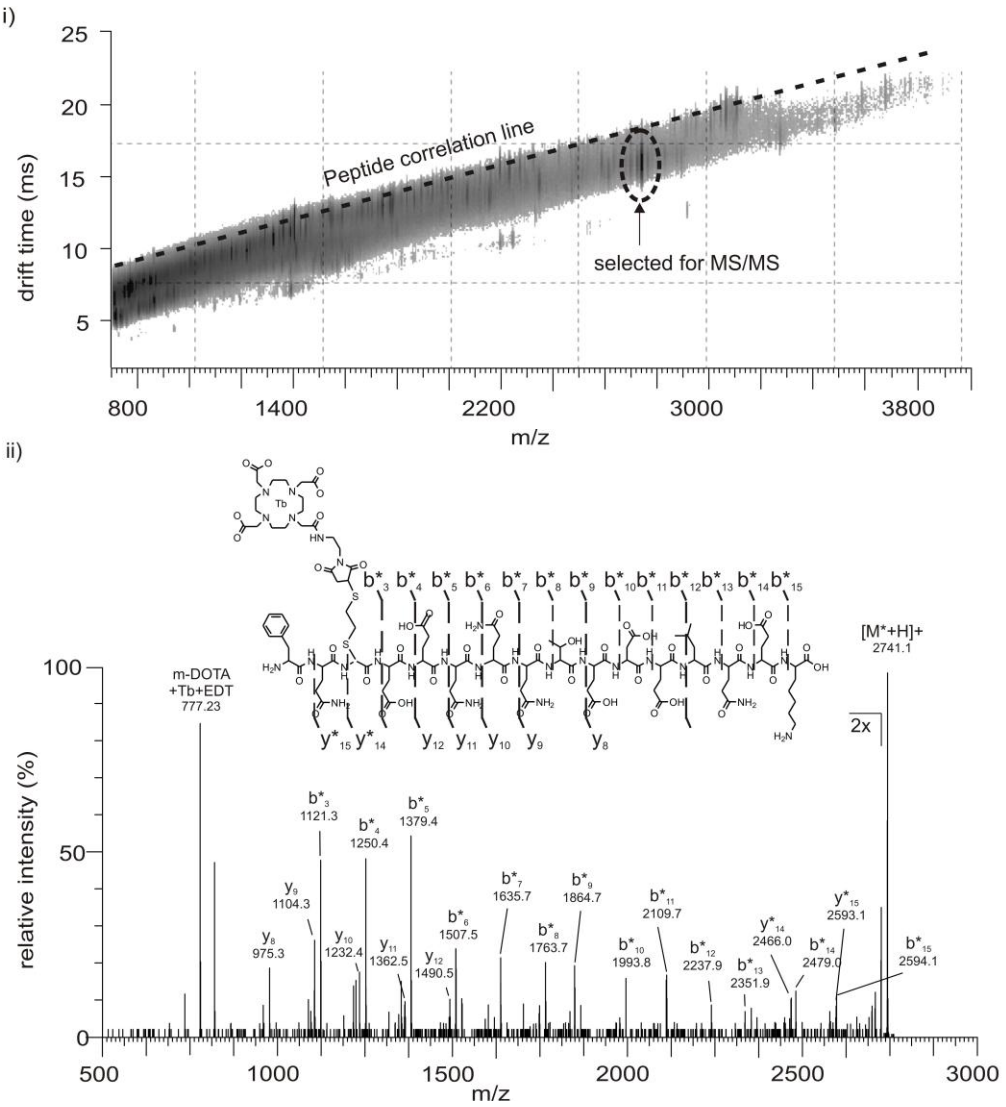

Figure 27. i) 2D IM-MS plot of derivatized tryptic beta-casein. Underivatized tryptic peaks establish the peptide correlation line, indicated by the dashed line. The signal corresponding to derivatized FQpSEEQQQTEDELQDK exhibits a negative deviation from the peptide correlation line, facilitating rapid identification prior to fragmentation. ii) Structure and fragmentation spectrum of a terbium-labeled tryptic beta-casein phosphorylated peptide having the sequence FQpSEEQQQTEDELQDK. An asterisk indicates that the ion is covalently modified with the PhECAT label. Fragmentation coverage of 86.7% and 46.7% of the labeled peptide was observed for b and y ions, respectively. Fragmentation coverage of 66.7% and 26.7% for the labeled peptide was observed for b and y water loss ions, respectively (an anticipated peak list and additional spectra from replicate experiments are provided in the supplementary material). Importantly, all of the anticipated ions corresponding to labeled positions are observed, demonstrating the utility of this label for phosphopeptide site identification as well as relative quantitation. It should also be noted that labeled fragment ion species exhibit greater intensity than non-labeled fragment ion species. Spectral peaks

from 500 m/z to 2600 m/z were intensified 2x to increase visibility of b and y spectral assignments.

covalently bound to the PhECAT label exhibit higher intensities than unlabeled fragment ions. The stability of this label enables predictable mass shifts of anticipated b and y ions which gives an indication of the site of modification previously phosphorylated.[44] Furthermore, because this tag is not labile and does not show phosphorylation site rearrangement (as is the case with phosphoric acid and phosphate plus water loss), it has an added advantage of more confident phosphorylation site assignment. Thus, complete phosphoproteomic characterization is accomplished using a single strategy.

4.4 Conclusions

Current methods of MS-based protein quantitation primarily focus on quantifying relative expression profiles through labeling non-post-translationally modified peptides. This offers a limited view of the biological activity of cells, because many biological functions are dependent on protein modifications, specifically, protein phosphorylation. The available methods for phosphoprotein quantitation provide good specificity for the site of phosphorylation, however, they have limited applicability for peptides of increasing mass and are seldom used for phosphorylation site identification. In this work, we have demonstrated the utility of lanthanide-based labels for phosphopeptides and proteins (PhECAT) for relative quantitation of phosphorylated peptides using MALDI-MS and as mobility shift labels using MALDI-IM-MS for rapid visual identification and subsequent quantitative and site analysis. We propose that this method may circumvent challenges encountered by quantitation and site localization, such as gas-phase phosphorylation site rearrangement, with the added utilities described above.

4.5 Acknowledgements

I would like to thank Dr. Thomas J. Kerr, Ms. Katie Dextraze (Georgia Institute of Technology), Dr. Larissa S. Fenn, Mr. Michal Kliman, and Dr. Brian Huffman for assistance in the initial stages of this work. Financial assistance for this work was provided by the Vanderbilt University College of Arts and Sciences, the Vanderbilt Institute for Chemical Biology (Pilot Project Grant), the Vanderbilt Institute for Integrative Biosystems Research and Education, and the American Society for Mass Spectrometry (Research Award to JAM).

CHAPTER 5

ENHANCED SEPARATION AND CHARACTERIZATION OF GLYCOSYLATED PROTEINS USING LANTHANIDE-BASED LABELING AND ION MOBILITY-MASS SPECTROMETRY

5.1 Introduction

Much like protein phosphorylation, protein glycosylation regulates numerous biological processes such as cell signaling, recognition, differentiation, and proliferation and is often observed to dynamically occupy the same sequence position that harbors phosphorylation as part of an ON/OFF switch in biological systems.[28] Thus, the stoichiometry between phosphorylation and glycosylation is significant for a complete understanding of a phosphorylated protein's role in a system. As with any PTM characterization, elucidation of the site of modification is critical to better understand the nature of modification-dependent protein function and to design and optimize protocol to quantify and structurally characterize the site of modification. Elucidation of the site of glycosylation is challenging for similar reasons as phosphorylation localization, namely – i) glycans are labile, and either beta-eliminate readily or fragment easily in MS ion sources and collision cells, ii) these labile modifications predominate in MS/MS spectra, as the bulk of fragmentation occurs at the site of modification confounding MS sequencing attempts, and iii) due to the temporal nature of the modification, only substoichiometric amounts are available and create difficulties in detection of the modification.

Application of the previously described lanthanide-based labeling strategies may provide relative quantitation information for glycosylated peptides

as well as phosphorylation occupation versus glycosylation occupation. Furthermore, by modifying the site of glycosylation prior to analysis, the labile glycosylation site is converted to a stable covalently bound label, which may circumvent challenges associated with glycosylation site identification. Moreover, removal of glycans through beta-elimination is routinely performed in glycan structural analysis, and this chemistry is compatible with structural analysis of glycans.

In this chapter, PhECAT strategies are applied toward the challenge of glycan site quantitation. In this benchmarking report, labeling of a glycosylated peptide from erythropoietin is demonstrated. In a manner similar to previously discussed, glycosylated tryptic peptides are selectively modified at the glycosylation site via beta-elimination/anionic thiol Michael addition chemistry. Thus, glycosylated peptides are converted to cysteine-like residues, which then readily react with cysteine-specific labels. This lanthanide-chelating label is added via maleimide chemistry and selected lanthanide metals are subsequently chelated to a macrocycle moiety.

5.2 Experimental

5.2.1 Materials

Model glycosylated peptides were investigated for proof-of-concept experiments. Glycosylated erythropoietin was purchased from Anaspec (Freemont, CA). Adrenocorticotropic hormone (ACTH) peptide clips 18-39, 1-17, and 7-38 were purchased from American Peptide (Sunnyvale, CA) and used without further purification. Polyacrylamide gel columns were purchased from Thermo (San Jose, CA). C-18 spin columns were purchased from Pierce

(Rockford, IL). Maleimido-mono-amide-DOTA was purchased from Macrocyclics (Dallas, TX) and dissolved in DMSO. 1,2-ethanedithiol (EDT) was purchased from Fluka (St. Gallen, Switzerland). 2,5-dihydroxybenzoic acid (DHB) was purchased from Sigma and dissolved in 50% methanol to a final concentration of 30 mg/mL. Lanthanide (in $LnCl_3$ form) metals were purchased from Strem Chemicals (Newburyport, MA) in chloride salt form and dissolved in distilled deionized water (18 MΩ cm^{-1}) to a final concentration of 25 mg/mL. Dimethylsulfoxide, acetonitrile, and ethanol were purchased from Sigma.

5.2.2 Selective derivatization of glycosylated peptides and proteins using lanthanide-based labeling strategies

Glycosylated erythropoietin peptide (sequence EAISPPDAAS*AAPLR, where * denotes glycosylation of serine) was subjected to a beta-elimination (Figure 28(i)) and anionic thiol Michael addition[35] reaction (Figure 28(ii)) resulting in the selective elimination of phosphoric acid followed by addition of ethanedithiol. In this reaction, each sample was derivatized in a reaction mixture containing 2.5 mM EDTA, 0.2 M ethanedithiol, 0.5 M NaOH, 1.5 M acetonitrile, 1.5 M ethanol, 5 M DMSO, and water for 2-3 hrs under nitrogen at 55ºC in a manner similar to reaction conditions described previously.[36-38] This resulted in conversion of O-GlnAc-modified serine and threonine into dehydroalanine or dehydroaminobutyric acid, respectively. The samples were then neutralized and purified by polyacrylamide 1800 desalting gel (Thermo) and reaction completion was confirmed by MALDI-TOFMS. Subsequently, the thiolated peptides were labeled with a 10-fold excess of maleimido-DOTA (Figure 28 (iii)) in a mixture containing acetate buffer (pH 5.5) and DMSO in 1:1 ratio (v/v), resulting in a

covalent bond between the free sulfhydryl group and the maleimide portion of the lanthanide-based tag. Finally, selected lanthanide

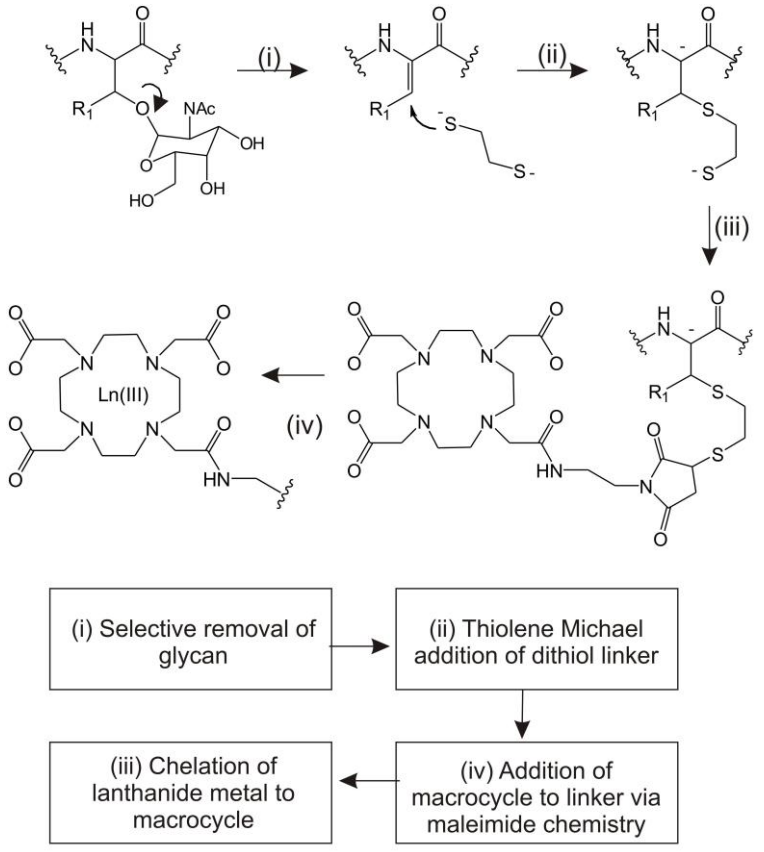

Figure 28. Reaction scheme for using PhECAT for O-linked glycans (i) O-linked glycans are removed via beta-elimination in basic conditions, generating a conjugated diene (ii) Ethanedithiol is subsequently added to the conjugated diene via anionic thiol Michael addition (iii) The remaining free thiol is attached to the macrocylic via maleimide chemistry (iv) Finally, samples are encoded by chelating lanthanides to the macrocyclic portion of the tag.

metals were chelated to the maleimide portion of the tag by adding a 100-fold molar excess of metal to peptide and heating to 80ºC to speed up chelation for 45 minutes (Figure 28(iv)).[39] Differentially labeled samples were then combined and purified by C-18 spin columns and analyzed using MALDI-IM-TOFMS.

5.2.3 Instrumentation and data analysis

Spectra were obtained using a Voyager MALDI-TOFMS in positive, reflector mode. MALDI matrix preparation consisted of 2,5-dihydroxybenzoic acid (DHB) in 50% methanol. The samples were spotted using the dried-droplet method.[40] Data analysis was performed using Data Explorer software version 4.3 (Applied Biosystems, Foster City, CA). At least 3 trials were analyzed for each relative quantitation experiment. Spectra were acquired by rastering the MALDI laser at random over the entire matrix spot.

Peaks were identified manually and quantitation spectra were processed using the baseline correction, noise filter/smooth, and centroiding processing tools of Data Explorer.

5.3 Results and Discussion

Here, we report successful labeling of a glycosylated peptide with lanthanide-based labels, termed “PhECAT” when used to characterize phosphorylated peptides. Lanthanide-based labeling of glycosylation sites circumvents challenges associated with the lability of the modification and provides quantitative information and selective separation of glycosylated peptides from concomitants. The stoichiometry of glycosylation vs. phosphorylation occupation may be elucidated with a selective purification

strategy outlined in Figure 29 prior to lanthanide encoding. In this proposed strategy, a glycosylated and phosphorylated protein mixture is digested before being subjected to antibody purification and divided out into two samples of phosphopeptides and glycopeptides. Each sample is then derivatized and encoded with a specific lanthanide and characterized by MS. If structural information is desired, the beta-elimination step of the labeling may be used to release the glycans for subsequent structural analysis. Simultaneous glycomics and proteomics has been reported in our group and can be applied toward comprehensive glycoproteomics as well.[70]

Preliminary data demonstrating the labeling of glycosylated peptides is presented in Figure 30. The GlcNAc-modified peptide was derivatized using beta-elimination/Michael addition chemistry followed by maleimide and lanthanide chelation chemistry as used previously for the derivatization of phosphorylated peptides. Erythropoietin (EAISPPDAAS*AAPLR, where * denotes glycosylation of serine) was derivatized in a 1:1 mixture of Tb to Ho-labeled peptides. A peptide mixture containing ACTH peptides was spiked into the sample to establish the underivatized peptide correlation line in IM-MS 2D conformation space (Figure 30, top). One sample was quantitated so that application of this strategy resembled characterization of an unknown biological sample, which is frequently limited in concentration. Labeled erythropoietin signal was identified by its negative deviation from the established peptide correlation line and mass spectra were subsequently extracted for quantitative information (Figure 30, bottom). Table 7 presents the results from this single quantitation experiment. Extracted mass spectra and quantitation raw data are provided in the Appendices. The relative percent error associated with this experiment was

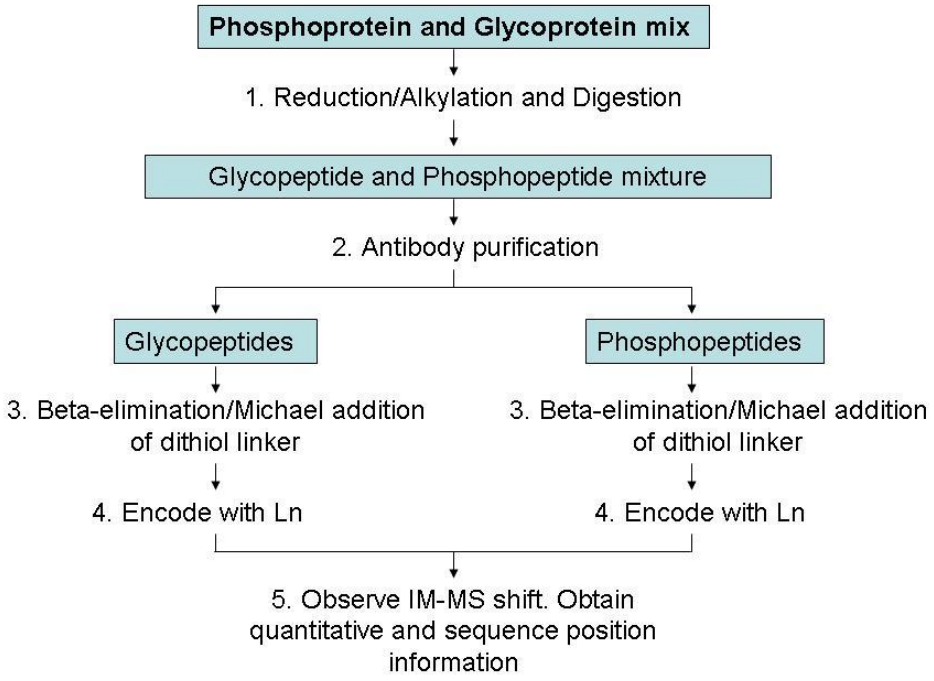

Figure 29. Proposed strategy for the selective separation, site identification, and relative quantitation of glycosylated and phosphorylated peptides and proteins.

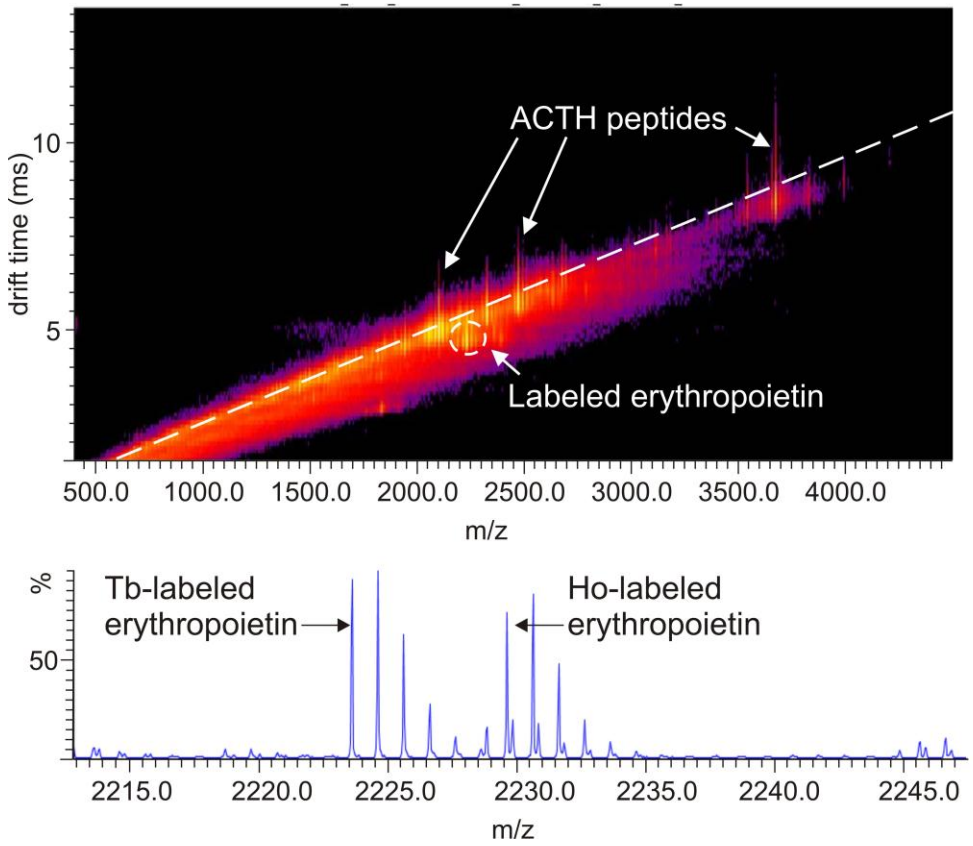

Figure 30. (top) O-GlcNAc-modified peptides are labeled by lanthanide-based labels and separated from a complex peptide mixture. The labeled peptide is indicated in a dashed circle. Underivatized ACTH clips 1-17, 7-38, and 18-39 are spiked in to the sample to establish the peptide correlation line and guide the eye for visual identification of labeled species. Peptide correlation line is indicated by a dashed line. (bottom) Extracted and zoomed mass spectra of Tb- and Ho-encoded erythropoietin. Here, a 1:1 mixture was quantitated. Normalized observed peak areas for this acquisition were 1.0 to 0.89.

Table 7. Relative Quantitation of O-GlcNAc modified peptide erythropoietin using lanthanide-chelating tags in MALDI-IM-TOFMS.

Peptide Sequence[a]	$[M+H]^{+}$ [b]	$[M^{*}+H]^{+}$ Tb, Ho[c]	Molar ratio of derivatized peptides	Measured molar ratio of peptides derivatized with Ho-tag and Tb-tag (average # of trials) [d]	Relative Percent Error[e]
^{117}EAISPPDAA**S**AAPLR ^{131} human	1670.7	2223.7‡, 2229.7‡	1.0: 1.0 (Tb:Ho)	0.833 (1)	-17.0

a. Bold denotes site of O-GlcNAc modification, sequence position indicated

b. Monoisotopic masses for unlabeled peptide.

c. Calculated monoisotopic peaks for labeled peptide. "*"denotes PhECAT labeling, "‡" denotes relative quantitation calculations where the peak having the highest relative abundance was selected for peak area quantitation rather than the monoisotopic peaks. This is primarily due to the fact that, here, the monoisotopic peak has the lowest intensity.

d. One sample was rastered 10 times and the result was averaged.

d. Percent errors are reported according to the following formula:

(Average Peak Area Ratio – Anticipated Peak Area Ratio) / Anticipated Peak Area Ratio

found to be 17%, which is comparable to current isotopologue quantitation strategies. It should also be noted that these isotopologue quantitation strategies are generally not demonstrated for PTMs and particularly not demonstrated as quantitative strategies between two PTMs occupying the same site of modification.

5.4 Conclusions

Glycosylation and phosphorylation have been shown to occupy the same site of modification in a number of cases, and switching modifications has been shown to be a critical regulatory mechanism for a number of cellular functions. Characterization of glycopeptides provides a more complete picture of a picture of the resident modification, and quantitation of phosphorylated vs. glycosylated species may provide a better understanding of the mechanisms controlled by modification switching. A 1:1 molar mixture of O-GlcNAc-modified peptide erythropoietin was quantitated using Tb- and Ho-chelated labels. In this initial experiment, performed with a single sample in the manner expected for unknown samples, the relative percent error was calculated to be 17%, which is comparable to current quantitative experiments that do not profile glycosylation stoichiometry. Moreover, labeled glycosylated species were visually identified by their negative deviation from the peptide correlation in 2D IM-MS conformation space, illustrating the additional advantage of lanthanide-based labeling for IM separations.

5.5 Acknowledgments

I would like to acknowledge Larissa S. Fenn for her assistance with setting up the experiments. This work was supported by the Vanderbilt University College of Arts and Sciences, the Vanderbilt Institute for Chemical Biology, the Vanderbilt Institute of Integrative Biosystems Research and Education, the American Society for Mass Spectrometry (Research Award to J.A.M.).

CHAPTER 6

CONCLUSIONS AND FUTURE DIRECTIONS

6.1 Summary and conclusions

The primary aim of this dissertation research was to simplify characterization of phosphorylated and glycosylated peptides and proteins. These post-translational modifications have profound significance in molecular biology and understanding the mechanisms of disease.

Complete phosphoproteomic characterization is accomplished through elucidating the site of phosphorylation and its stoichiometry. These are typically performed in separate experiments, and each determination has demonstrated challenges. Site identification by data-dependent tandem MS is often confounded by phosphorylation site rearrangement, HPLC co-elution, and heterogeneous phosphorylation. Quantitation between two states is typically accomplished using isotopologue labeling and subsequent MS analysis, which provides limited mass shift and requires high resolution instrumentation. These challenges are described in detail in Chapters 1 and 2. Chapters 3 and 4 address these challenges using lanthanide-based labeling. Chapter 4 introduces the utility of ion mobility-mass spectrometry separations and the use of these labels as mobility shift reagents for rapid visual identification of labeled ions. Lanthanide-based tagging provides increased mass separation to quantitate peptides of increasing mass and also provides separation from concomitant species in IM-MS conformation space so that site identification is more easily achieved. Together,

these strategies provide comprehensive phosphoproteomic characterization. This was demonstrated in a benchmarking experiment using the model phosphorylated protein, bovine beta-casein. In Chapter 3, the quantitative advantages of lanthanide-based labeling were first explored. Error comparable to current isotopologue strategies (including those that do not label phosphopeptides) was achieved. Moreover, fragmentation of labeled species indicated that derivatization of the phosphorylation site produced a more stable modification in which to identify the site of phosphorylation. In Chapter 4, the additional utility of lanthanide-based labeling as mobility shift tags for separation from unphosphorylated peptides in IM-MS conformation space was explored. Lanthanide tags provided sufficient mobility and mass shift to successfully separate phosphorylated peptides away from the anticipated peptide conformation space, facilitating further characterization without concomitant contamination.

A number of reports have described a dynamic “ON/OFF” switching of phosphorylation sites with glycosylation. Thus, contemporary phosphoproteomics must incorporate glycoproteomic identification and quantitation. Contemporary glycoproteomic characterization includes identification of the site of modification and determination of the glycan’s stoichiometry. Glycoproteomic characterization entails the same challenges as phosphoproteomic characterization. Lanthanide-based labeling and IM-MS separations for selective separation may circumvent these challenges and moreover provide quantitative information. This is discussed in detail in Chapter 5. In this experiment, a O-GlcNAc-modified peptide, human erythropoietin, was labeled and visually identified by its negative deviation form the peptide correlation line in 2D conformation space.

Furthermore, a 1:1 molar ratio of Tb- to Ho-labeled sample was quantitated with comparable error to current isotopologue-based quantitation strategies.

6.2 Future directions

6.2.1 Custom labels for labeling and ionization efficiency

Through these studies, significant progress was made in developing a simplified, comprehensive strategy for multiplexed characterization of phosphorylated and glycosylated peptides and proteins, but there are many opportunities for further research. Our laboratory is presently pursuing a number of custom labels that further enhance the ionization efficiency of the label and that accommodate single reaction, or “one-pot,” phosphoproteomic labeling.

One label that was conceptualized in our laboratory, illustrated in Figure 30a, contains an arginine residue, which through labeling substitutes the negatively charged phosphorylation or glycosylation residue for a positively charged residue. This is especially advantageous to improve ionization efficiency and to enhance detection of phosphopeptides or glycopeptides for relative quantitation strategies. Another label envisioned, illustrated in Figure 30b, contains a DOTA macrocycle and a reactive thiol replacing the maleimide. Using this label, phosphopeptides may be labeled without a dithiol linker, reducing reaction time and desalting steps required when converting the phosphorylation site to a thiol-terminated residue. Reducing desalting and chromatographic steps in phosphoproteomic labeling reduces losses associated with each process, and can potentially improve the overall limit of detection of the method.

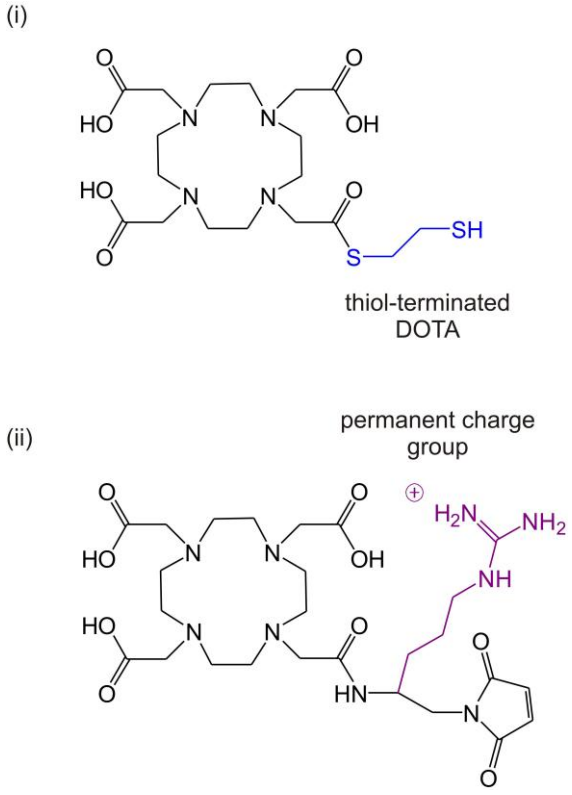

Figure 31. Custom labels that may provided added utility to the overall labeling strategy. i) Thiol-terminated labels circumvent sample losses associated with chromatography cleanup of the intermediate labeling steps. ii) Lanthanide-based labels that contain an arginine or other positive charges may enhance signal from substoichiometric modifications and enhance phosphoproteomic characterization.

6.2.2 Mobility shift labeling for selective separation and structural analysis of glycosylated peptides

Another avenue envisioned for future research is the use of mobility shift "balloon" labels for structural analysis of glycans, illustrated in detail in Chapter 1. Although lanthanide-based labeling provides quantitative and site identification information of the glycan, structural information is lost. A number of biological processes are highly dependent on glycan structure and the composition of terminal saccharides on the glycan.[3, 4, 8, 33-35, 37, 108-110] Thus, this information is of critical importance to comprehensive glycoproteomics.

The potential for balloon mobility shift labeling of post-translationally modified peptides in IM-MS has not been explored. Due to the curvature of each biomolecular class, mobility shift separation experiments must be tuned to the target biomolecule class to achieve maximum separation. For underivatized glycosylated peptides and proteins, mobility shift strategies that place labeled glycopeptides signals above the carbohydrate/protein correlation line may provide the optimal separation for rapid visual identification and further characterization. Characteristics of "balloon" shift reagents include labels with high surface area and low mass such that surface area scales disproportionately with mass.

Addition of a balloon mobility shift reagent may provide enhanced separation of a glycosylated peptide having a labeled terminal group from its isobaric counterparts. This separation also provides added utility by reducing concomitant species fragmented in structural elucidation. Moreover, O-GlcNAc-modified peptides separated by labeling strategies may be selected for fragmentation to obtain structural information on the glycan.

6.2.3 Relative quantitation of dynamic interchange between protein phosphorylation and protein glycosylation

Lanthanide-based quantitative mobility-shift labeling may also be applied toward characterization between PTM states such as glycosylation vs. phosphorylation states. As mentioned previously, glycosylation and phosphorylation are known to occupy the same sequence position, and dynamic regulation between the modifications are known to control signaling functions of the cell. A strategy for glyco/phospho quantitation is illustrated in figure 29 in Chapter 5.

APPENDIX A

Supplementary Information for Mass Spectrometry Data Acquisition according to MIAPE-MS format.

General Features

Global Descriptors

Dates obtained can be found in the file names behind "sh_RG_1270_" or "sh_RG_1368_."

These samples were processed and analyzed by the Vanderbilt Proteomics Core.

Contact info: Hayes McDonald – Assistant Director
Email: hayes.mcdonald@Vanderbilt.Edu
Contact info: Salisha Hill – Laboratory Technician
Email: salisha.sobratee@vanderbilt.edu
Phone: (615) 343-7334

Instrument Manufacturer and Model :

LTQMS : ThermoFinnigan LTQ LC-MS-MS
LTQ-Orbitrap : Thermo Scientific LTQ XL™
Customizations : none

Control and Analysis Software :

Software Name and Version: Thermo Xcalibur 1.3 and Bioworks 3.1 software

Switching criteria: available in supplementary raw MS files

Isolation Width: 2.00

Ion Sources: Electrospray Ionisation (ESI): Instrumental, source, and tune parameter settings are available in the raw data files provided at the following url: http://www.mc.vanderbilt.edu/msrc/bioinformatics/data.php or at the following link: https://proteomecommons.org/tranche/data-downloader.jsp?fileName=ZEb8WJQd75%2Fi4%2FPOlusCyfWI7czMK%2BUT3kcIGy8P6caR3iYgUJdGR958BvUpwYS8v6Q56Pe1eiGKjK5H2Y8L%2FYG%2FA3kAAAAAAAAEDg%3D%3D

Post-Source Component:

Ion Trap Final MS Stage Achieved: MS^3

APPENDIX B

Table of initial APPL1 phosphorylation site identifications by LTQ-MS and reasons for acceptance or rejection.

LTQ-MS/MS DATA						
Sequence	position	X-corr	z	mh	MS_3	comments
F.SKVIDELSS@CHAVL.S	90-103	2.49	2	1580.77	NO	Top 3 ions don't match prospector output, losses
Y.IFESNNEGEKICDS@VGLAKQIAL.H	605-627	**4.10**	3	2558.25	NO	Top 4 out of 10 ions don't match prospector output
F.DIIS@PVC*EDQPGQAKAF.G	456-472	**3.76**	2	1954.93	YES	Triggered MS3, top ions match prospector output
F.DIIS@PVC*EDQPGQAKAF.G	456-472	**3.85**	2	1954.93	YES	Top ions match prospector output
E.GQFVVLSSS@QSEESDLGEGGKKRE.S	683-706	**4.62**	3	2633.24	YES	Triggered MS3, top ions match prospector output
E.GQFVVLSSS@QSEESDLGEGGKKRE.S	683-706	**5.53**	3	2633.24	----	Replicate of previously confirmed assignment.
E.GQFVVLSSSQS@EES@DLGEGGKKRE.S	683-706	4.40	3	2713.24	YES	Top ions match prospector output. Some ambiguity of site assignment. Reasonably confident.
E.GQFVVLSSS@QSEESDLGEGGKKRE.S	683-706	5.38	3	2633.24	----	Replicate of previously confirmed assignment.
E.GQFVVLSSS@QSEESDLGEGGKKRE.S	683-706	5.03	3	2633.24	----	Replicate of previously confirmed assignment.
E.GQFVVLSSSQS@EESDLGEGGKKRE.S	683-706	3.23	3	2633.24	NO	No neutral loss, some mismatched assignments, sites of phosphorylation not bracketed.
Q.IY@LS@ENPEETAARVNQSALE.A	377-396	2.19	2	2394.09	YES	Top 6 of 10 ions don't correspond to b ions, y ions or any losses of b and y ions.
E.GQFVVLSSSQS@EESDLGEGGKKRE.S	683-706	4.52	3	2633.24	YES	Ions bracketing sites not confident.
A.AS@S@RPNQASSEGQFVVLSSSQSEESDLGEGGKKRE.S	672-706	3.27	3	3827.74	NO	Proposed phosphorylation sites not bracketed
R.LIAASSRPNQASSEGQFVVLS@SSQSEESDLGEGGK.K	669-703	6.32	3	3631.71	YES	Top ions match prospector output. Some ambiguity of site assignment. Reasonably confident.
R.VIDELSS@CHAVLSTQLADAMMFPITQFK.E	92-119	5.56	3	3175.53	NO	Top ions match prospector output. Some ambiguity of site assignment. Reasonably confident.
R.LIAASSRPNQASSEGQFVVLS@SSQSEESDLGEGGK.K	669-703	5.86	3	3631.71	----	Replicate of previously confirmed assignment.
K.MGS@ENLNEQLEEFLANIGTSVQNVR.R	213-237	3.46	3	2872.35	NO	Top ions don't match prospector output.
R.LIAASSRPNQASSEGQFVVLS@SSQSE	669-703	5.94	3	3631.71	---	Replicate of previously confirmed assignment.

ESDLGEGGK.K						
R.TNPFGESGGSTKS@ETEDSILHQLFIVR.F	479-505	3.85	3	3029.46	YES	Top ions above 1000m/z match
R.LIAASSRPNQASSEGQFVVLS@SSQSEESDLGEGGK.K	669-703	4.88	3	3631.71	----	Replicate of previously confirmed assignment.
R.LIAASSRPNQASSEGQFVVLS@SSQSEESDLGEGGK.K	669-703	6.11	3	3631.71	----	Replicate of previously confirmed assignment.
R.SESNLSSVCY@IFESNNEGEK.I	595-614	4.14	3	2315.97	NO	Top ions match prospector output. Some ambiguity of site assignment. Reasonably confident.
R.LIAASSRPNQASSEGQFVVLS@SSQSEESDLGEGGK.K	669-703	5.99	3	3631.71	----	Replicate of previously confirmed assignment.
R.LIAASSRPNQASSEGQFVVLS@SSQSEESDLGEGGK.K	669-703	5.46	3	3631.71	----	Replicate of previously confirmed assignment.
R.LIAASSRPNQASSEGQFVVLS@SSQSEESDLGEGGK.K	669-703	5.99	3	3631.71	----	Replicate of previously confirmed assignment.
R.LIAASSRPNQASSEGQFVVLS@SSQSEESDLGEGGK.K	669-703	5.52	3	3631.71	----	Replicate of previously confirmed assignment.
R.SESNLSS@VCYIFESNNEGEK.I	595-614	3.00	3	2315.97		Ions do not bracket site of phosphorylation. Numerous mismatches.
R.LIAASSRPNQASSEGQFVVLS@SSQSEESDLGEGGK.K	669-703	4.37	3	3631.71	----	Replicate of previously confirmed assignment.
R.LIAASSRPNQASSEGQFVVLS@SSQSEESDLGEGGK.K	669-703	6.12	3	3631.71	----	Replicate of previously confirmed assignment.
R.SESNLSSVCY@IFESNNEGEK.I	595-614	3.15	2	2315.97	NO	Top ions match prospector output. Some ambiguity of site assignment. Reasonably confident.
R.VNQSALEAVTPS@PSFQQR.H	390-407	4.95	2	2038.99	NO	Top ions match prospector output. Some ambiguity of site assignment. Reasonably confident.
R.SESNLSSVCY@IFESNNEGEK.I	595-614	4.75	2	2315.97	NO	Numerous low intensity peaks do not match.
K.QIY@LSENPEETAAR.V	376-389	3.65	2	1700.79	NO	Top ions match prospector output.
R.LIAASSRPNQASSEGQFVVLS@SSQSEESDLGEGGK.K	669-703	4.05	3	3631.71	**----**	Replicate of previously confirmed assignment.

APPENDIX C

Table of initial APPL1 phosphorylation site identifications by LTQ-Orbitrap-MS and reasons for acceptance or rejection.

LTQ-ORBITRAP-MS/MS DATA	Pos-ition	X corr	ppm	MS3 triggered	Conf-irmed	comments
Q.SRPPTARTSS@SGS@LGSESTNL.A	418-438	2.52	0.93	YES	YES	Ions bracket site of phosphorylation, reasonably confident but some ambiguity of exact site.
A.AGQSRPPTARTSS@SGSLGSESTNL.A	415-438	2.68	-0.62	NO	YES	Bracket site of phosphorylation and appear to support site assignment.
L.SLDSLVAPDTPIQFDIIS@PVC*EDQPGQAKAF.G	442-472	4.43	0.87	NO	NO	Numerous unassigned peaks.
D.TPIQFDIIS@PVC*EDQPGQAKAF.G	451-472	4.36	-0.08	YES	YES	Confident assignments, site bracketed, neutral loss observed.
W.IC*TINNIS@KQIYLSENPEETAARVNQSAL.E	367-395	4.77	3.30	NO	YES	Ions bracket site of phosphorylation, reasonably confident but some ambiguity of exact site.
Q.SRPPTARTSSSGS@LGSESTNL.A	418-438	2.97	1.10	YES	YES	Confident assignments, site bracketed, neutral loss observed.
D.SLVAPDTPIQFDIIS@PVC*EDQPGQAKAF.G	445-472	4.65	-0.77	NO	NO	Some mismatched peaks, no neutral loss observed, site uncertain.
F.DIIS@PVC*EDQPGQAKAF.G	456-472	3.55	0.82	YES	NO	Can't confirm charge state by precursor peaks.
D.IIS@PVC*EDQPGQAKAF.G	457-472	3.2	0.33	YES	YES	Confident assignments, site bracketed, neutral loss observed.
E.GQFVVLSSSQS@EESDLGEGGKKRE.S	683-706	4.92	383.76	YES	NO	Parts per million error too large.
E.GQFVVLSSSQS@EESDLGEGGKKRE.S	683-706	4.04	11.61	NO	YES	Ions bracket site of phosphorylation, reasonably confident but some ambiguity of exact site.
A.AS@S@RPNQASSEGQFVVLSSSQSEESDLGEGGKKRE.S	672-706	3.8	435.00	NO	NO	Parts per million error too large.
E.GQFVVLSSSQS@EESDLGEGGKKRE.S	683-706	5.16	0.91	YES	YES	Confident assignments, site bracketed, neutral loss observed.
I.AASSRPNQASS@EGQFVVLSSSQSEESDLGEGGKKRE.S	671-706	3.44	292.72	NO	NO	Parts per million error too large.
E.GQFVVLSSS@QSEESDLG	683-	5.93	-0.23	NO	YES	Ions bracket site of

EGGKKRE.S	706					phosphorylation, reasonably confident but some ambiguity of exact site.
E.GQFVVLSSS@QSEESDLG EGGKKRE.S	683-706	4.08	2.28	YES	YES	Replicate of previously confirmed assignment.
E.GQFVVLSSSQS@EESDLG EGGKKRESE.A	683-708	4.45	5.58	YES	YES	Replicate of previously confirmed assignment.
F.VVLSSSQS@EES@DLGEG GKKRE.S	686-706	2.83	-4.53	YES	YES	Confident assignments, site bracketed, neutral loss observed.
G.QFVVLS@S@S@QSEESDLG EGGKKRE.S	684-706	3.41	-858.54	NO	NO	Parts per million error too large.
E.GEKICDS@VGLAKQIALHAE.L	612-630	3.65		YES	NO	Isotopic overlap of potential precursor peaks confounds precursor assignment.
E.GQFVVLSSSQS@EESDLGEG GKKRE.S	683-706	4.75	378.98	NO	NO	Parts per million error too large.
A.AS@S@RPNQASSEGQFVVL SSSQSEESDL GEGGKKRE.S	672-706	3.96	445.65	NO	NO	Parts per million error too large.
E.GQFVVLSSSQS@EESDLGEG GKKRE.S	683-706	5.66	0.23	YES	----	Replicate of previously confirmed assignment.
F.VVLSSS@QSEESDLGEGGKK RE.S	686-706	2.9	-2.34	YES	YES	Ions bracket site of phosphorylation, reasonably confident but some ambiguity of exact site.
P.NQAS@S@EGQFVVLSSSQS EESDLGEGGKKRE.S	677-706	3.73	516.98	NO	NO	Parts per million error too large.
R.LIAASSRPNQASSEGQFVVL S@SSQSEESDLGEGGK.K	669-703	6.99	-7.93	YES	YES	Ions bracket site of phosphorylation, reasonably confident but some ambiguity of exact site.
R.SESNLSSVCY@IFESNNEG EK.I	595-614	4.08	-415.58	NO	NO	Parts per million error too large.
R.TSSSGS@LGSESTNLAAL SLDSLVAPDTPIQFDIISPVC* EDQPGQAK.A	425-470	4.68	210.77	NO	NO	Parts per million error too large.
R.TNPFGESGGSTKS@ETE DSILHQLFIVR.F	479-505	4.67		YES	NO	Isotopic overlap of potential precursor peaks confounds precursor assignment.
R.SESNLSSVCY@IFESNNE GEK.I	595-614	4.49	-836.53	NO	NO	Precursor peak not readily evident, error too large.
R.LIAASSRPNQASSEGQFV VLS@SSQSEESDLGEGGK.K	669-703	5.17		NO	NO	Isotopic overlap of potential precursor peaks confounds precursor assignment.
R.LIAASSRPNQASSEGQFV VLS@SSQSEESDLGEGGK.K	669-703	7.16	277.49	NO	NO	Parts per million error too large.

K.DHEEWICT@INNISK.Q	362-375	3.02	-533.48	NO	NO	Parts per million error too large.
R.LIAASSRPNQASSEGQFVVLS@SSQSEESDLGEGGK.K	669-703	6.88	3.96	YES	Yes	Replicate, good parts per million error.
R.LIAASSRPNQASSEGQFVVLS@SSQSEESDLGEGGK.K	669-703	7.54	5.28	NO	----------	Replicate of previously confirmed assignment.
R.LIAASSRPNQASSEGQFVVLS@SSQSEESDLGEGGK.K	669-703	5.13		NO	NO	Isotopic overlap of potential precursor peaks confounds precursor assignment.
K.MGS@ENLNEQLEEFLANIGTSVQNVR.R	213-237	4.6		YES	NO	Isotopic overlap of potential precursor peaks confounds precursor assignment.
R.VNQSALEAVTPS@PSFQQR.H	390-407	3.92	-2.45	NO	YES	Some bracketing of assignments, error within confident range, ambiguity of exact phosphorylation sites.
R.LIAASSRPNQASSEGQFVVLS@SSQSEESDLGEGGK.K	669-703	5.15	0.50	NO	----------	Replicate of previously confirmed assignment.

APPENDIX D

Supplementary data for confirmation of BEMA in labeling on beta-casein.

The confirmation of beta-casein fragment 48-63 (FQpSEEQQQTEDELQDK) is shown. For this peptide, the BEMA reaction is near quantitative.

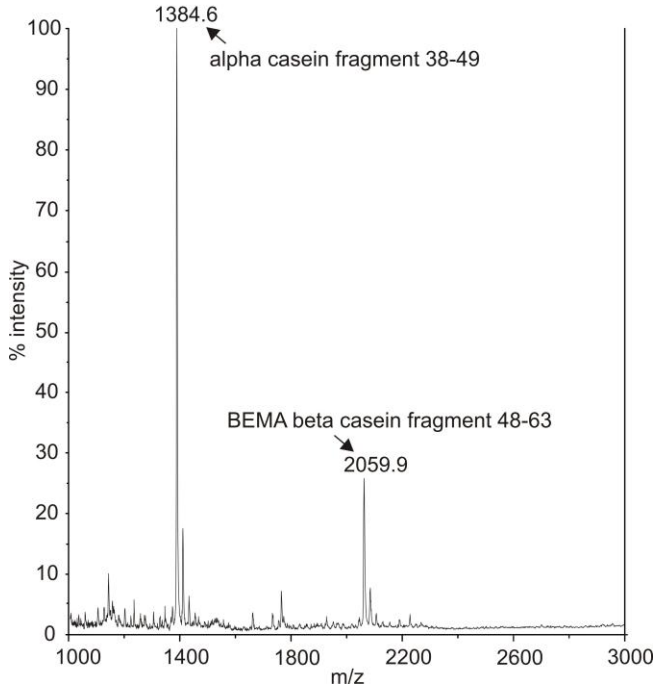

APPENDIX E

Normalized peak area ratios for varying molar concentrations of Tb and Ho labeled phosphorylated peptides in MALDI-TOFMS.

5 (Tb-labeled):1 (Ho-labeled) molar ratio WAGGDApSGE analyzed by MALDI-TOFMS

					1 (Tb):1 (Ho)
sample #	Selected Tb-labeled m/z	Tb-labeled peak area	Selected Ho-labeled m/z	Ho-labeled peak area	Relative Peak Area Ratio
1	1607.43	1423.22	1613.43	172.99	8.23
1	1607.28	9851.83	1613.27	2517.59	3.91
1	1607.24	3715.28	1613.16	526.79	7.05
1	1607.24	2506.79	1613.21	837.87	2.99
1	1607.25	1420.09	1613.21	191.52	7.41
2	1607.59	2622.48	1613.62	587.23	4.47
2	1607.58	2603.36	1613.60	660.74	3.94
2	peak intensity too low				
2	1607.66	2429.36	1613.59	390.70	6.22
2	peak intensity too low				
3	1607.56	441.06	1613.66	104.41	4.22
3	1607.67	1087.55	1613.66	309.52	3.51
3	peak intensity too low				
3	1607.63	1413.01	1613.62	198.66	7.11
3	1607.41	3781.71	1613.28	477.87	7.91
		average	**5.4075**	**relative error**	**0.08**

1 (Tb-labeled):5 (Ho-labeled) molar ratio WAGGDApSGE analyzed by MALDI-TOFMS

Sample #	Selected Tb-labeled m/z	Tb-labeled peak area	Selected Ho-labeled m/z	Ho-labeled peak area	Relative Peak Area Ratio
1	1607.14	774.93	1613.20	3816.00	0.20
1	1607.23	1490.58	1613.21	5142.25	0.29
1	1607.28	1107.85	1613.27	4087.57	0.27
1	1607.14	722.26	1613.20	2357.26	0.31
1	1607.18	705.90	1613.16	3710.51	0.19

2	1607.98	1726.10	1613.00	10414.48	0.17
2	1607.11	714.03	1613.14	6500.69	0.11
2	1606.89	217.05	1613.04	1965.50	0.11
2	1606.99	352.08	1613.99	1974.91	0.18
2	1607.10	1047.98	1613.12	5465.97	0.19
3	1607.23	1904.65	1613.20	11115.08	0.17
3	1607.14	714.90	1613.11	2986.33	0.24
3	1607.99	852.08	1613.00	5932.84	0.14
3	1607.04	729.15	1613.07	3967.66	0.18
3	1607.27	2295.76	1613.27	12673.50	0.18
4	1607.13	3004.65	1613.12	14170.80	0.21
4	1607.12	5066.96	1613.12	24952.40	0.20
4	1606.99	1427.47	1612.98	5494.21	0.26
4	1607.04	1898.93	1613.03	9520.45	0.20
4	1607.17	3071.98	1613.18	13470.76	0.23
5	1607.20	615.82	1613.25	4392.40	0.14
5	1607.23	1596.99	1613.22	7732.68	0.21
5	1607.21	2735.46	1613.19	9531.61	0.29
5	1606.91	744.02	1612.91	2987.99	0.25
5	1607.09	2055.87	1613.09	8062.50	0.25
		average	**0.2070**	**relative error**	**0.04**

1 (Tb-labeled):1 (Ho-labeled) molar ratio WAGGDApSGE analyzed by MALDI-TOFMS

sample #	Selected Tb-labeled m/z	Tb-labeled peak area	Selected Ho-labeled m/z	Ho-labeled peak area	Relative Peak Area Ratio
1	1607.72	3228.61	1613.69	4625.82	1.43
1	1607.70	7004.42	1613.70	7856.04	1.12
1	1607.72	12904.85	1613.74	14640.67	1.13
1	1607.70	7874.79	1613.69	8990.98	1.14
1	1607.70	7619.63	1613.30	8047.21	1.06
2	1607.66	8426.09	1613.66	6004.65	0.71
2	1607.56	8586.85	1613.53	6870.04	0.80
2	1607.60	15273.02	1613.57	12639.61	0.83
2	1607.57	5338.15	1613.57	1892.91	0.35
2	1607.58	5206.04	1613.55	4319.97	0.83
3	1607.46	12767.89	1613.44	9846.99	0.77
3	1607.38	5605.78	1613.40	6690.62	1.19
3	1607.35	6125.84	1613.36	5709.91	0.93
3	1607.36	1025.96	1613.33	1681.95	1.64
3	1607.54	14342.52	1613.46	10558.51	0.74
4	1607.43	4255.02	1613.39	2219.92	0.52

4	1607.41	14361.34	1613.38	17776.02	1.24
4	1607.58	4985.82	1613.59	4702.94	0.94
4	1607.63	4988.10	1613.57	11084.98	2.22
4	1607.58	3721.85	1613.52	3615.98	0.97
		average	**1.0290**	**relative error**	**0.03**

1 (Tb-labeled):1 (Ho-labeled) molar ratio FQpSEEQQQTEDELQDK analyzed by MALDI-TOFMS

					1 (Tb):1 (Ho)
sample #	Selected Tb-labeled m/z	Tb-labeled peak area	Selected Ho-labeled m/z	Ho-labeled peak area	Relative Peak Area Ratio
1	2741.60	1705.80	2747.57	1793.72	0.95
1	2741.49	1420.79	2747.52	1391.32	1.02
1	2741.46	1705.03	2747.47	1666.97	1.02
2	2741.22	1107.12	2747.18	1069.85	1.03
2	2741.25	1239.22	2747.22	1230.74	1.01
2	2741.84	457.16	2747.78	587.11	0.78
3	2741.18	987.30	2747.18	989.74	1.00
3	2741.25	1251.91	2747.26	1194.11	1.05
3	2741.53	801.12	2747.58	598.75	1.34
		average	**1.0330**	**relative error**	**0.03**

1 (Tb-labeled):5 (Ho-labeled) molar ratio FQpSEEQQQTEDELQDK analyzed by MALDI-TOFMS

					1 (Tb):5 (Ho)
sample #	Selected Tb-labeled m/z	Tb-labeled peak area	Selected Ho-labeled m/z	Ho-labeled peak area	Relative Peak Area Ratio
1	2741.34	82.97	2747.35	481.98	0.17
1	2741.22	226.92	2747.22	725.12	0.31
1	2741.49	804.28	2747.45	3436.81	0.23
2	2741.52	305.00	2747.49	1535.90	0.20
2	2741.51	400.34	2747.49	1867.19	0.21
2	2741.77	455.77	2747.76	2241.51	0.20
3	2741.31	665.05	2747.26	2688.99	0.25
3	2741.07	241.02	2747.01	963.76	0.25
3	2741.83	223.55	2747.90	1130.44	0.20
		average	**0.2256**	**relative error**	**0.13**

5 (Tb-labeled):1 (Ho-labeled) molar ratio FQpSEEQQQTEDELQDK analyzed by MALDI-TOFMS

					1 (Ho):5 (Tb)
sample #	Selected Tb-labeled m/z	Tb-labeled peak area	Selected Ho-labeled m/z	Ho-labeled peak area	Relative Peak Area Ratio
1	2740.60	2961.21	2746.63	581.79	0.20
1	2741.54	2665.33	2747.46	410.48	0.15
1	2741.38	2370.88	2747.41	522.00	0.22
2	2740.59	1465.75	2746.55	406.55	0.28
2	2741.39	2898.14	2747.40	546.68	0.19
2	2741.30	2287.42	2747.32	509.73	0.22
3	2741.55	1309.88	2747.56	297.34	0.23
3	2741.56	2985.48	2747.55	566.89	0.19
3	2741.54	1275.04	2747.59	245.97	0.19
		average	**0.2077**	**relative error**	**0.04**

APPENDIX F

Spectra of relative quantitation of phosphorylated peptides by PhECAT in MALDI-TOFMS.

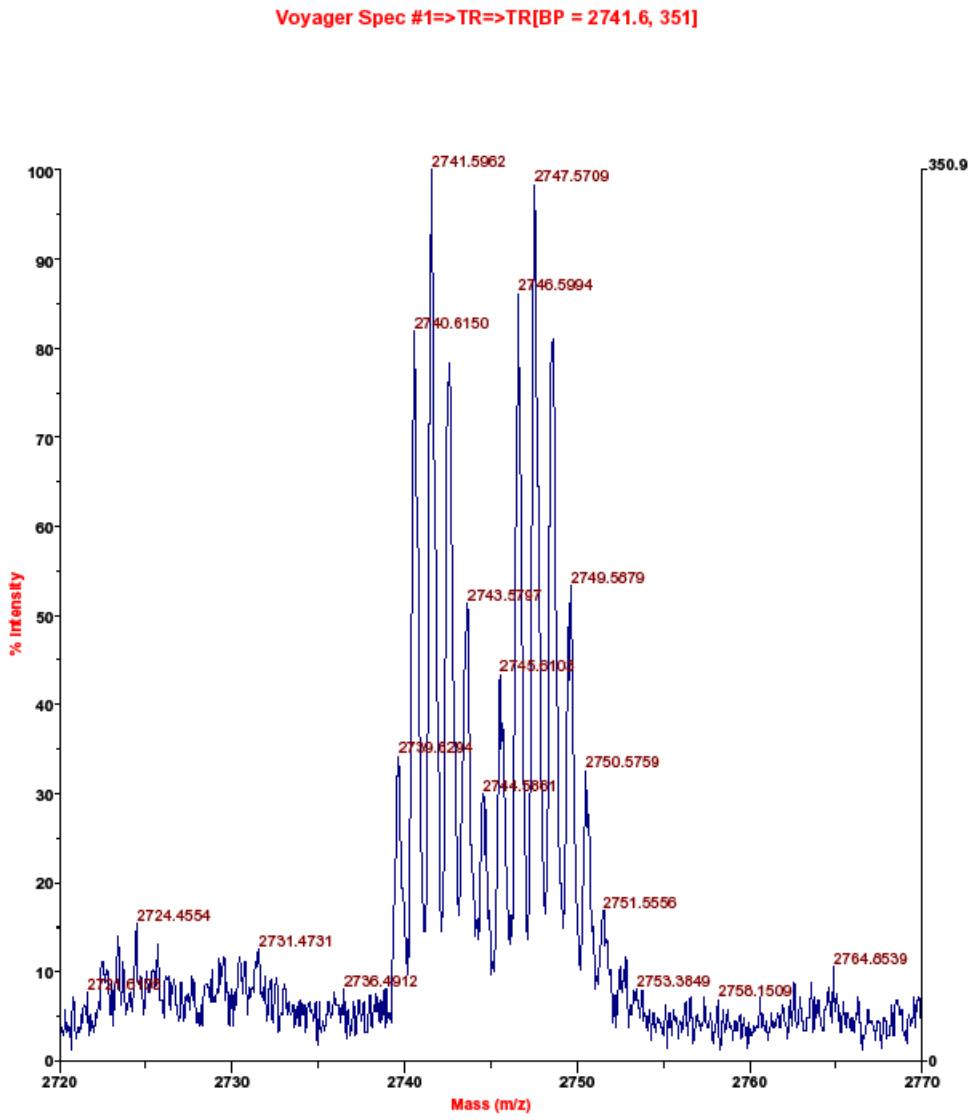

Voyager Spec #1=>TR=>TR[BP = 2741.4, 275]

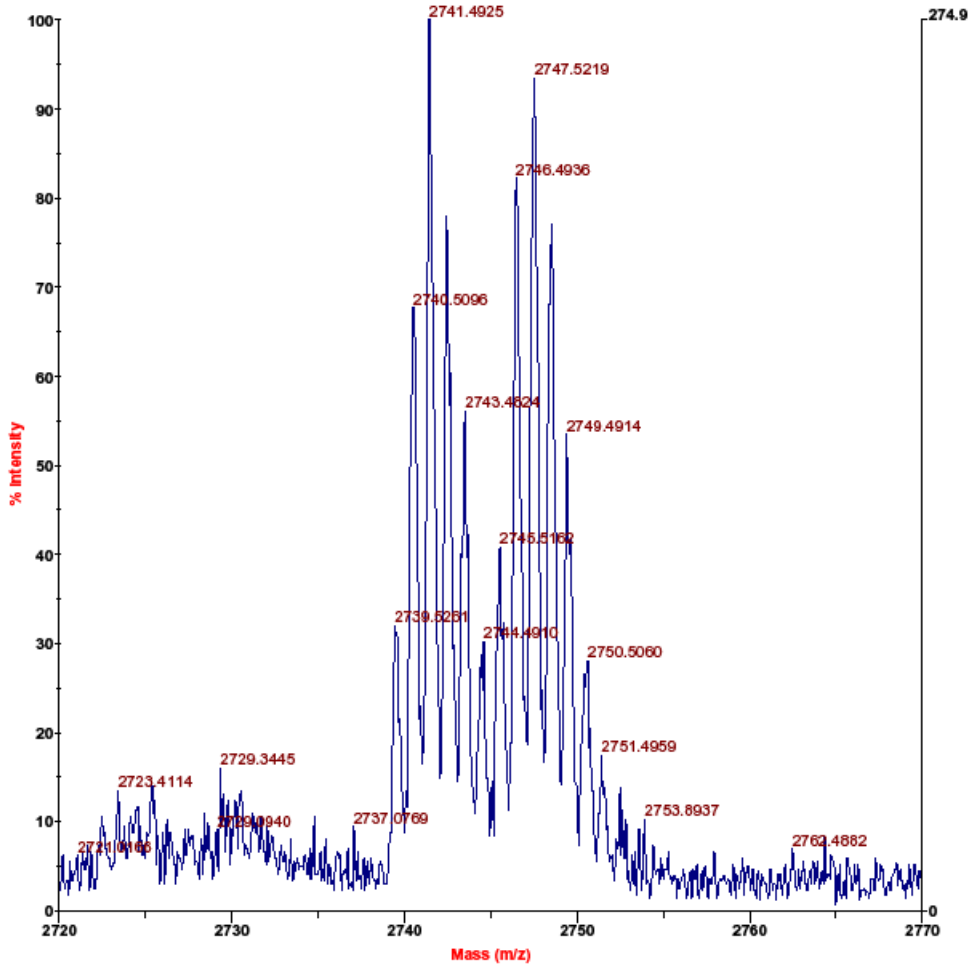

C:\...\042309 1to1 TbHo spot 1_0002.dat
Acquired: 09:55:00, April 23, 2009

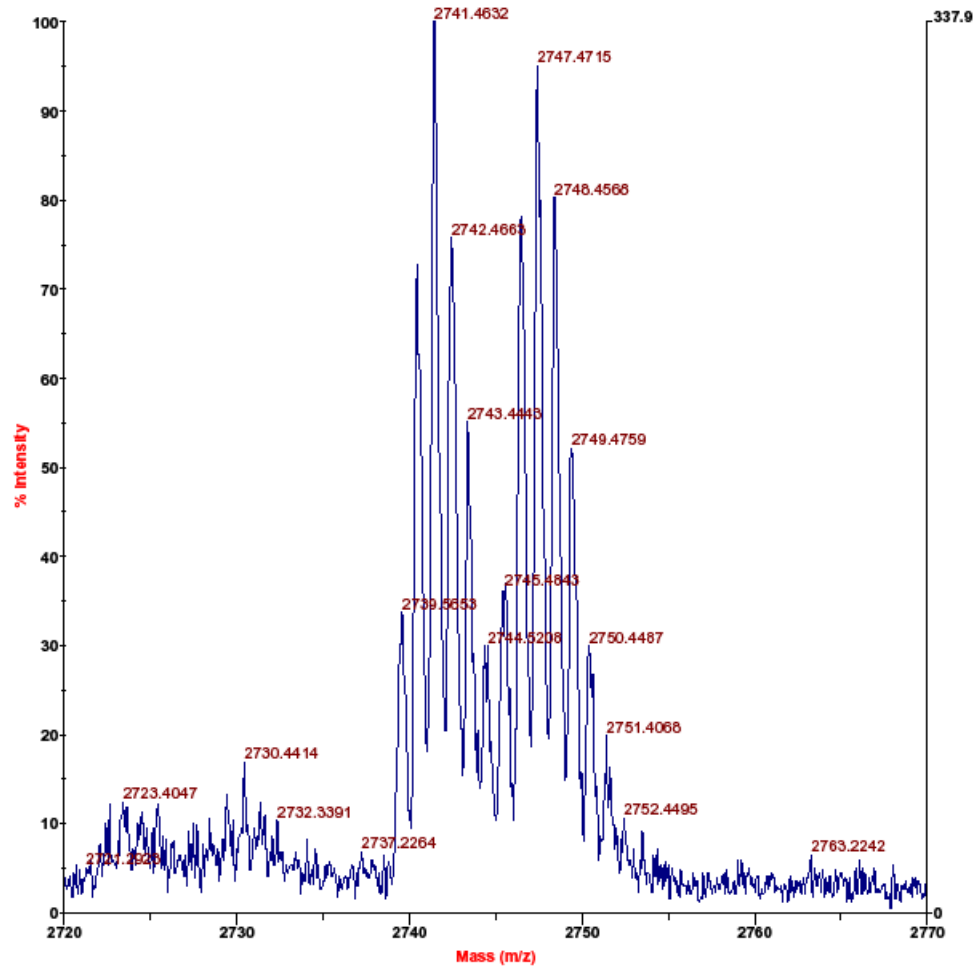

C:\...\042309 1to1 TbHo spot 1_0003.dat
Acquired: 09:56:00, April 23, 2009

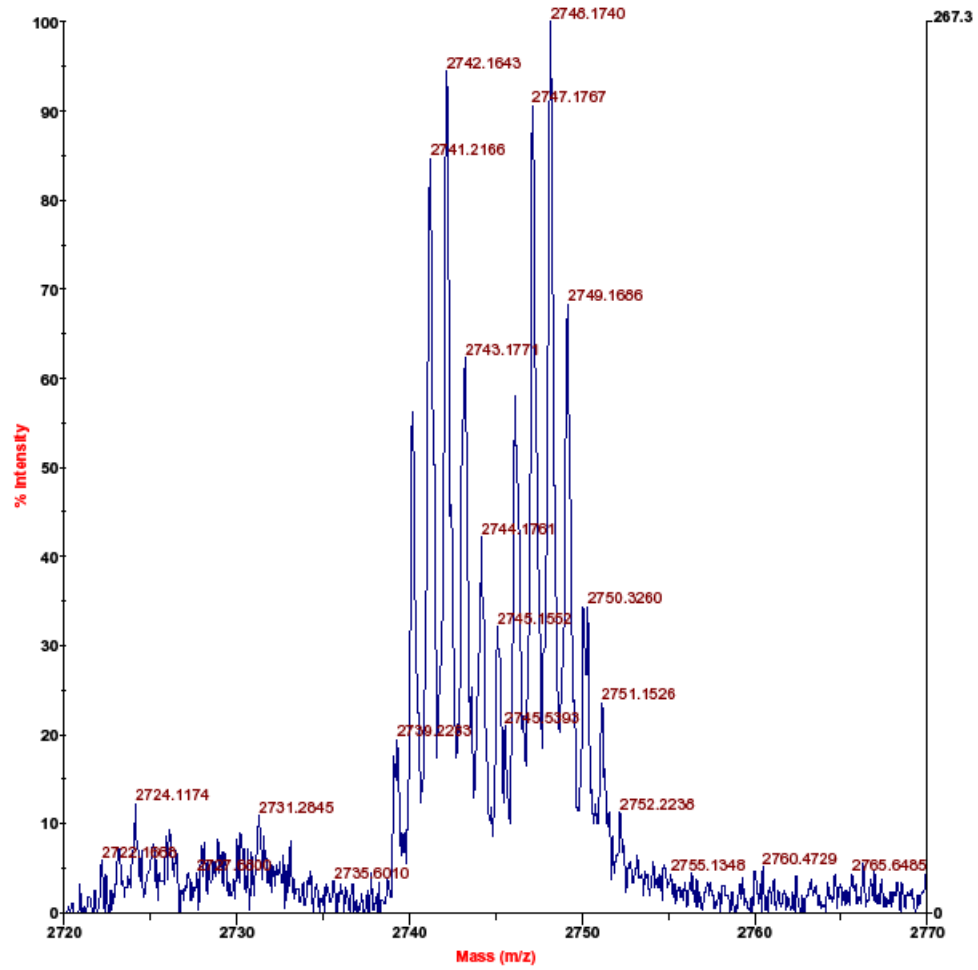

C:\...\042309 1to1 TbHo spot 2_0001.dat
Acquired: 13:51:00, April 23, 2009

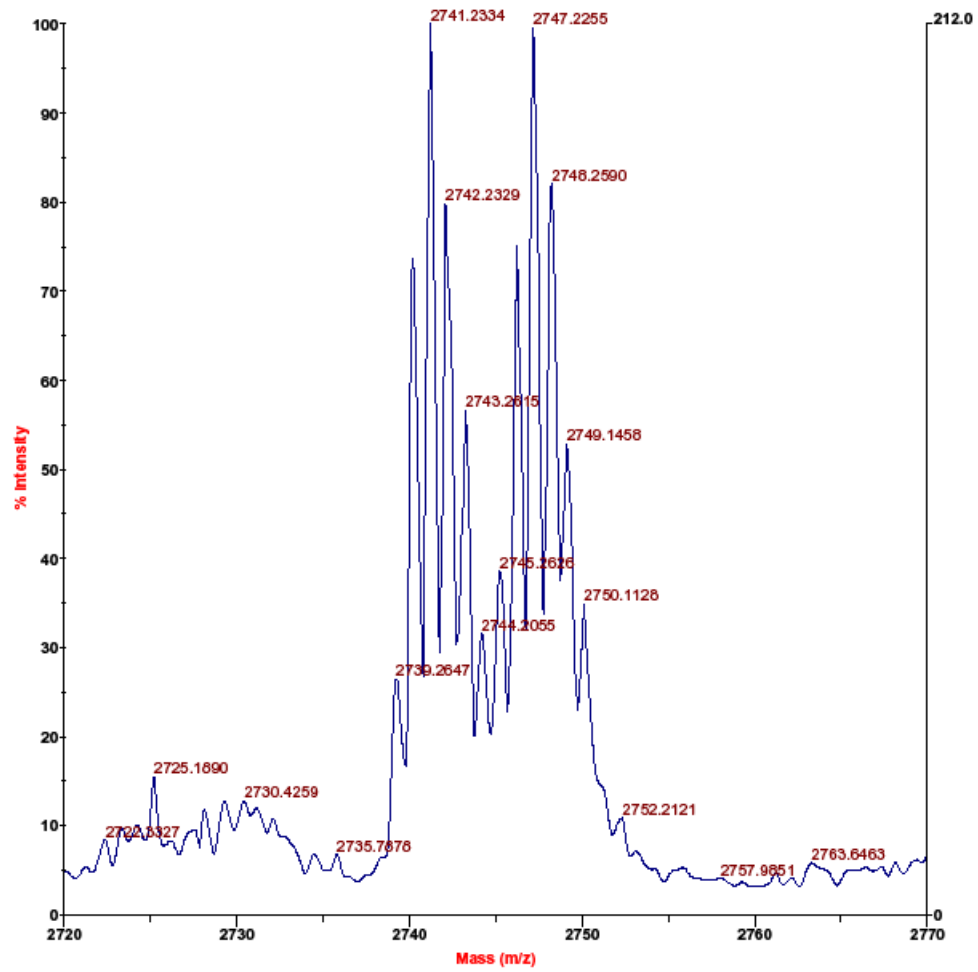

C:\...\042309 1to1 TbHo spot 2_0002.dat
Acquired: 13:55:00, April 23, 2009

Voyager Spec #1=>TR=>BC=>NF0.7=>TR[BP = 2747.7, 148]

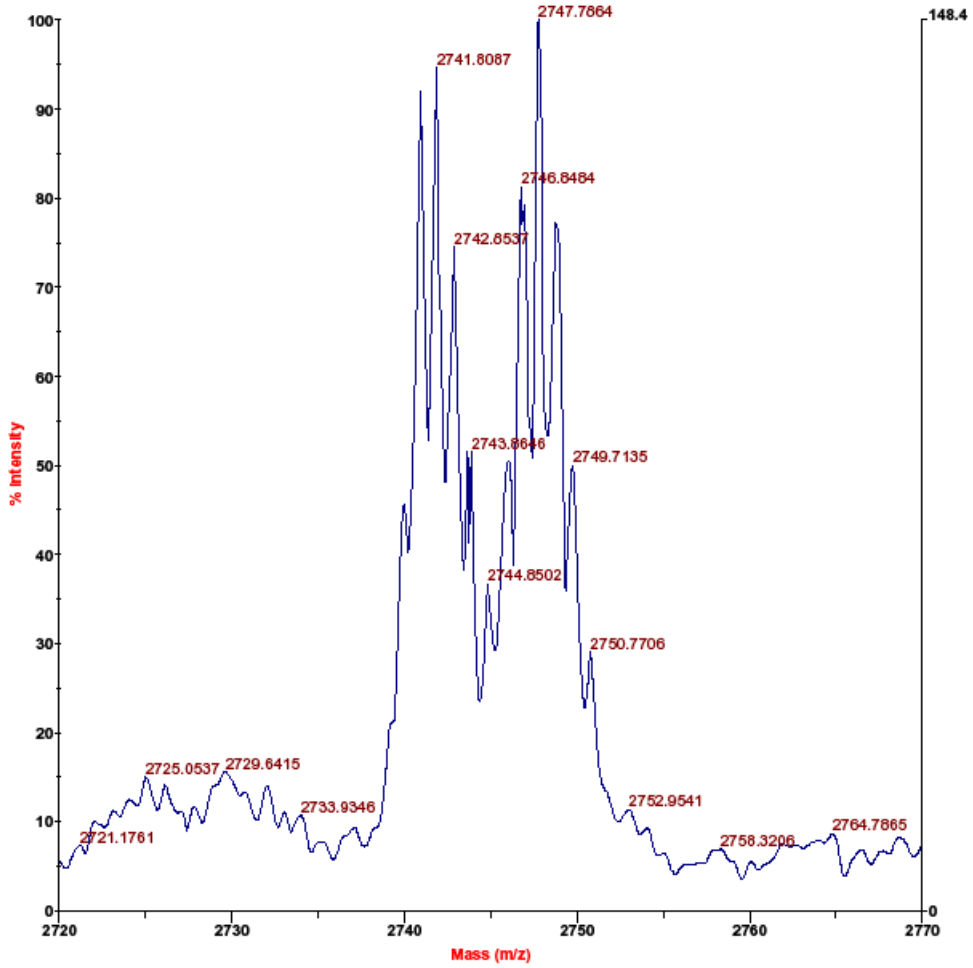

C:\...\042309 1to1 TbHo spot 2_0003.dat
Acquired: 13:57:00, April 23, 2009

Voyager Spec #1=>TR=>TR=>NF0.7[BP = 2741.2, 171]

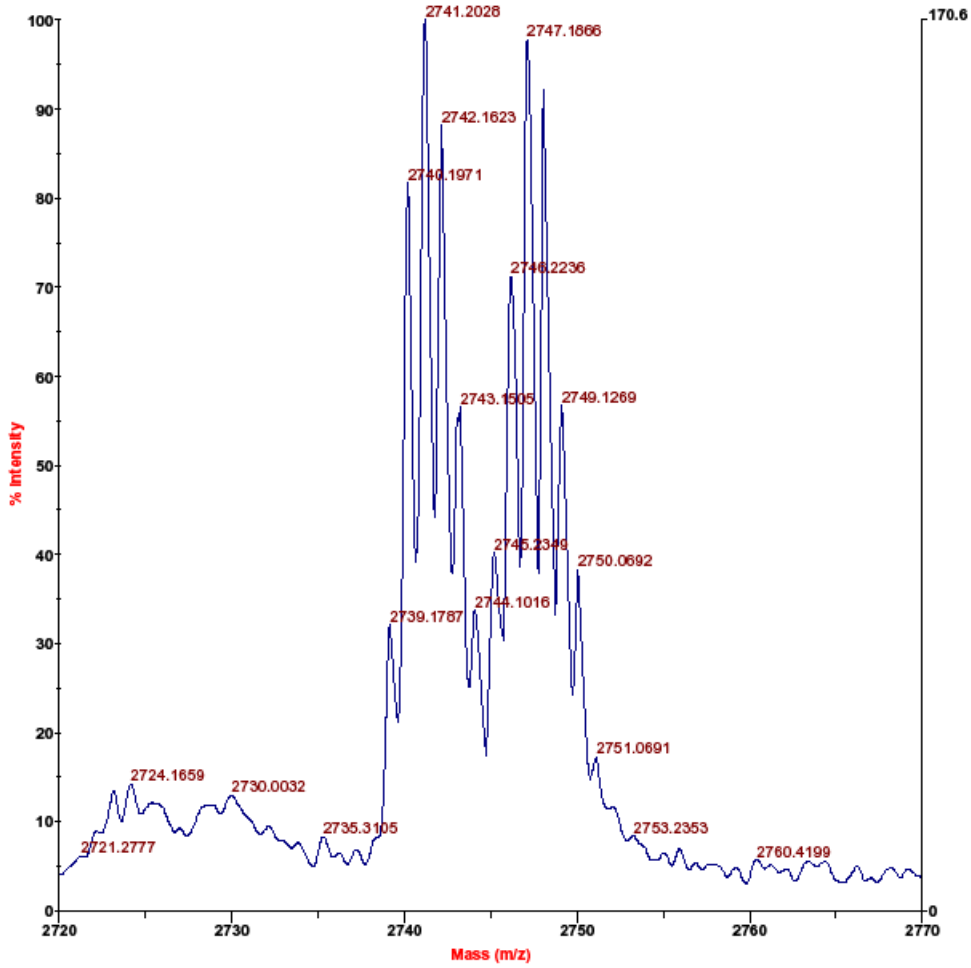

C:\...\042309 1to1 TbHo spot 3_0001.dat
Acquired: 14:03:00, April 23, 2009

Voyager Spec #1=>TR=>BC=>NF0.7=>TR[BP = 2741.3, 260]

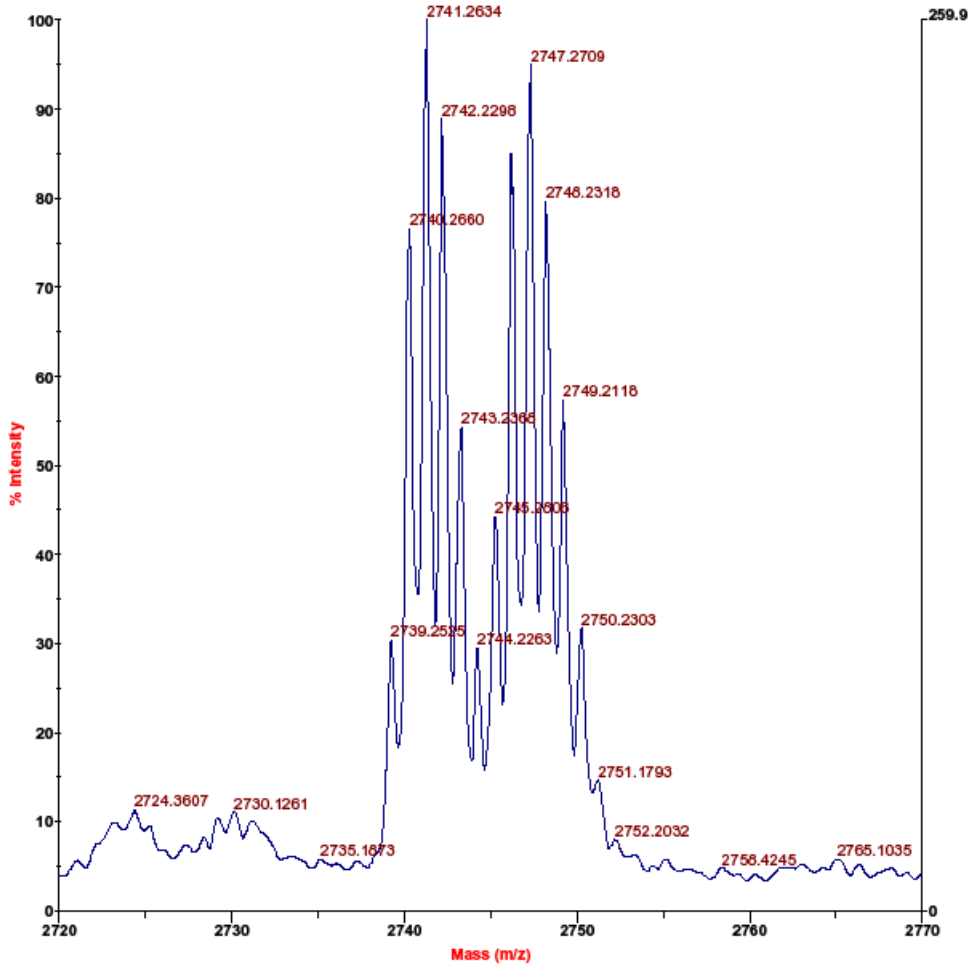

C:\...\042309 1to1 TbHo spot 3_0002.dat
Acquired: 14:05:00, April 23, 2009

Voyager Spec #1=>TR=>BC=>NF0.7=>TR[BP = 2747.6, 172]

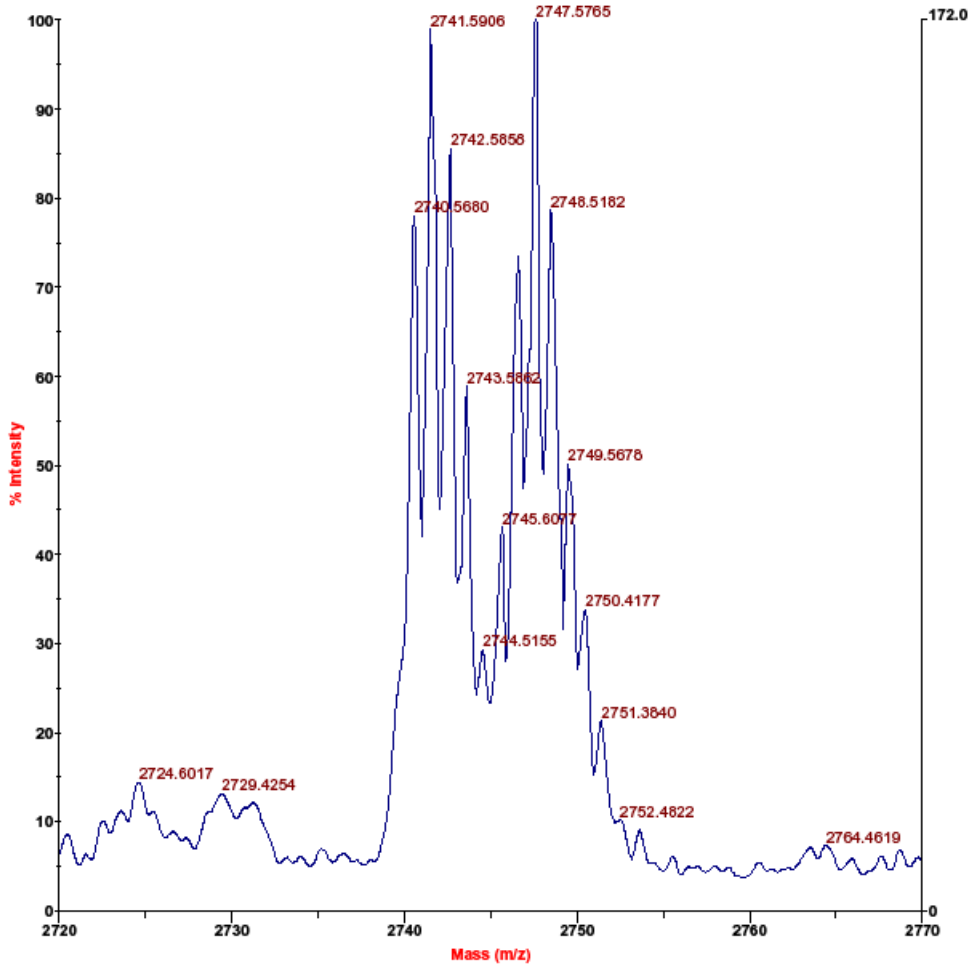

C:\...\042309 1to1 TbHo spot 3_0003.dat
Acquired: 14:08:00, April 23, 2009

Voyager Spec #1=>TR=>NF0.7[BP = 2747.3, 88]

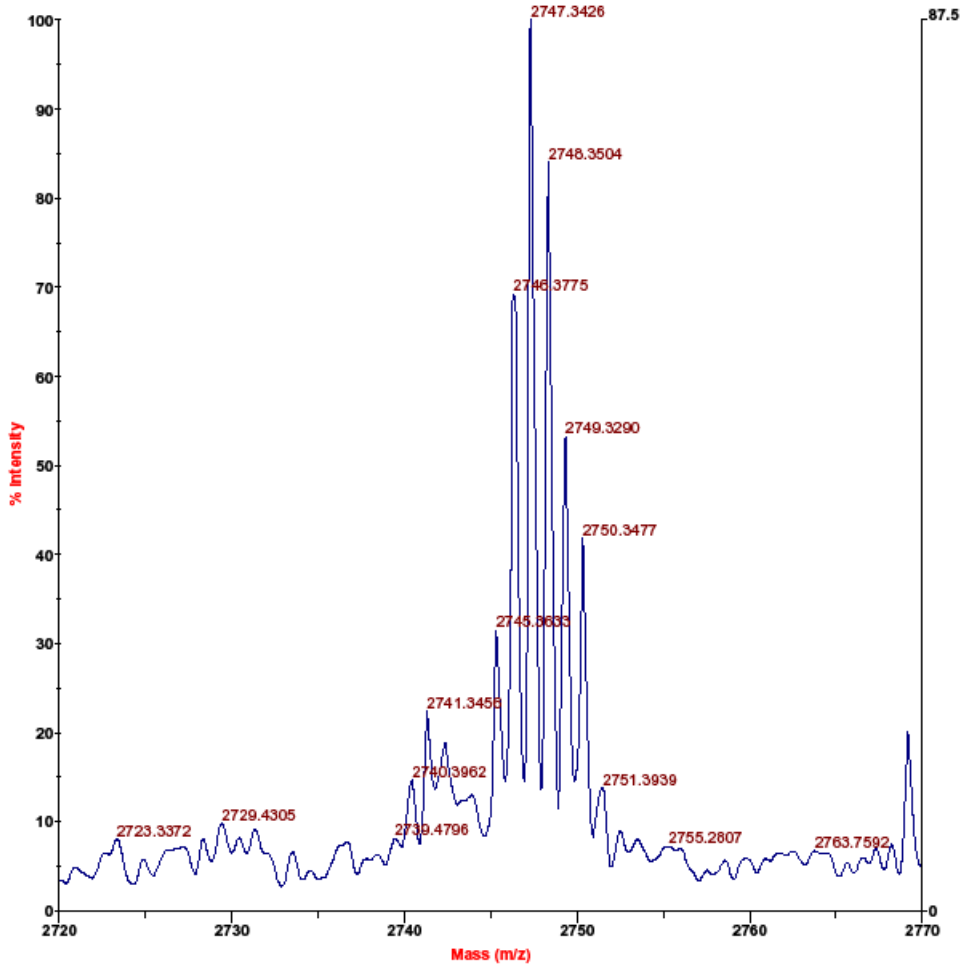

C:\...\042309 1to5 TbHo spot 1_0001.dat
Acquired: 08:55:00, April 23, 2009

Voyager Spec #1=>TR=>BC=>NF0.7=>TR[BP = 2747.2, 145]

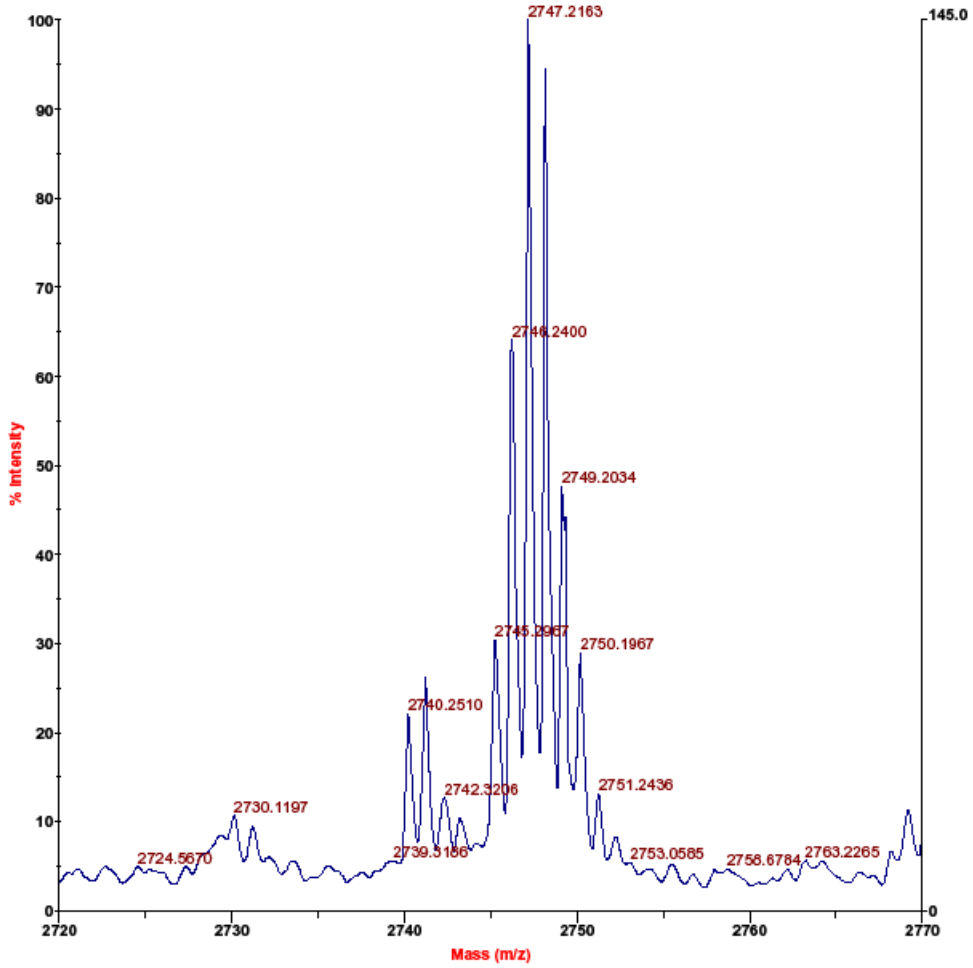

C:\...\042309 1to5 TbHo spot 1_0002.dat
Acquired: 09:05:00, April 23, 2009

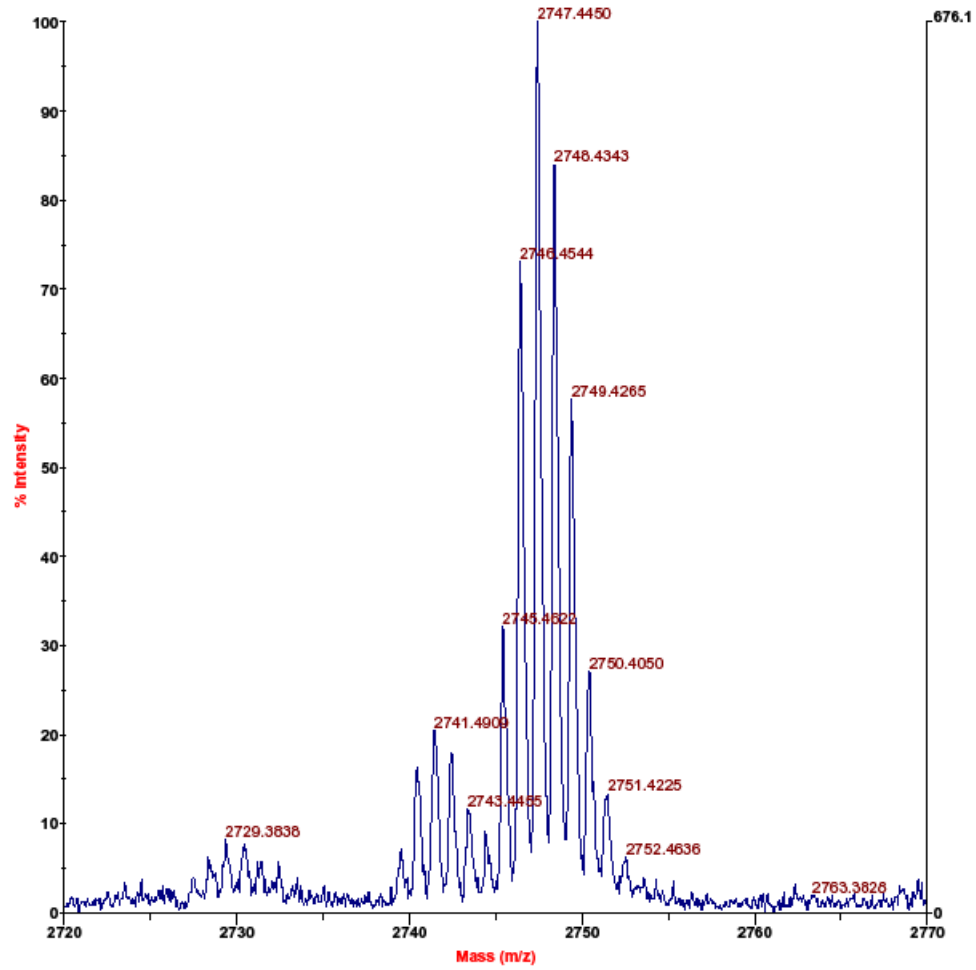

C:\...\042309 1to5 TbHo spot 1_0003.dat
Acquired: 09:10:00, April 23, 2009

Voyager Spec #1=>BC=>TR=>TR=>NF0.7[BP = 2747.5, 268]

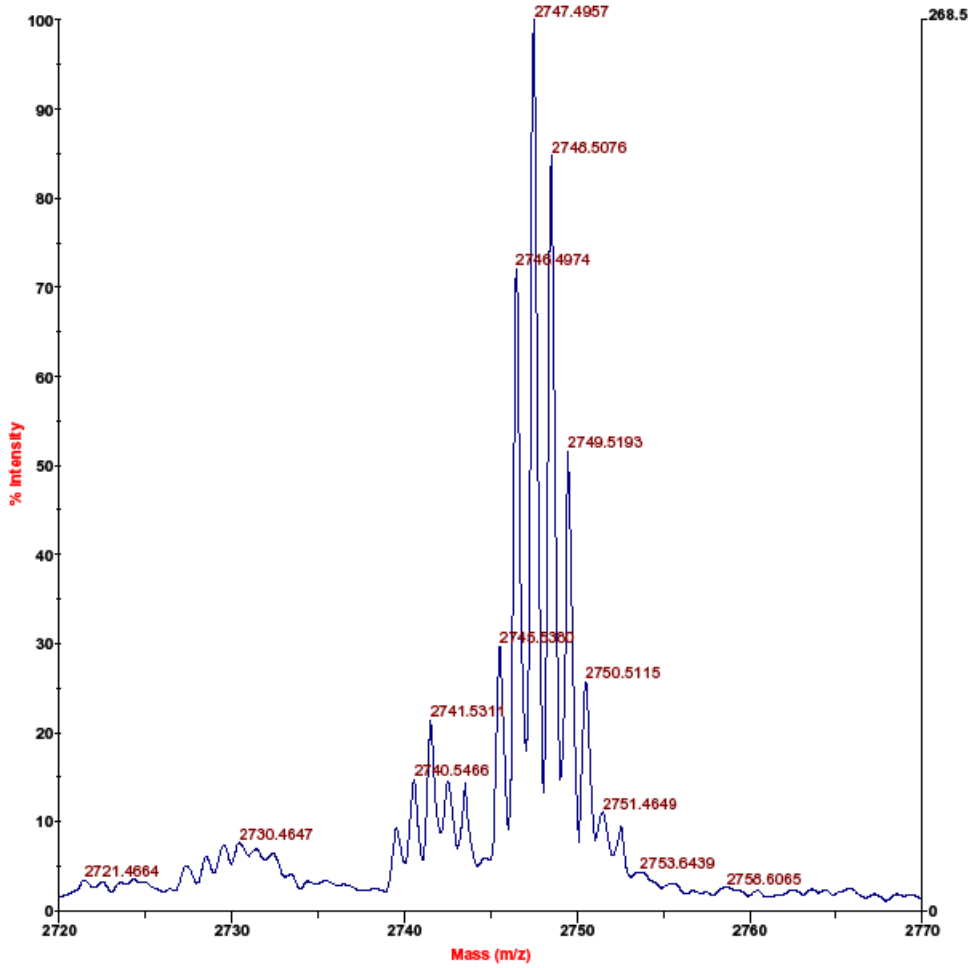

C:\...\042309 1to5 TbHo spot 2_0001.dat
Acquired: 09:16:00, April 23, 2009

Voyager Spec #1=>TR=>TR=>NF0.7[BP = 2747.4, 305]

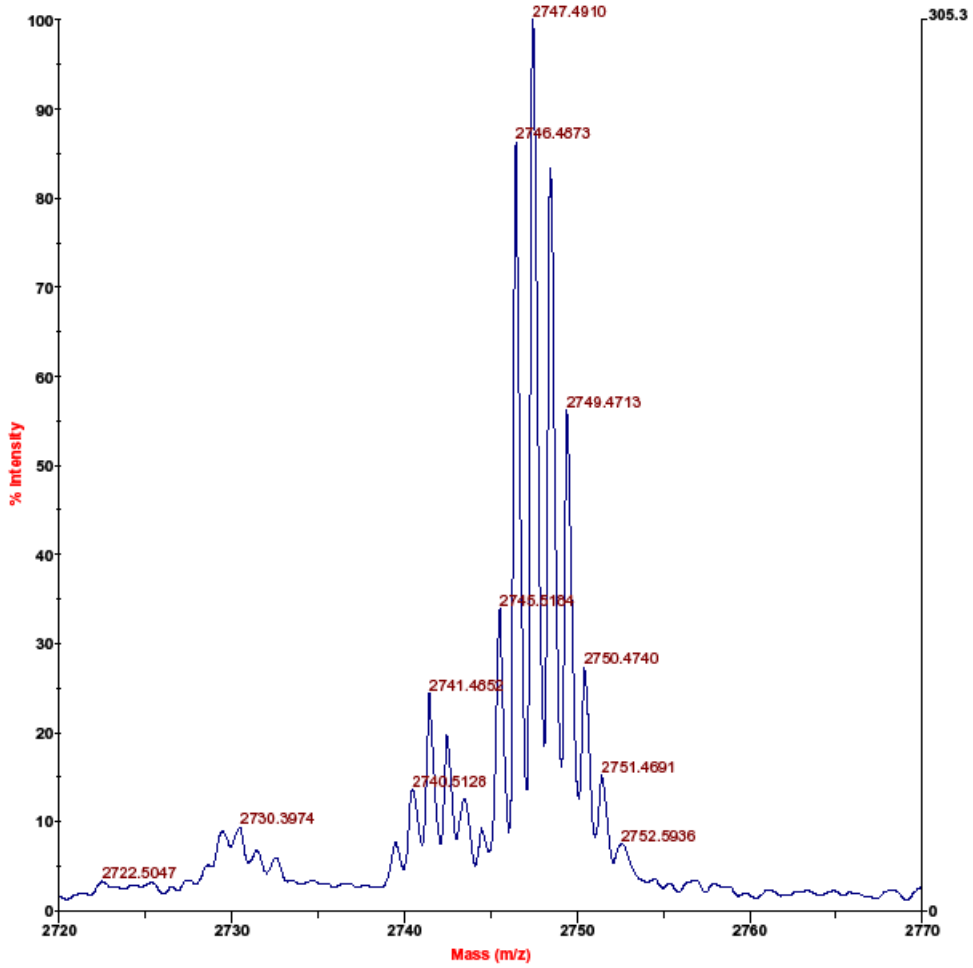

C:\...\042309 1to5 TbHo spot 2_0002.dat
Acquired: 09:17:00, April 23, 2009

Voyager Spec #1=>TR=>BC=>NF0.7=>TR[BP = 2747.7, 532]

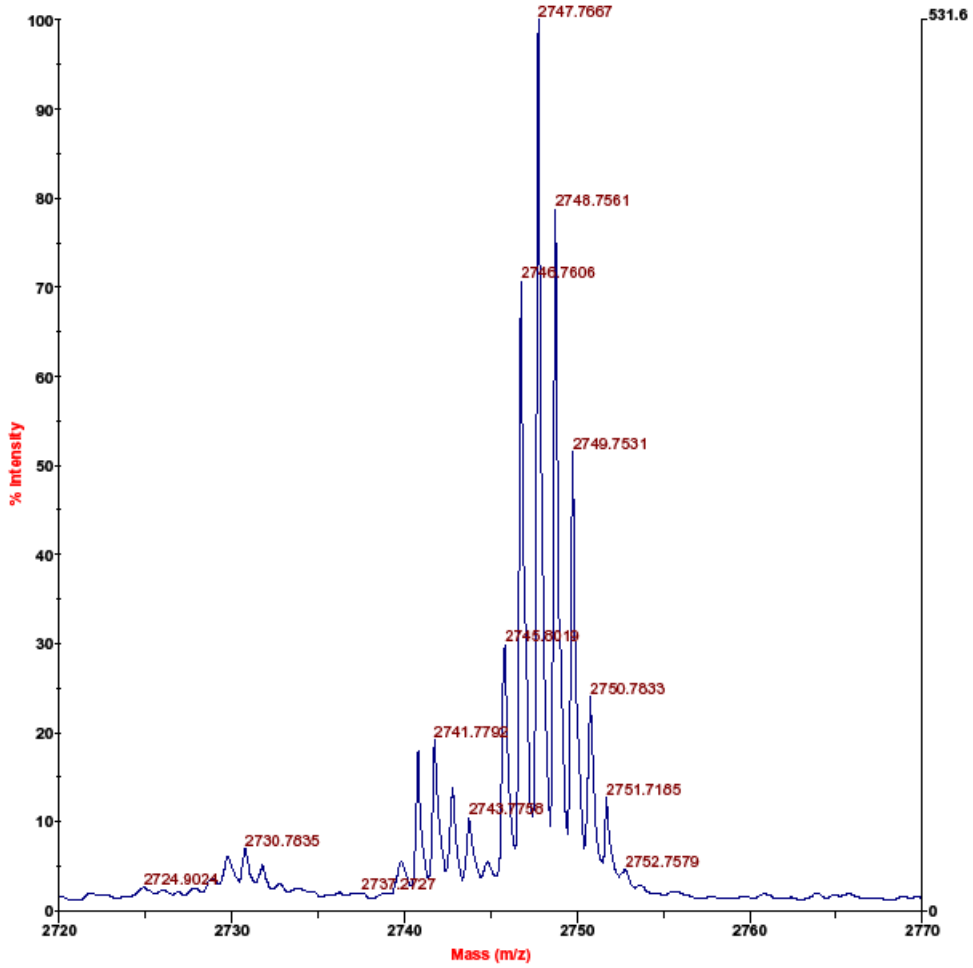

C:\...\042309 1to5 TbHo spot 2_0003.dat
Acquired: 12:32:00, April 23, 2009

Voyager Spec #1=>TR=>TR=>NF0.7[BP = 2748.2, 526]

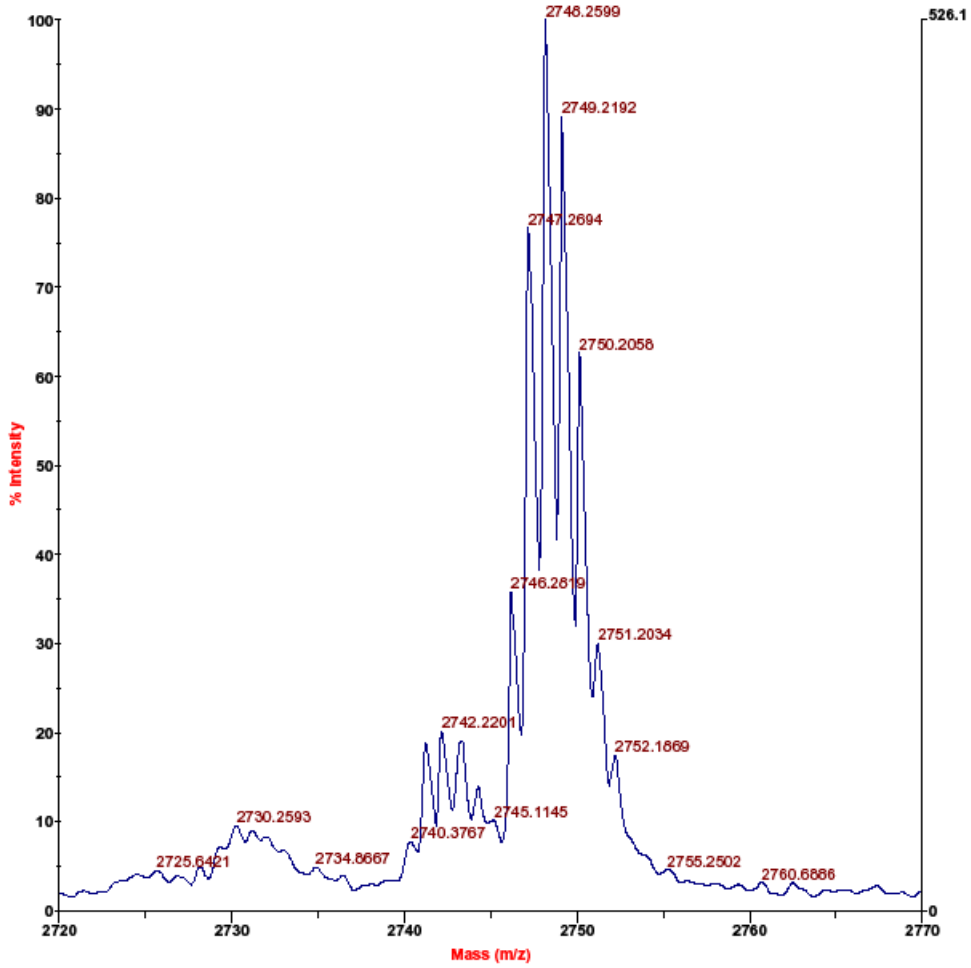

C:\...\042309 1to5 TbHo spot 3_0001.dat
Acquired: 12:41:00, April 23, 2009

Voyager Spec #1=>TR=>BC=>NF0.7=>TR[BP = 2748.0, 186]

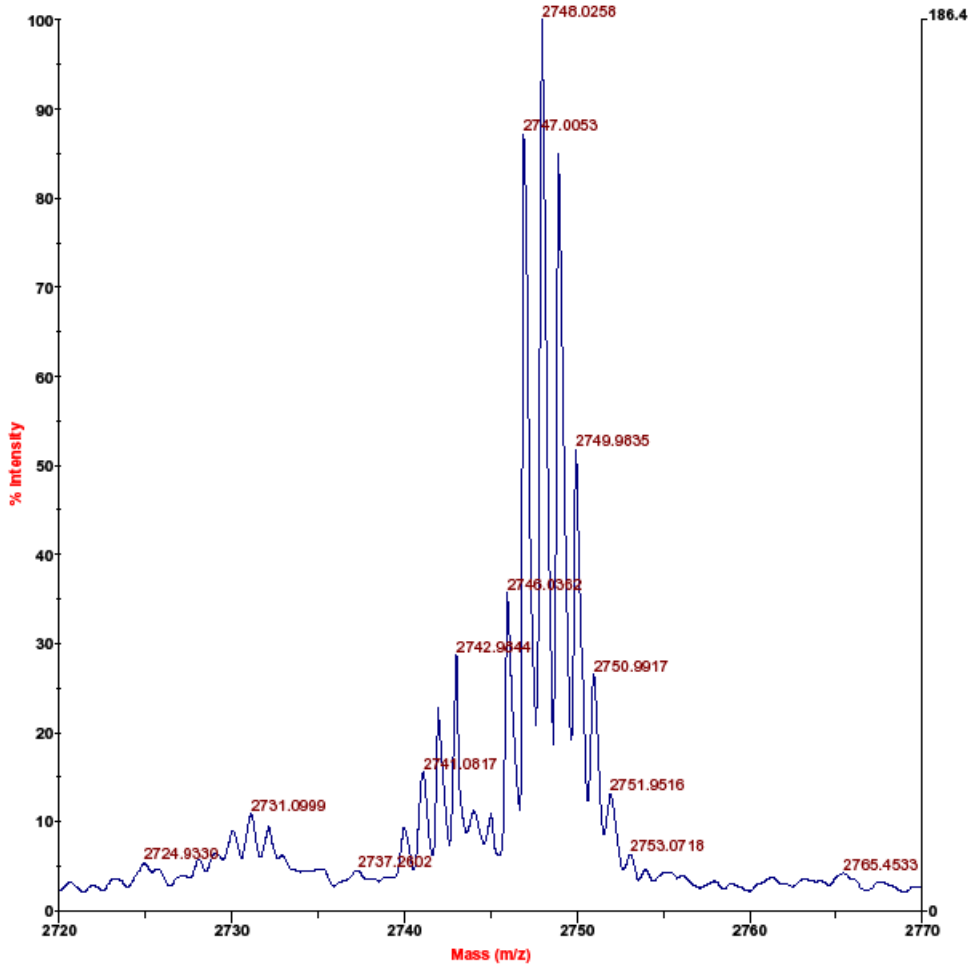

C:\...\042309 1to5 TbHo spot 3_0002.dat
Acquired: 12:46:00, April 23, 2009

Voyager Spec #1=>TR=>BC=>NF0.7=>TR[BP = 2747.9, 253]

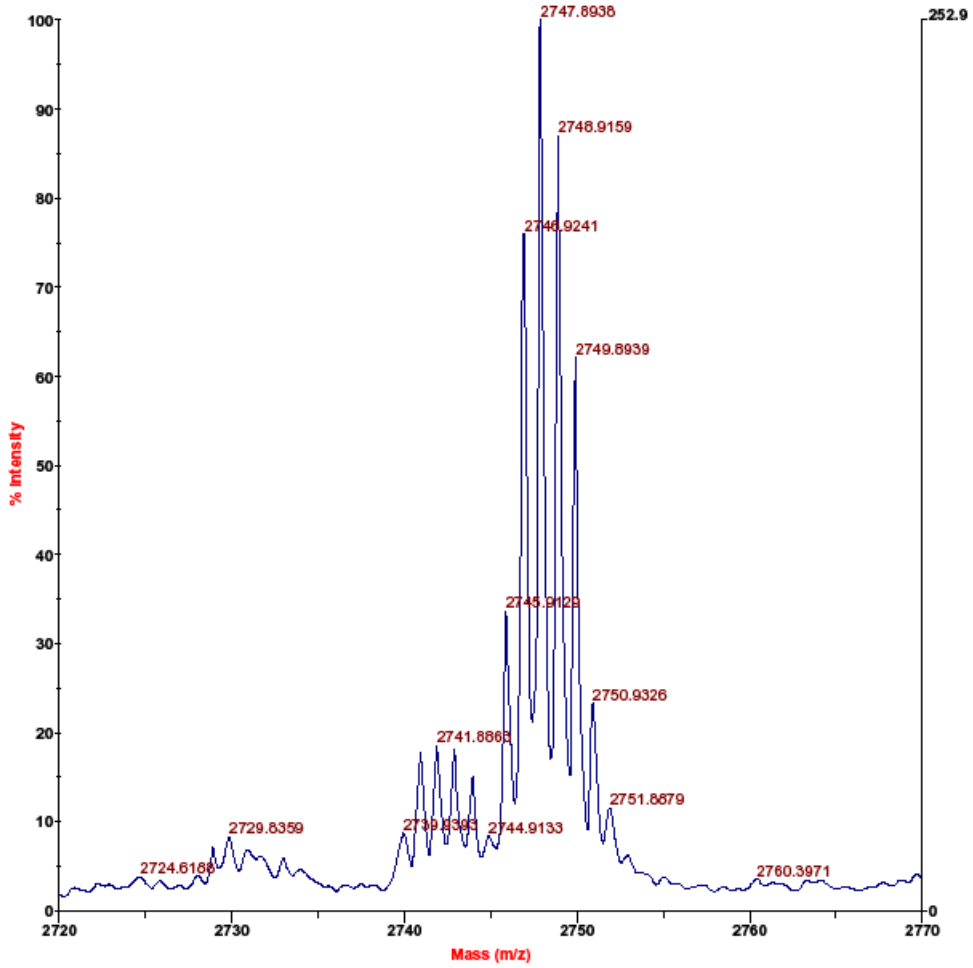

C:\...\042309 1to5 TbHo spot 3_0003.dat
Acquired: 13:04:00, April 23, 2009

Voyager Spec #1=>TR=>BC=>NF0.7=>TR[BP = 2741.4, 257]

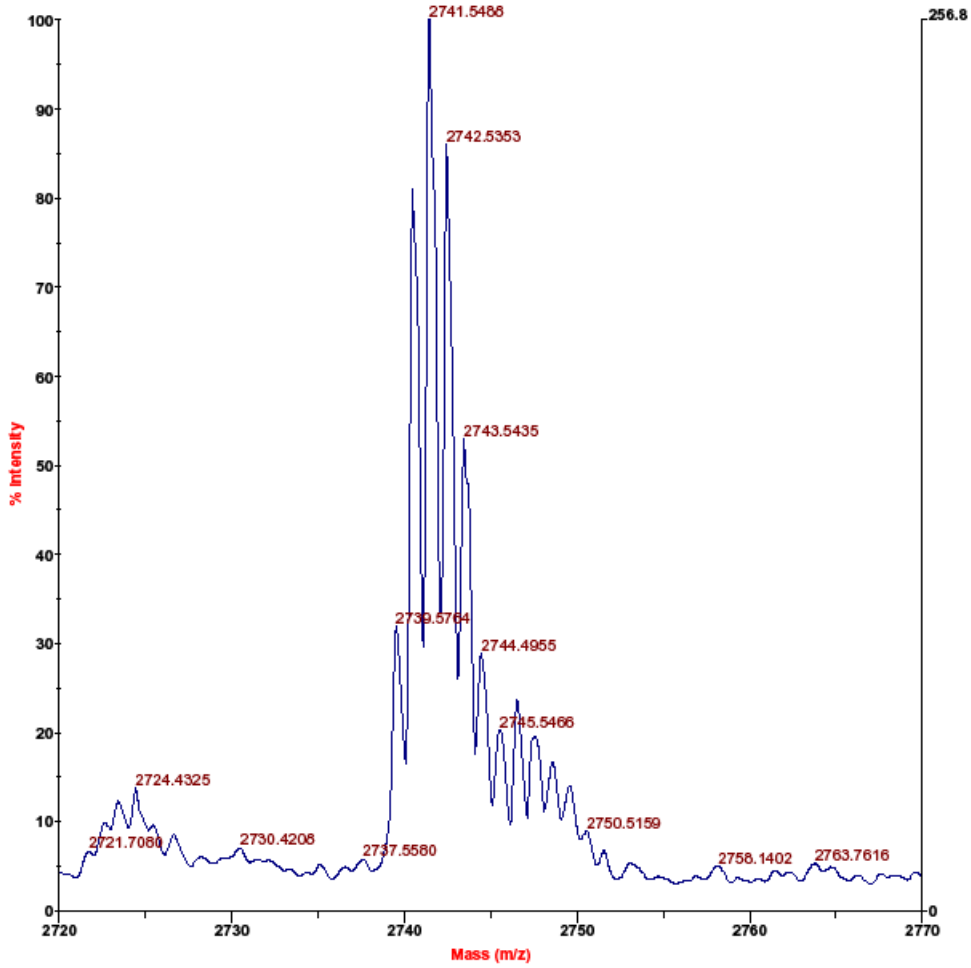

C:\...\042309 5to1 TbHo spot 2_0001.dat
Acquired: 11:28:00, April 23, 2009

Voyager Spec #1=>TR=>NF0.7=>TR[BP = 2741.4, 567]

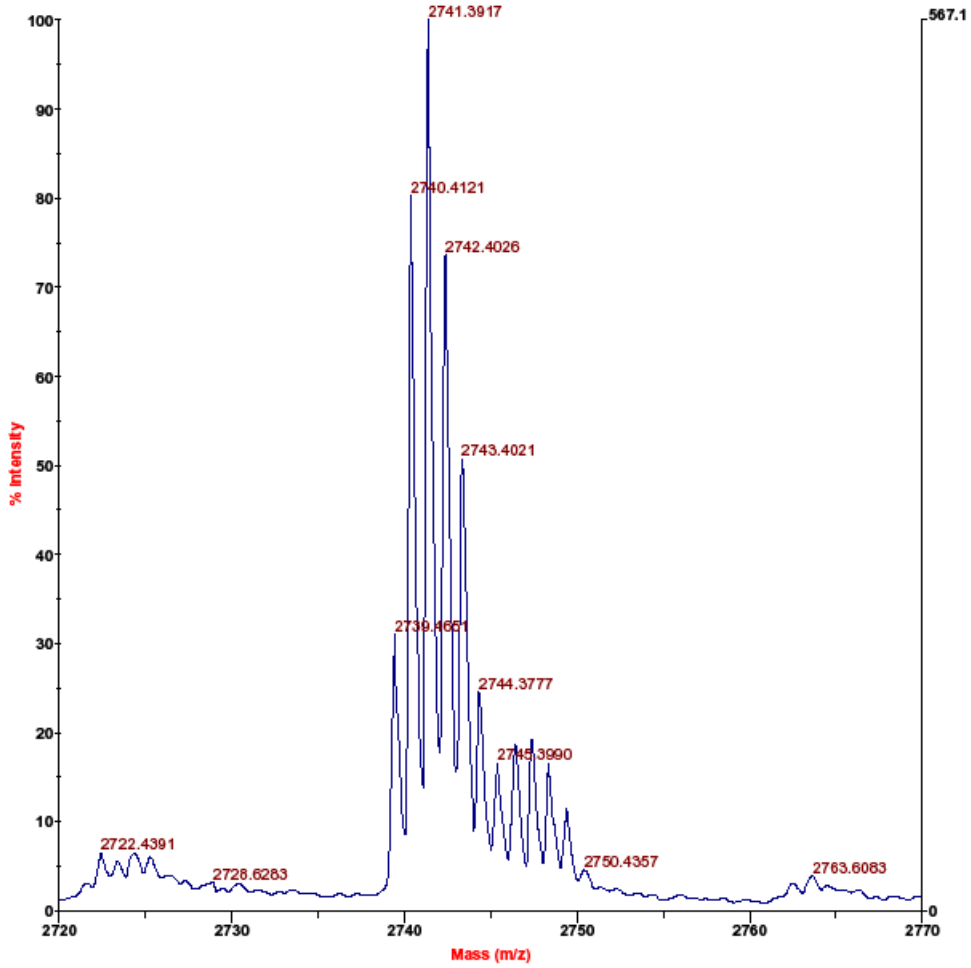

C:\...\042309 5to1 TbHo spot 2_0002.dat
Acquired: 11:34:00, April 23, 2009

Voyager Spec #1=>TR=>BC=>TR=>NF0.7[BP = 2741.3, 396]

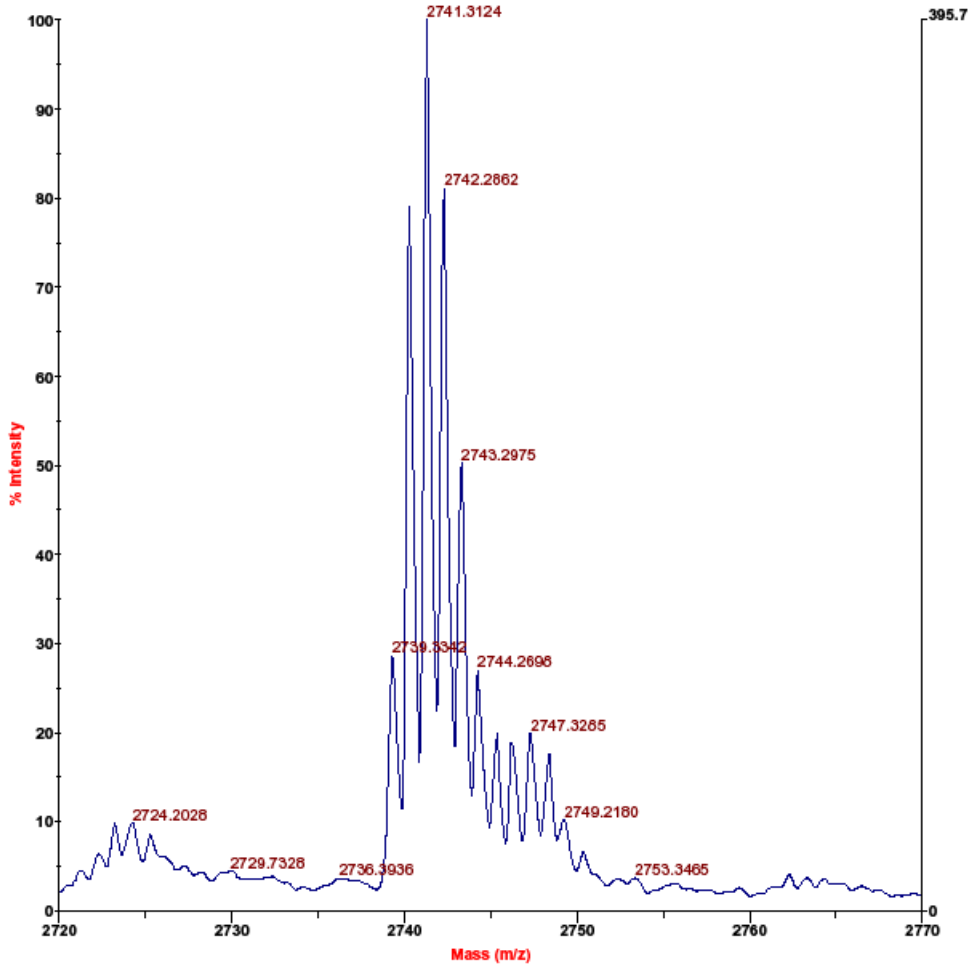

C:\...\042309 5to1 TbHo spot 2_0003.dat
Acquired: 11:38:00, April 23, 2009

Voyager Spec #1=>TR=>BC=>NF0.7=>TR[BP = 2741.6, 241]

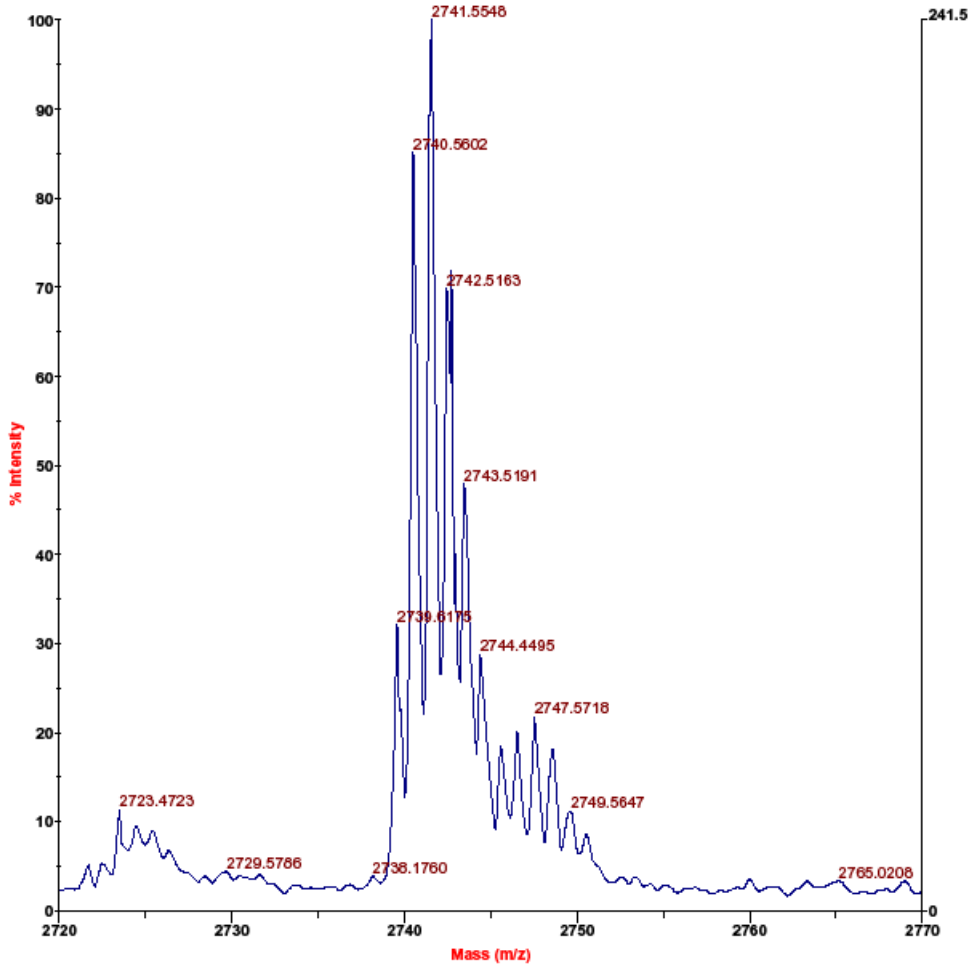

C:\...\042309 5to1 TbHo spot 3_0001.dat
Acquired: 11:44:00, April 23, 2009

Voyager Spec #1=>NF0.7=>BC=>TR=>TR[BP = 2741.5, 517]

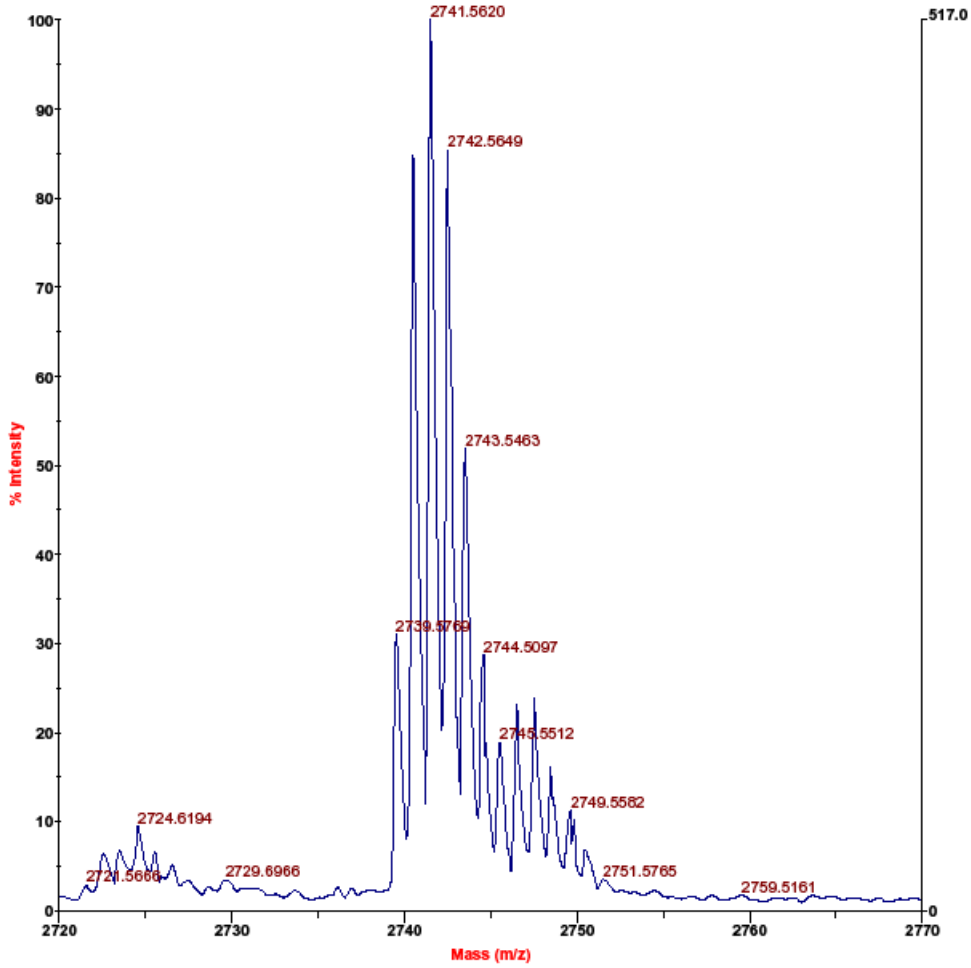

C:\...\042309 5to1 TbHo spot 3_0002.dat
Acquired: 11:45:00, April 23, 2009

Voyager Spec #1=>TR=>NF0.7=>BC=>TR[BP = 2741.4, 227]

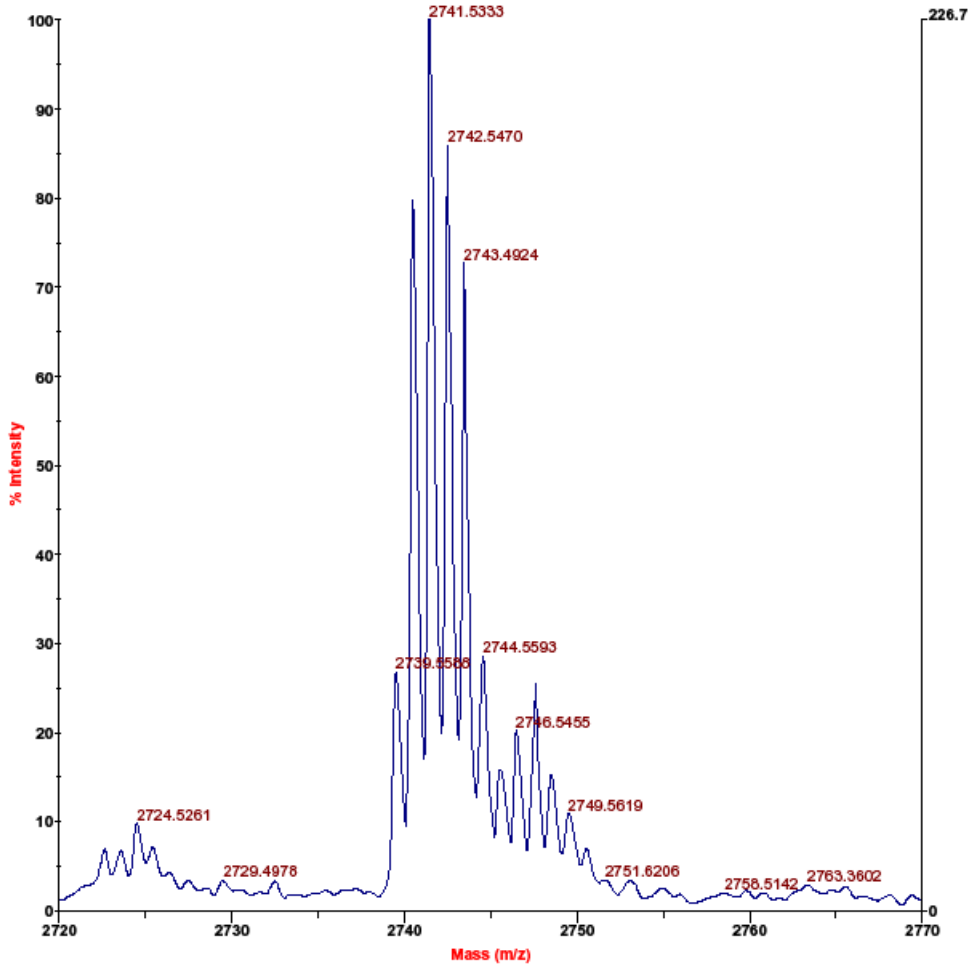

C:\...\042309 5to1 TbHo spot 3_0003.dat
Acquired: 11:47:00, April 23, 2009

APPENDIX G

G. Predicted and observed ions for Tb-labeled FQSEEQQQTEDELQDK as represented in Figure 18.

Predicted b ion m/z				
	#	Predicted b ion m/z	Tb-labeled	Observed
F	1	---	---	---
Q	2	276.13	---	---
s*	3	443.13	1121.58	1121.33
E	4	572.18	1250.62	1250.62
E	5	701.22	1379.66	1379.47
Q	6	829.28	1507.72	1507.50
Q	7	957.34	1635.78	1635.51
Q	8	1085.39	1763.84	1763.60
T	9	1186.44	1864.89	1865.58
E	10	1315.48	1993.93	1993.68
D	11	1430.51	2108.95	2108.74
E	12	1559.55	2238.00	2237.80
L	13	1672.64	2351.08	2350.86
Q	14	1800.70	2479.14	2479.96
D	15	1915.72	2594.17	2594.97
K	16	---		---

Predicted b-H2O ion m/z		
Predicted b-H2O ion m/z	Tb-labeled	Observed
---	---	---
---	---	---
---		---
554.16	1232.61	1232.53
683.21	1361.65	1361.73
811.27	1489.71	---
939.32	1617.77	1618.54
1067.38	1745.83	1745.51
1168.43	1846.87	1846.73
1297.47	1975.92	1975.82
1412.50	2090.94	2090.29
1541.54	2219.99	---
1654.63	2333.07	2332.80
1782.69	2461.13	2461.77
1897.71	2576.16	2576.87
---	---	---

Predicted y ion m/z				
	ion #	Predicted y ion m/z	Tb-Labeled	Observed
F	16	---	---	---
Q	15	1914.76	2593.20	2593.55
s*	14	1786.70	2465.15	2465.85
E	13	1619.70	---	---
E	12	**1490.66**	---	---
Q	11	**1361.62**	---	---
Q	10	1233.56	---	---
Q	9	**1105.50**	---	---
T	8	977.44	---	---
E	7	876.39	---	---
D	6	747.35	---	---
E	5	632.33	---	---
L	4	503.28	---	---
Q	3	390.20	---	---
D	2	262.14	---	---
K	1	147.11	---	---

Predicted y-H2O ion m/z		
Predicted y-H2O ion m/z	Tb-labeled	Observed
---	---	---
1896.75	2575.19	---
1768.69	2447.13	2447.90
1601.69	---	---
1472.65	---	---
1343.61	---	---
1215.55	---	---
1087.49	---	---
959.43	---	---
858.38	---	---
729.34	---	---
614.31	---	---
485.27	---	---
372.19	---	---
244.13	---	---
---	---	---

*s,y,t = phosphorylated S,Y,T

APPENDIX H

Normalized peak area ratios for varying molar concentrations of Tb and Ho labeled phosphorylated peptides in MALDI-IM-TOFMS.

	1(Pr-labeled):1(Tb-labeled):5(Ho-labeled) FQpSEEQQQTEDELQDK analyzed by MALDI-IM-TOFMS				1(Pr):5(Ho), 1(Tb):5(Ho)
sam-ple #	Pr, Tb, and Ho-labeled m/z	Pr-labeled peak area	Tb-labeled peak area	Ho-labeled peak area	Relative Peak Area Ratio
1	2723.30, 2741.77, 2747.20	36.31	31.14	375.00	0.10, 0.08
1	2723.17, 2741.23, 2747.21	27.81	30.19	451.00	0.06, 0.07
1	2723.25, 2741.09, 2747.19	55.64	42.56	551.70	0.10, 0.08
2	2723.30, 2741.50, 2747.23	79.97	74.28	380.40	0.21, 0.20
2	2723.37, 2741.42, 2747.24	101.00	81.28	458.40	0.22, 0.18
2	2723.27, 2741.43, 2747.24	65.38	66.75	448.60	0.15, 0.15
3	2723.37, 2741.43, 2747.23	85.00	179.00	507.00	0.17, 0.35
3	2723.22, 2741.68, 2747.23	43.25	52.57	364.40	0.12, 0.14
3	2723.30, 2741.72, 2747.23	55.58	39.42	413.80	0.13, 0.10
		average	**0.1400, 0.1300**	**relative error**	**-0.30, -0.35**
	3 (Tb-labeled):1 (Ho-labeled) molar ratio FQpSEEQQQTEDELQDK analyzed by MALDI-IM-TOFMS				3 (Tb):1 (Ho)
sam-ple #	Selected Tb-labeled m/z	Tb-labeled peak area	Selected Ho-labeled m/z	Ho-labeled peak area	Relative Peak Area Ratio
1	2741.99	168.40	2747.01	64.19	2.62
2	2741.00	142.40	2747.01	58.98	2.41
3	2740.98	377.10	2747.01	132.00	2.86
4	2740.99	61.52	2747.00	36.29	1.70
5	2740.98	559.70	2747.00	241.50	2.32
6	2740.99	485.00	2747.01	226.40	2.14
		average	**2.3416**	**relative error**	**-0.22**
	1 (Tb-labeled):1 (Ho-labeled) molar ratio FQpSEEQQQTEDELQDK				1 (Tb):1 (Ho)

	analyzed by MALDI-IM-TOFMS				
acq #	Selected Tb-labeled m/z	Tb-labeled peak area	Selected Ho-labeled m/z	Ho-labeled peak area	Relative Peak Area Ratio
1	2741.03	2767.00	2747.04	2512.00	1.10
2	2741.02	3449.00	2747.03	2877.00	1.20
3	2741.01	5924.00	2747.02	4981.00	1.19
4	2741.03	2697.00	2747.03	2315.00	1.17
5	2741.02	3312.00	2747.03	2910.00	1.14
		average	**1.1586**	**relative error**	**0.16**
	1 (Tb-labeled):5 (Ho-labeled) molar ratio FQpSEEQQQTEDELQDK analyzed by MALDI-IM-TOFMS				1 (Tb):5 (Ho)
acq #	Selected Tb-labeled m/z	Tb-labeled peak area	Selected Ho-labeled m/z	Ho-labeled peak area	Relative Peak Area Ratio
1	2741.04	1275.00	2747.01	4451.00	0.29
2	2741.04	1599.00	2747.01	5222.00	0.31
3	2741.04	1102.00	2747.01	3907.00	0.28
4	2741.04	1234.00	2747.01	4274.00	0.29
5	2741.03	1198.00	2747.01	3964.00	0.30
		average	**0.2931**	**relative error**	**0.47**
	5 (Tb-labeled):1 (Ho-labeled) molar ratio FQpSEEQQQTEDELQDK analyzed by MALDI-IM-TOFMS				1 (Ho):5 (Tb)
acq #	Selected Tb-labeled m/z	Tb-labeled peak area	Selected Ho-labeled m/z	Ho-labeled peak area	Relative Peak Area Ratio
1	2741.99	12050.00	2748.04	2105.00	0.17
2	2741.99	6300.00	2748.03	1075.00	0.17
3	2742.00	3153.00	2748.04	575.20	0.18
4	2741.98	8306.00	2747.04	1371.00	0.17
5	2741.98	6976.00	2747.04	1170.00	0.17
		average	**0.1721**	**relative error**	**-0.14**

APPENDIX I

Sample spectra and data from relative quantitation of phosphorylated peptides by PhECAT in MALDI-IM-TOFMS.

I. 1. 1 to 1 Tb to Ho-labeled beta-casein.

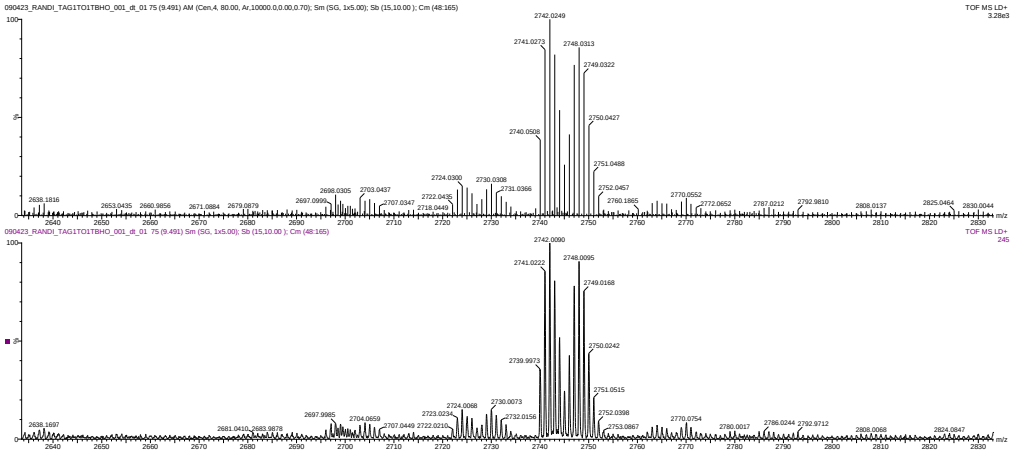

Sample 01 – 1

	mass	peak area
Tb	2741.0273	2.767e3
Ho	2747.0354	2.512e3

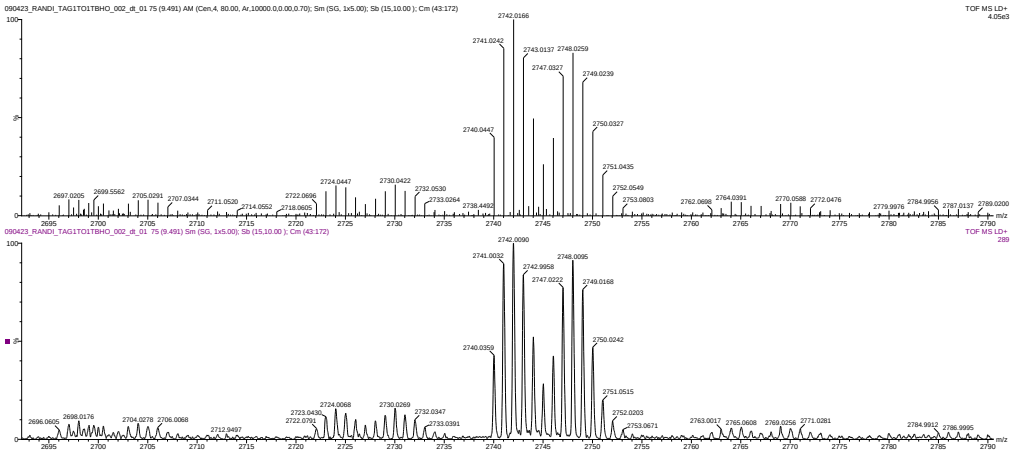

Sample 01-2

	mass	peak area
Tb	2741.0242	3.449e3
Ho	2747.0327	2.877e3

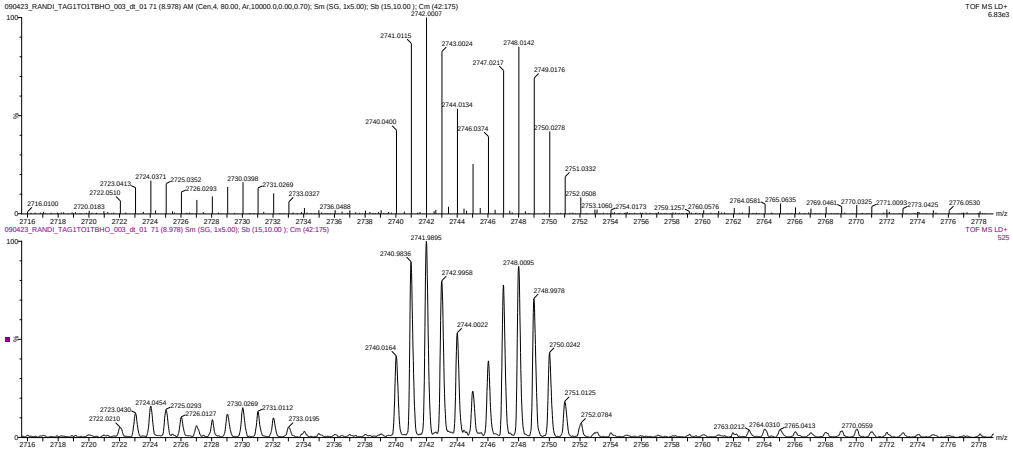

Sample 01-3

	mass	peak area
Tb	2741.0115	5.924e3
Ho	2747.0217	4.981e3

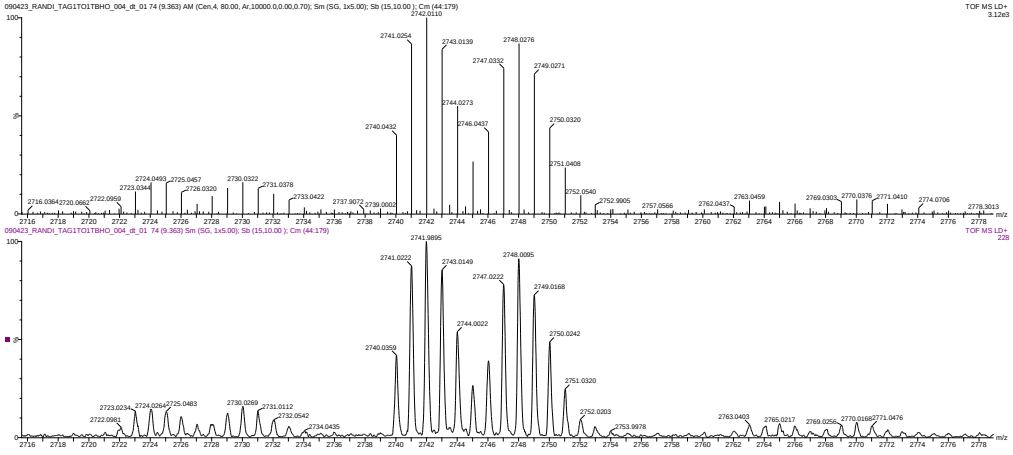

Sample 01-4

	mass	peak area
Tb	2741.0254	2.697e3
Ho	2747.0332	2.315e3

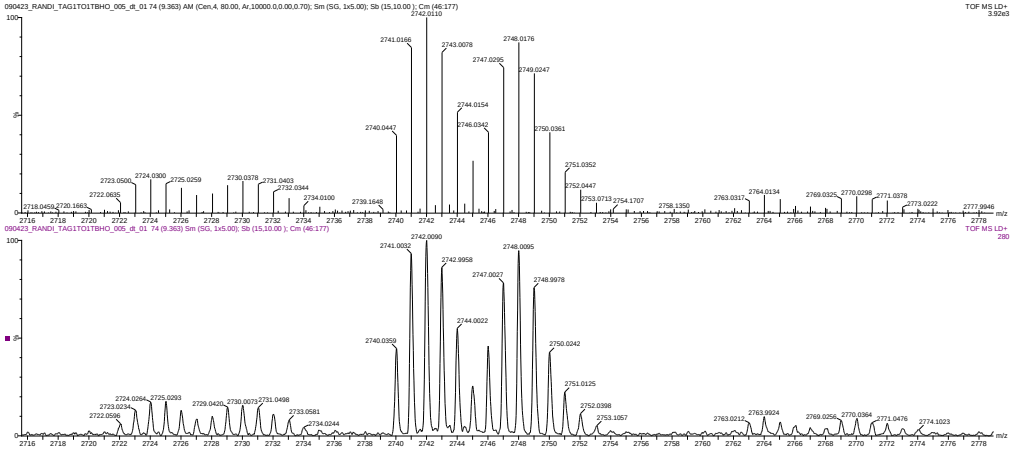

Sample 01-5

	mass	peak area
Tb	2741.0166	3.312e3
Ho	2747.0295	2.910e3

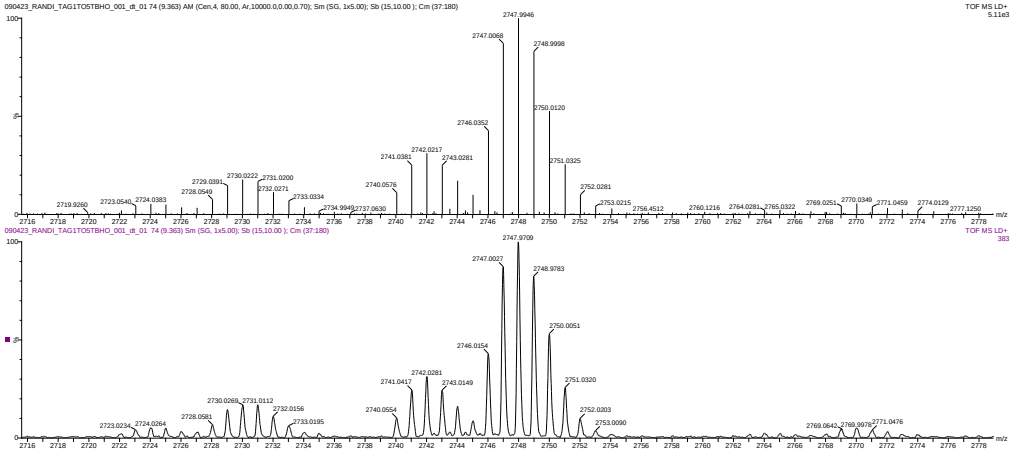

Sample 02-1

	mass	peak area
Tb	2741.0381	1.279e3
Ho	2747.0068	4.451e3

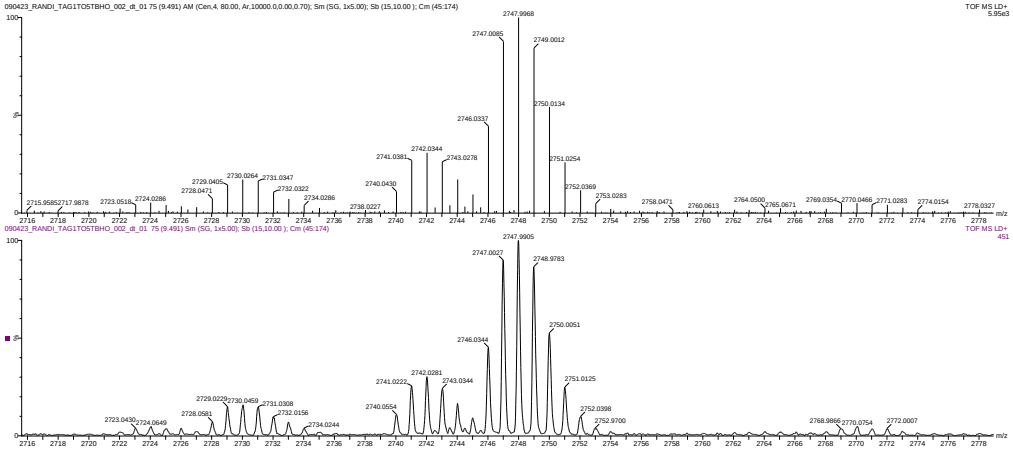

Sample 02-2

	mass	peak area
Tb	2741.0381	1.599e3
Ho	2747.0085	5.222e3

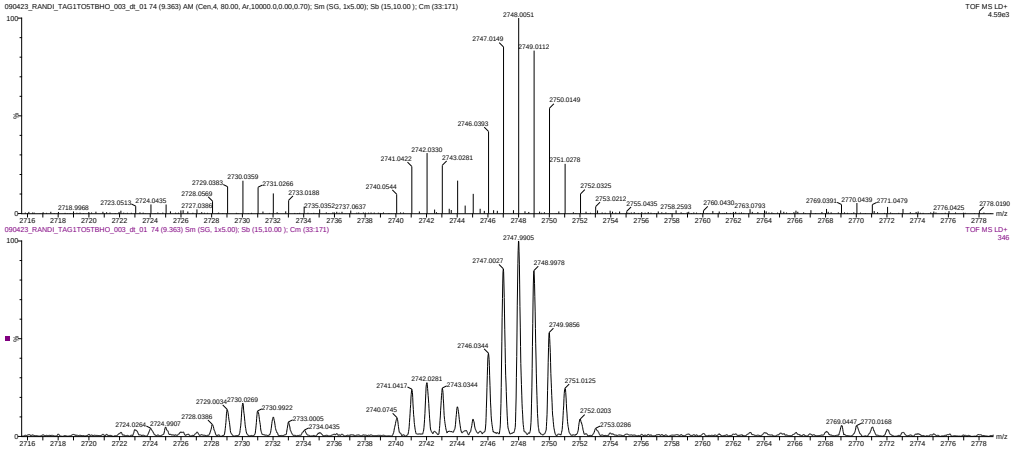

Sample 02-3

	mass	peak area
Tb	2741.0422	1.102e3
Ho	2747.0149	3.907e3

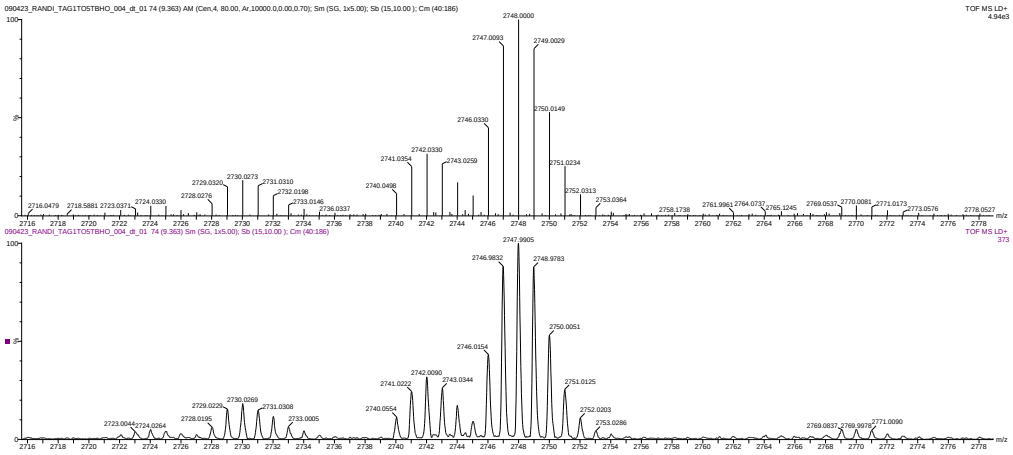

Sample 02-4

	mass	peak area
Tb	2741.0354	1.234e3
Ho	2747.0093	4.274e3

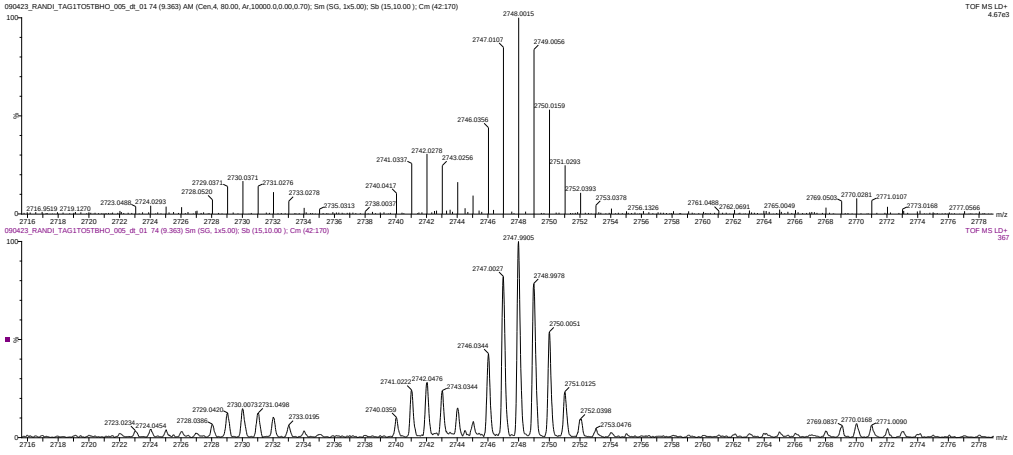

Sample 02-5

	mass	peak area
Tb	2741.0337	1.198e3
Ho	2747.0107	3.964e3

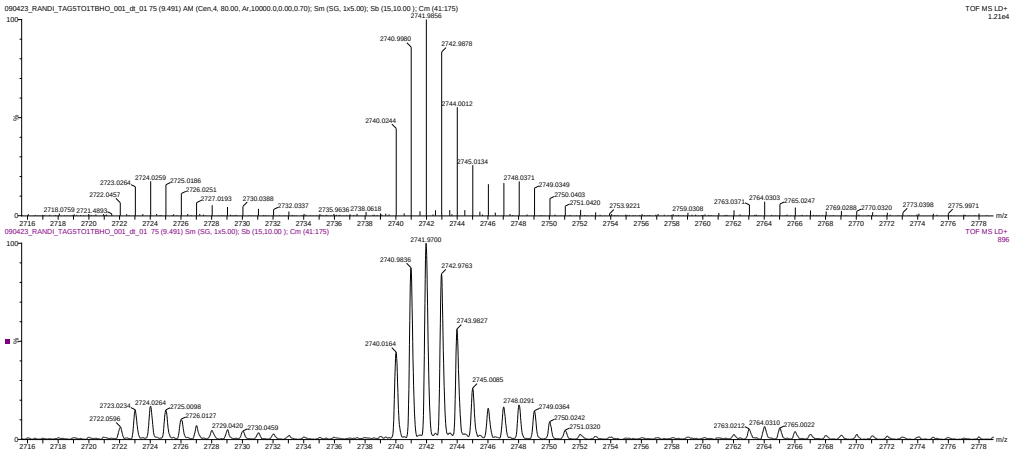

Sample 03-1

	mass	peak area
Tb	2741.9856	1.205e4
Ho	2748.0371	2.105e3

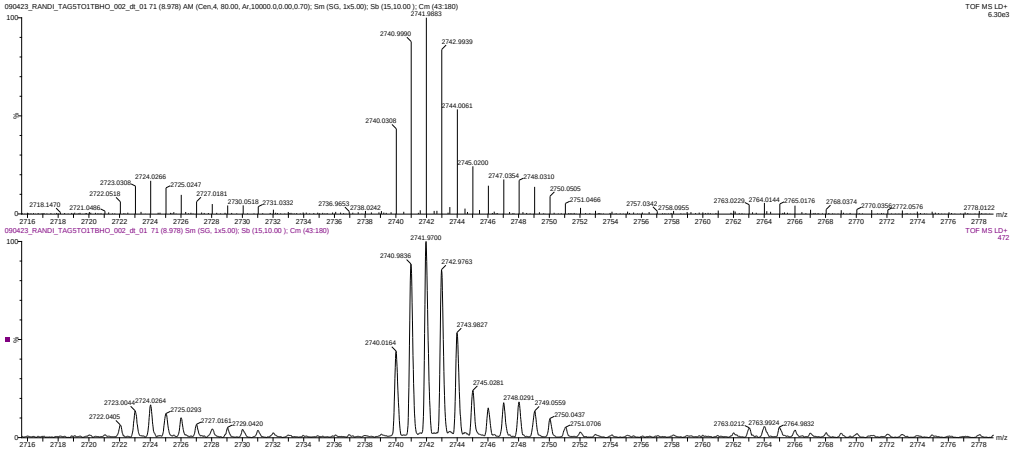

Sample 03-2

	mass	peak area
Tb	2741.9883	6.300e3
Ho	2748.0310	1.075e3

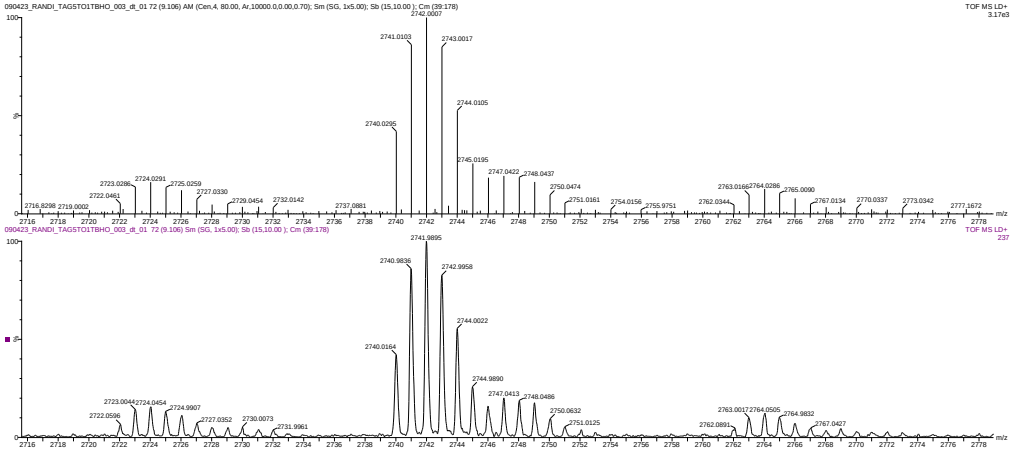

Sample 03-3

	mass	peak area
Tb	2741.0103	2.729e3
Ho	2742.0007	3.168e3

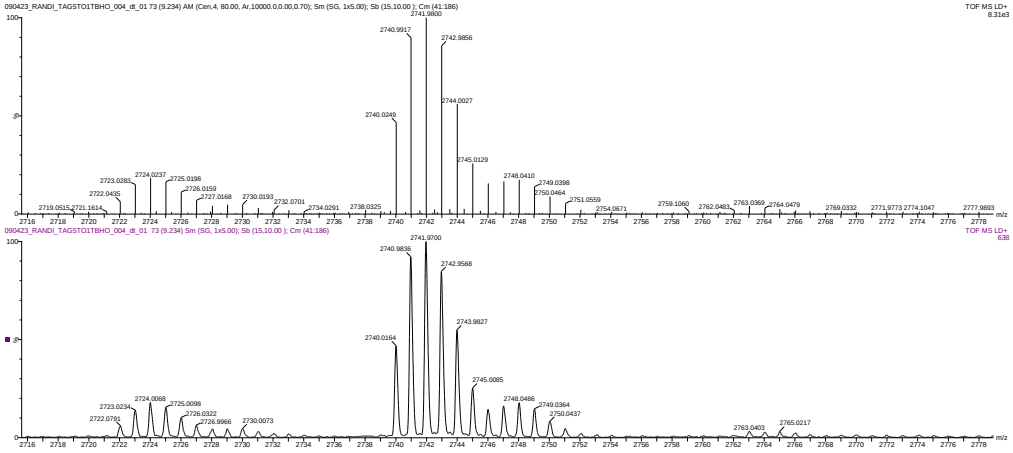

Sample 03-4

	mass	peak area
Tb	2741.9800	8.306e3
Ho	2747.0408	1.371e3

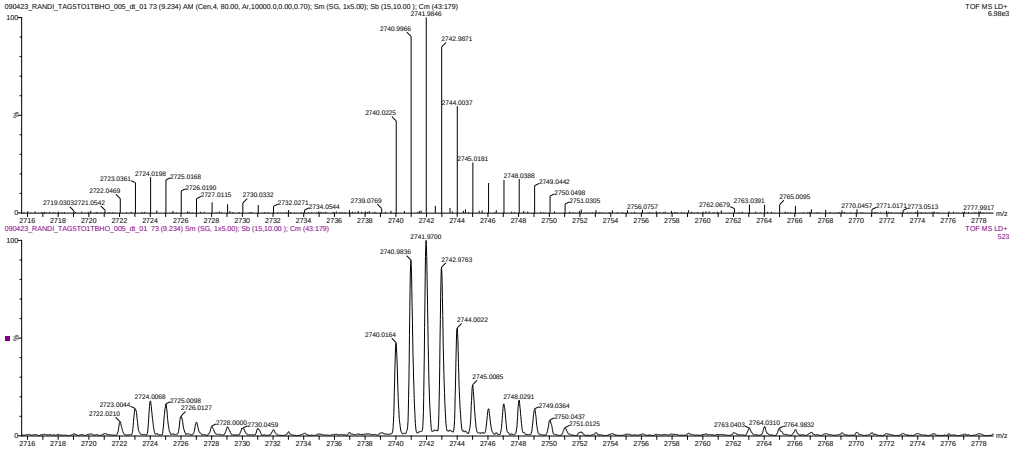

Sample 03-5

	mass	peak area
Tb	2741.9846	6.976e3
Ho	2747.0439	1.170e3

APPENDIX I. PART 2.

1 to 3 Tb to Ho-labeled beta-casein.

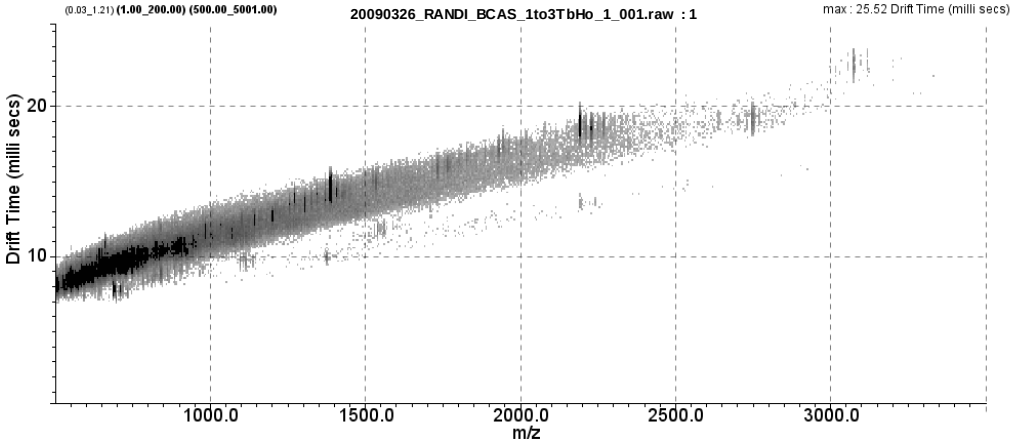

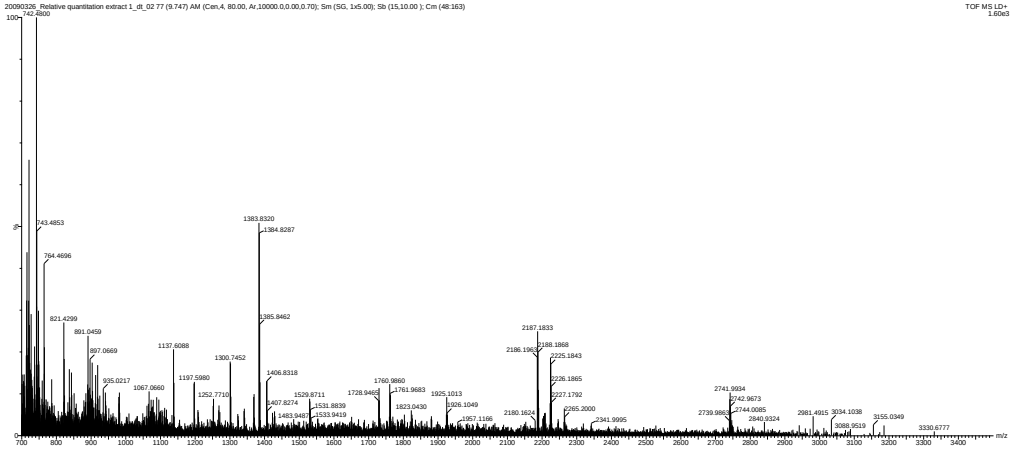

Sample 01 – 1

	mass	peak area
Tb	2741.9939	1.684e2
Ho	2747.0100	6.419e1

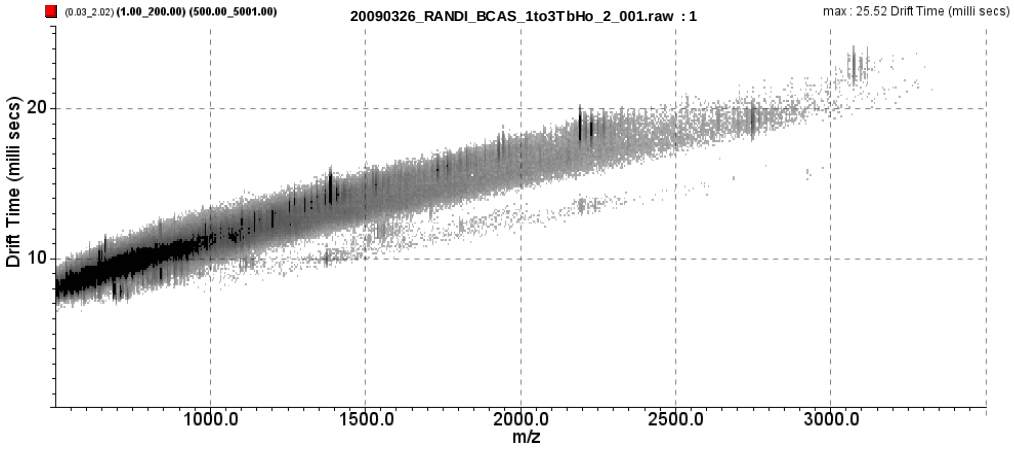

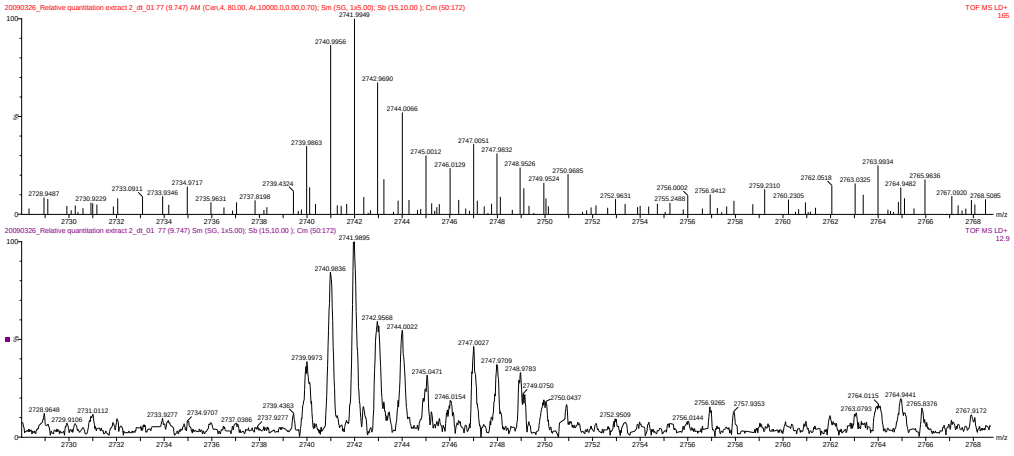

Sample 01-2

	mass	peak area
Tb	2740.9956	1.424e2
Ho	2747.0051	5.898e1

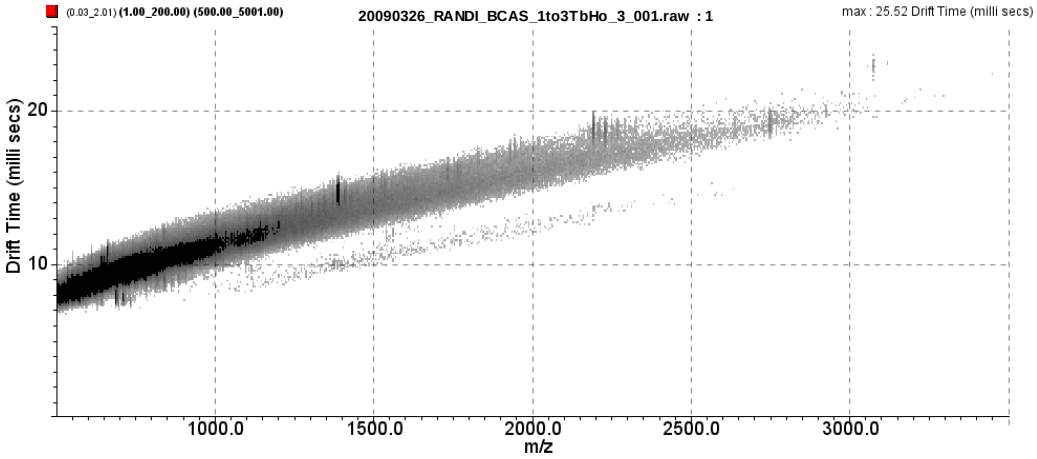

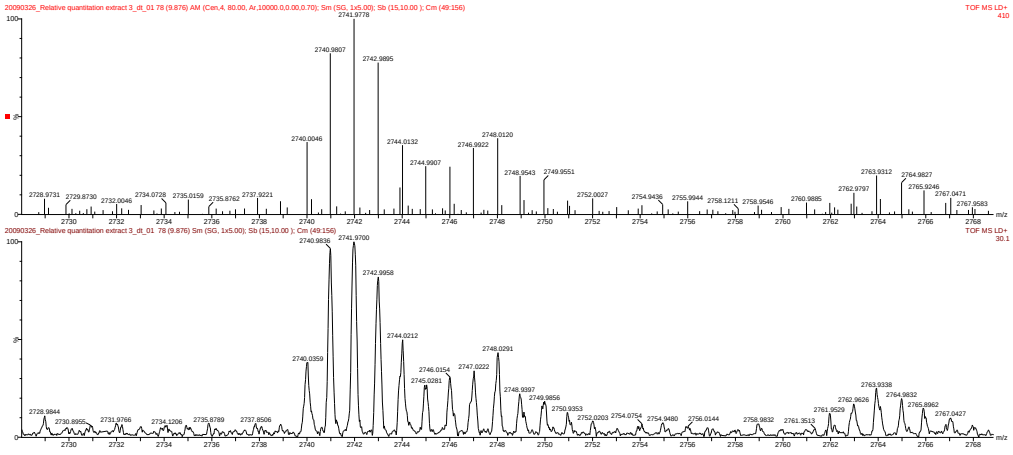

Sample 01-3

	mass	peak area
Tb	2740.9812	3.771e2
Ho	2747.0063	1.320e2

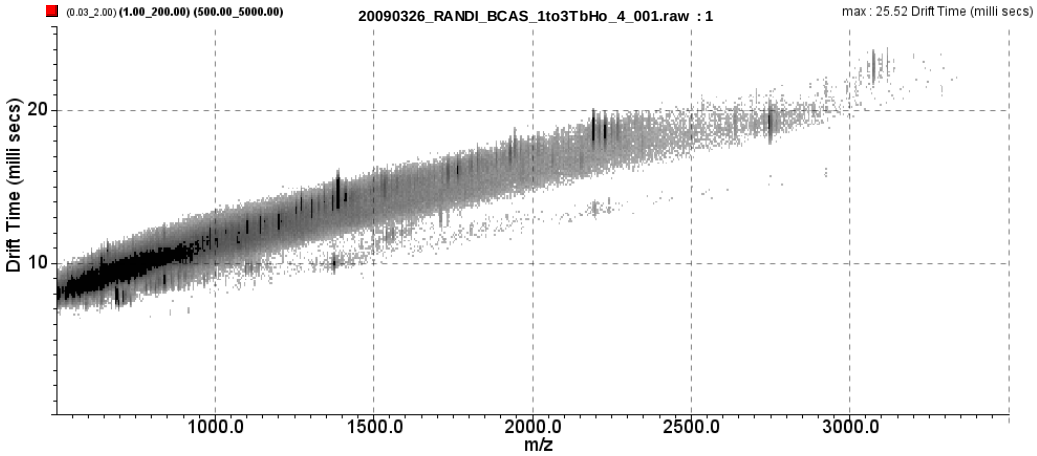

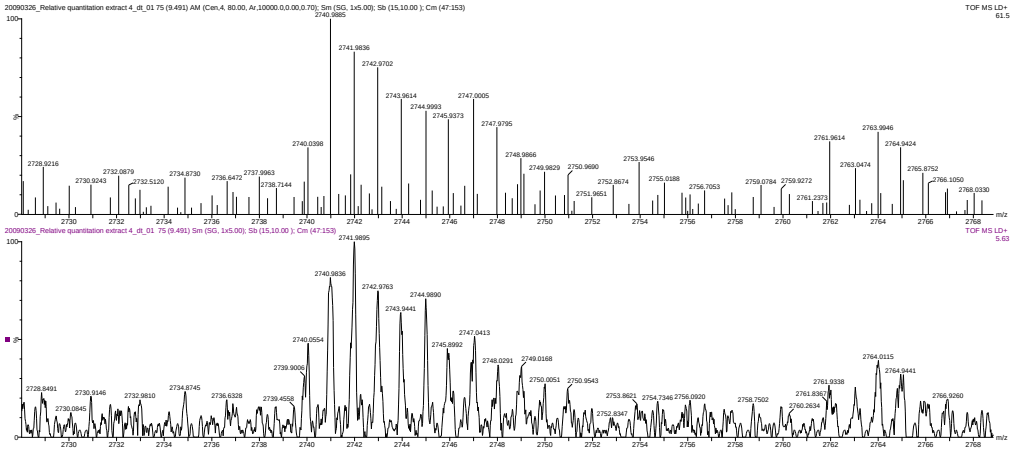

Sample 4

	mass	peak area
Tb	2740.9885	6.152e1
Ho	2747.0005	3.629e1

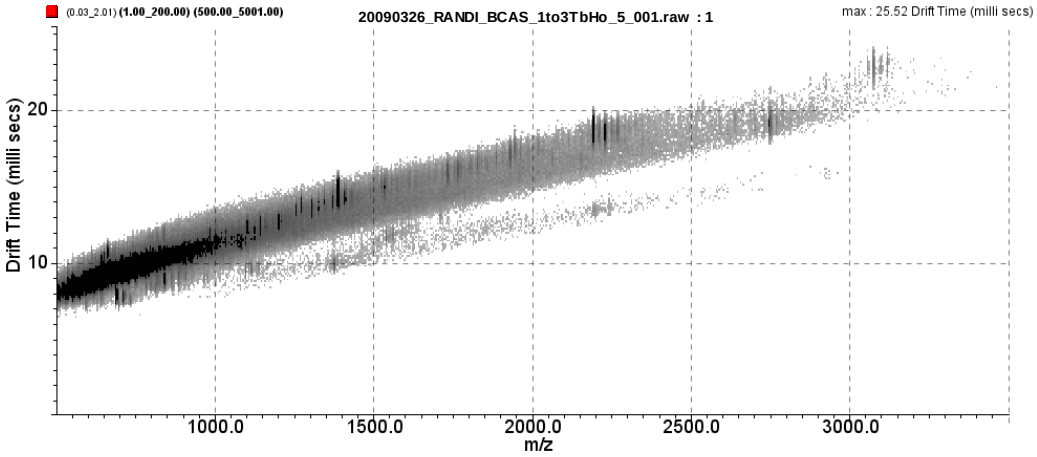

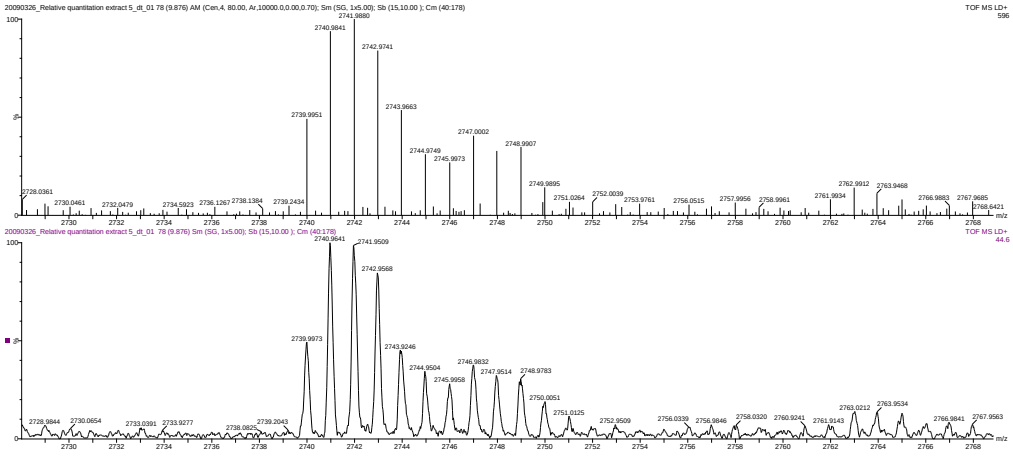

Sample 5

	mass	peak area
Tb	2740.9841	5.597e2
Ho	2747.0002	2.415e2

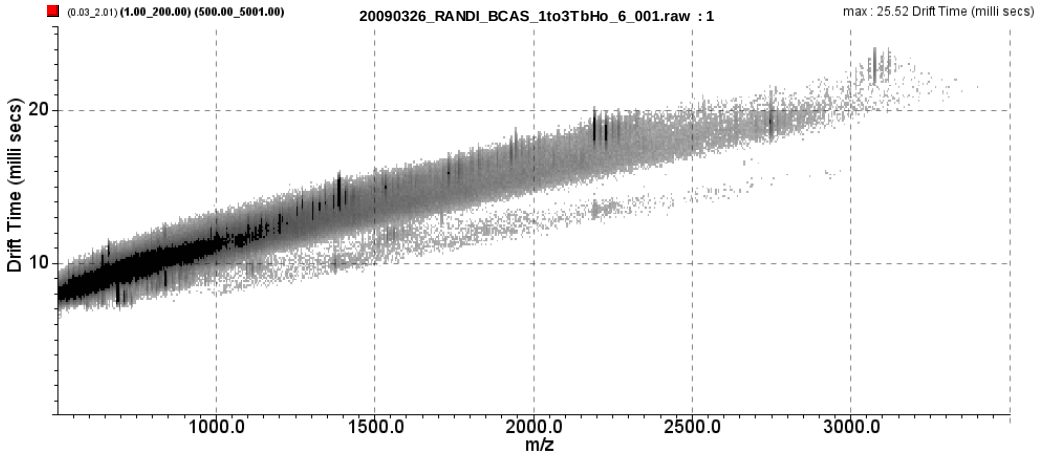

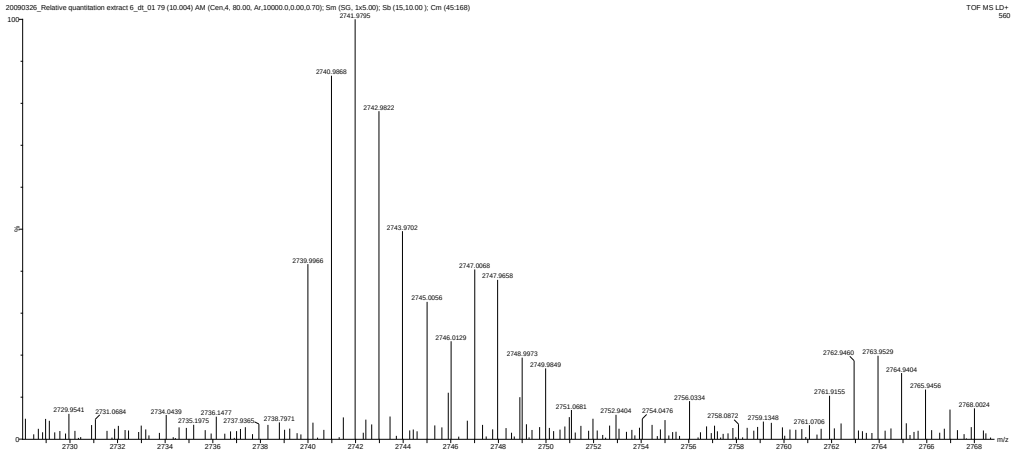

Sample 6

	mass	peak area
Tb	2740.9868	4.850e2
Ho	2747.0068	2.264e2

APPENDIX J

Predicted and observed ions for Tb-labeled FQSEEQQQTEDELQDK as represented in Figure 27.

Predicted b ion m/z				
	ion #	unlabeled **	Tb-labeled	Observed
F	1	---	---	---
Q	2	276.13	---	---
s*	3	443.13	1121.5766	1121.3558
E	4	572.18	1250.6192	1250.4181
E	5	701.22	1379.6618	1379.4369
Q	6	829.28	1507.7204	1507.5013
Q	7	957.34	1635.7790	1635.6525
Q	8	**1085.39**	1763.8375	1763.7114
T	9	1186.44	1864.8852	1864.681
E	10	1315.48	1993.9278	1993.8141
D	11	1430.51	2108.9548	2109.7825
E	12	1559.55	2237.9974	2237.8542
L	13	1672.64	2351.0814	2351.8511
Q	14	1800.70	2479.1400	2478.9624
D	15	1915.72	2594.1669	2594.0896
K	16	---		---

Predicted b-H2O ion m/z		
unlabeled **	Tb-labeled	Observed
---	---	---
---	---	---
---		---
554.1647	1232.6087	1232.3909
683.2072	1361.6512	1362.4300
811.2658	1489.7098	1490.47
939.3244	1617.7684	1617.6461
1067.383	1745.827	1745.6090
1168.4307	1846.8747	1846.7239
1297.4733	1975.9173	1975.7067
1412.5002	2090.9442	---
1541.5428	2219.9868	---
1654.6269	2333.0709	2333.9512
1782.6854	2461.1294	2461.7742
1897.7124	2576.1564	2576.0229
---	---	---

Predicted y ion m/z				
	ion #	unlabeled **	Tb-Labeled	Observed
F	16	---	---	---
Q	15	1914.7601	2593.2041	2593.052
s*	14	1786.7015	2465.1455	2466.0413
E	13	1619.7031	---	---
E	12	**1490.6605**	---	---
Q	11	**1361.6179**	---	---
Q	10	**1233.5594**	---	---
Q	9	**1105.5008**	---	---
T	8	**977.4422**	---	---
E	7	876.3945	---	---
D	6	747.3519	---	---
E	5	632.325	---	---
L	4	503.2824	---	---
Q	3	390.1983	---	---
D	2	262.1397	---	---
K	1	147.1128	---	---

Predicted y-H2O ion m/z		
unlabeled **	Tb-labeled	Observed
---	---	---
1896.7495	2575.1935	2575.0928
1768.6909	2447.1349	2446.9009
1601.6926	---	---
1472.65	---	---
1343.6074	---	---
1215.5488	---	---
1087.4902	---	---
959.4316	---	---
858.384	---	---
729.3414	---	---
614.3114	---	---
485.2718	---	---
372.1878	---	---
244.1292	---	---
---	---	---

*s,y,t = phosphorylated S,Y,T
** identified unlabeled ions indicated in bold

APPENDIX K

Beta-elimination/Michael addition typical spectra for labeled Erythropoietin as discussed in Chapter 5.

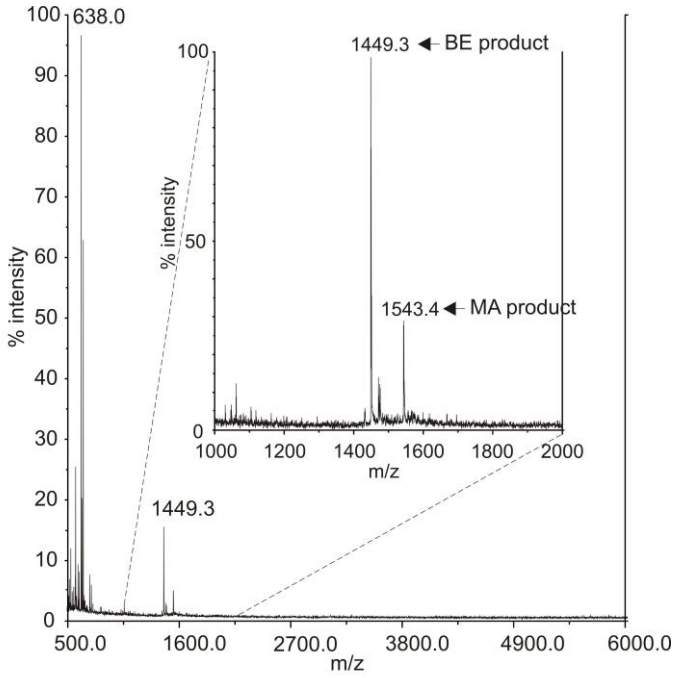

For the model O-linked GlcNAc glycopeptide Erythropoietin, beta-elimination was observed to go to completion. Michael addition was observed to be limited, and further work will show optimization of BEMA conditions to maximize the Michael addition product. Nonetheless, relative quantitation data may be achieved as the percent product yield is consistent between varying stoichiometries of samples.

APPENDIX L

Preliminary relative quantitation data for 1:1 molar ratios of Tb- and Ho-labeled erythropoietin.

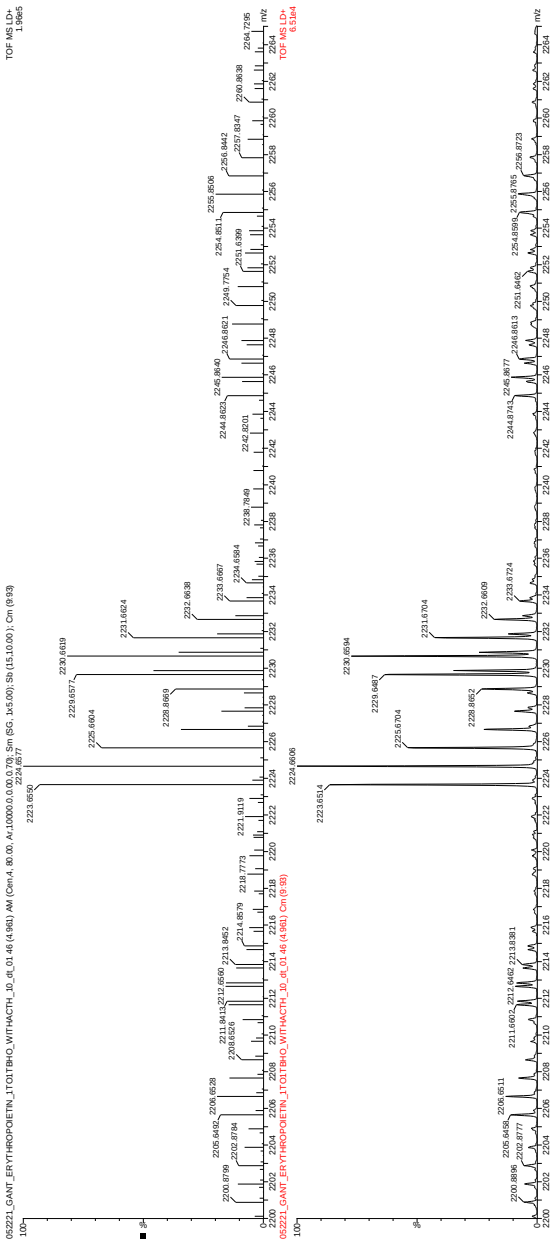

	m/z	peak area
Tb-label	2223.6550	1.829e5
Ho-labeled	2229.6577	1.527e5

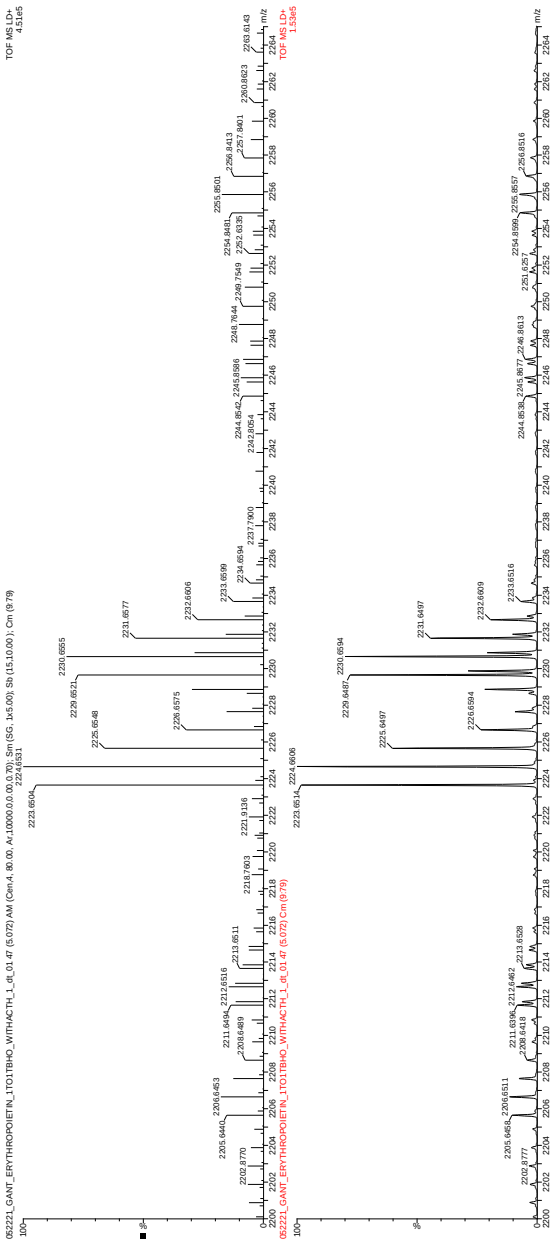

	m/z	peak area
Tb-labeled	2223.6504	4.267e5
Ho-labeled	2229.6521	3.480e5

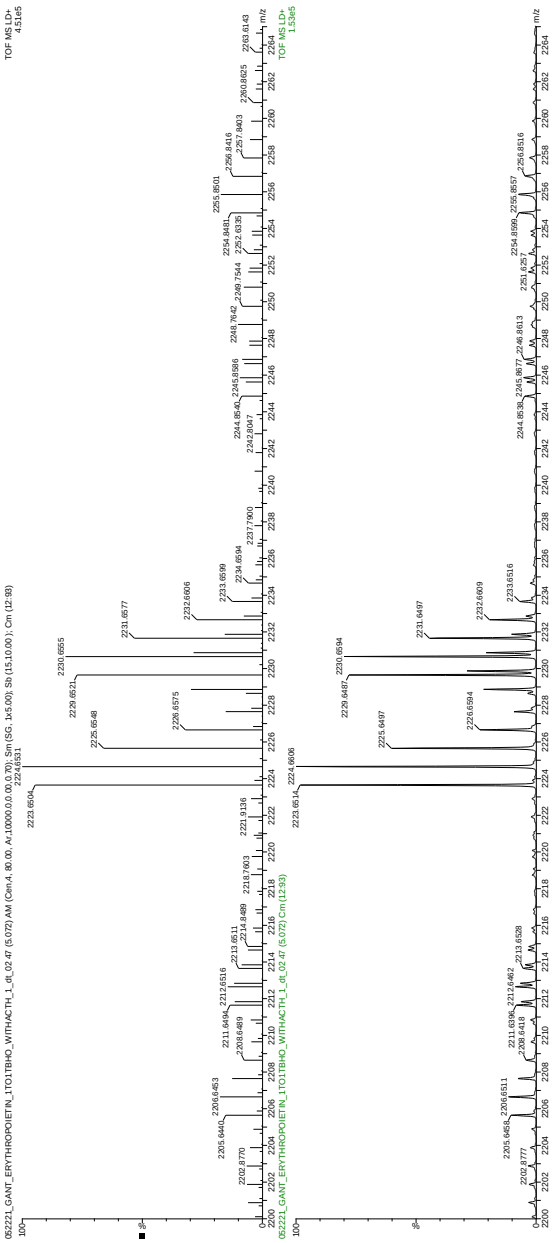

	m/z	peak area
Tb-labeled	2223.6504	4.265e5
Ho-labeled	2229.6521	3.479e5

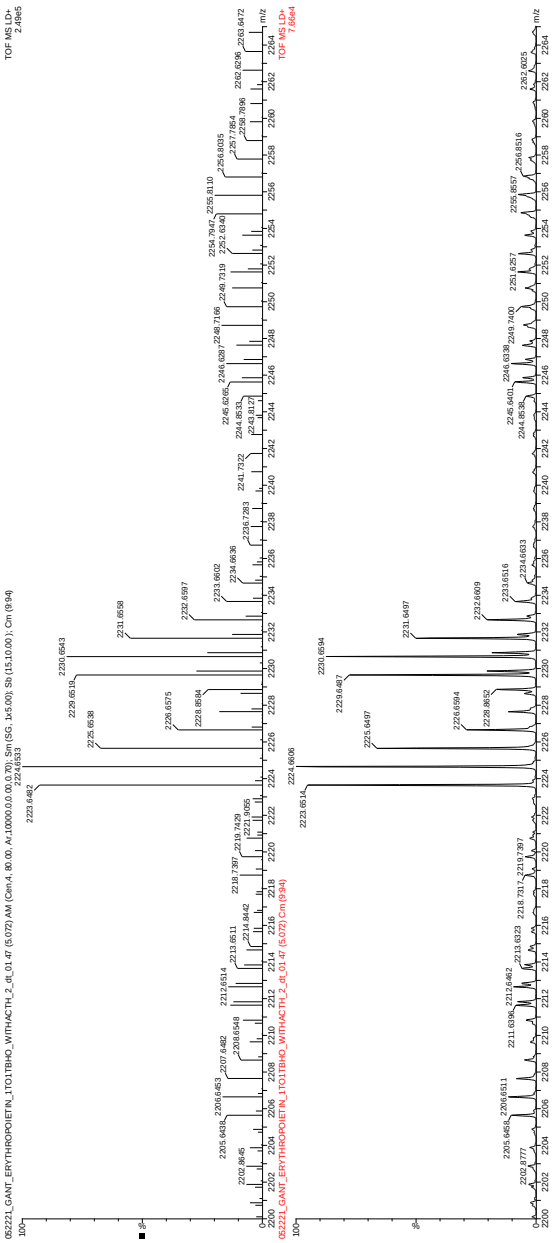

	m/z	peak area
Tb-labeled	2223.6482	2.309e5
Ho-labeled	2229.6519	1.925e5

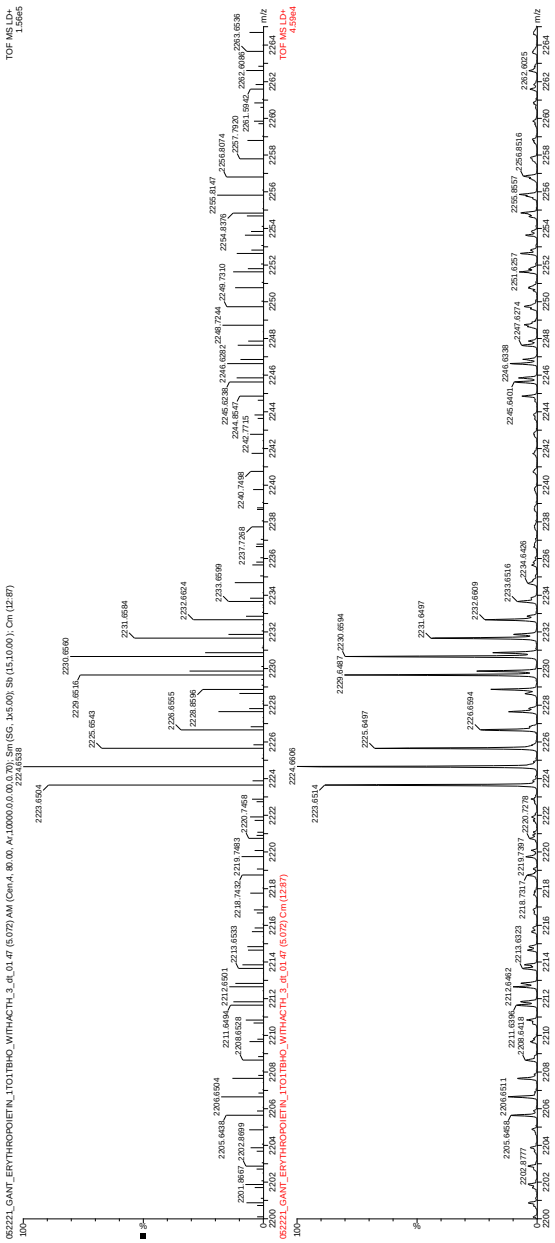

	m/z	peak area
Tb-labled	2223.6504	1.397e5
Ho-labeled	2229.6516	1.191e5

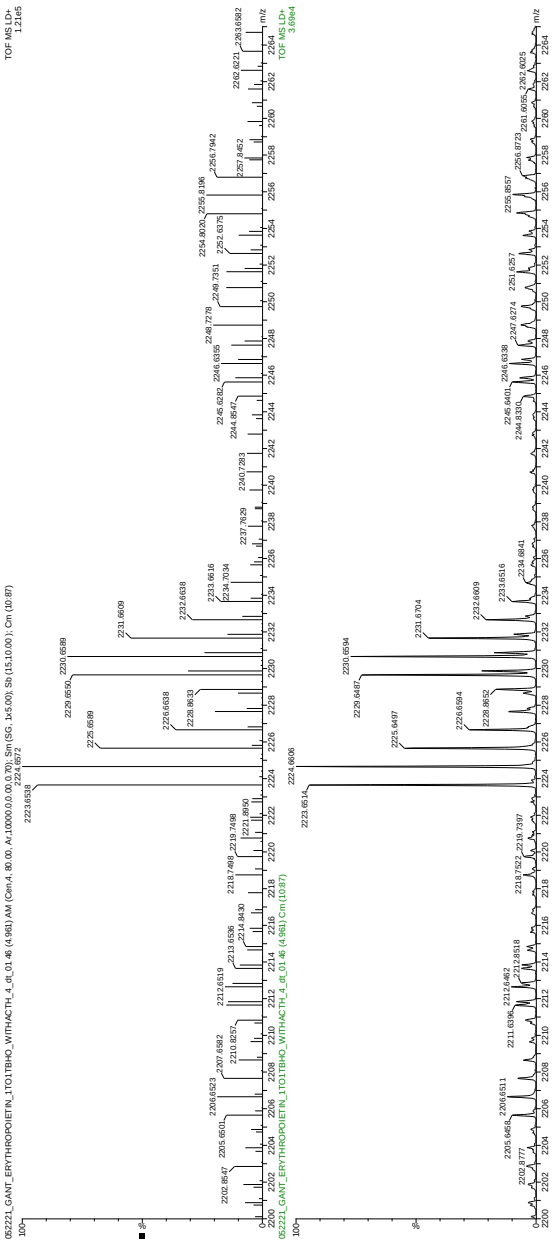

	m/z	peak area
Tb-labeled	2223.6538	1.129e5
Ho-labeled	2229.6550	9.525e4

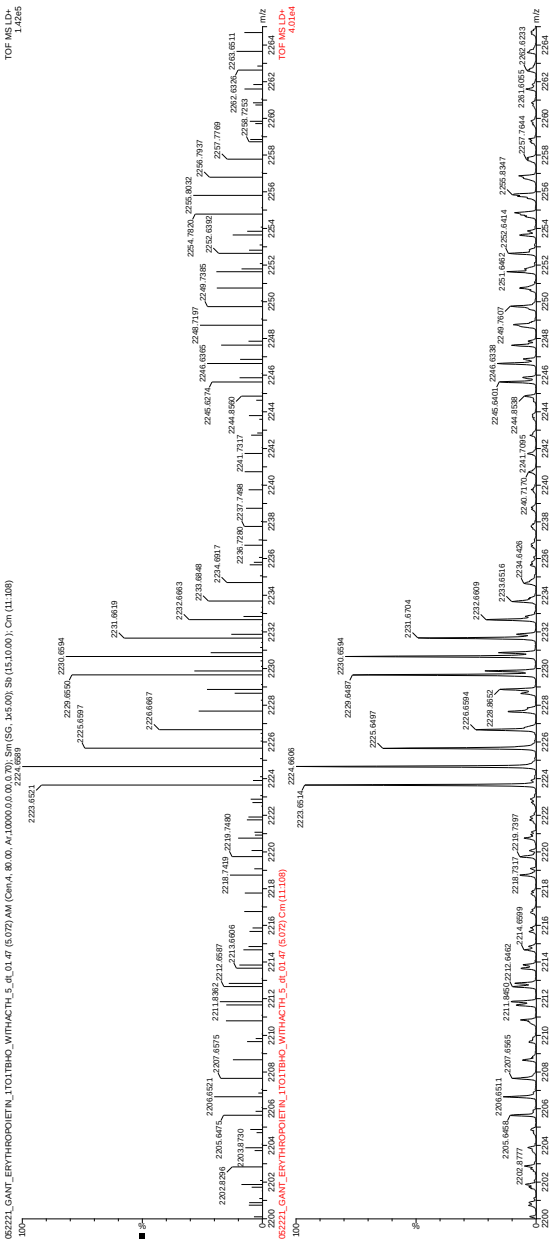

	m/z	peak area
Tb-labeled	2223.6521	1.303e5
Ho-labeled	2229.6550	1.124e5

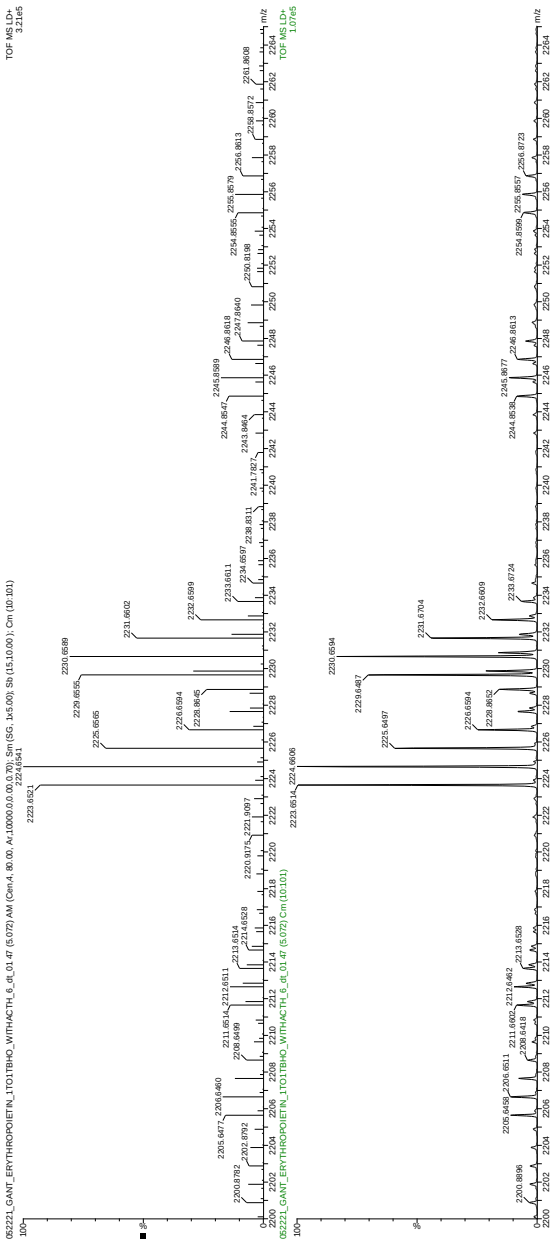

	m/z	peak area
Tb-labeled	2223.6521	2.984e5
Ho-labeled	2229.6555	2.435e5

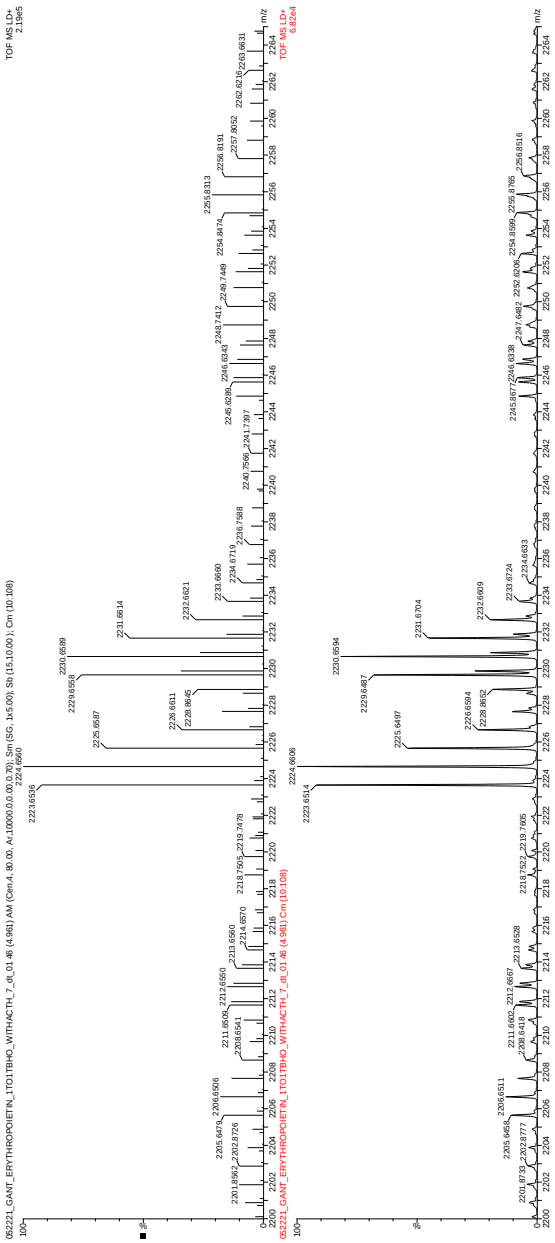

	m/z	peak area
Tb-labeled	2223.6536	2.017e5
Ho-labeled	2229.6558	1.654e5

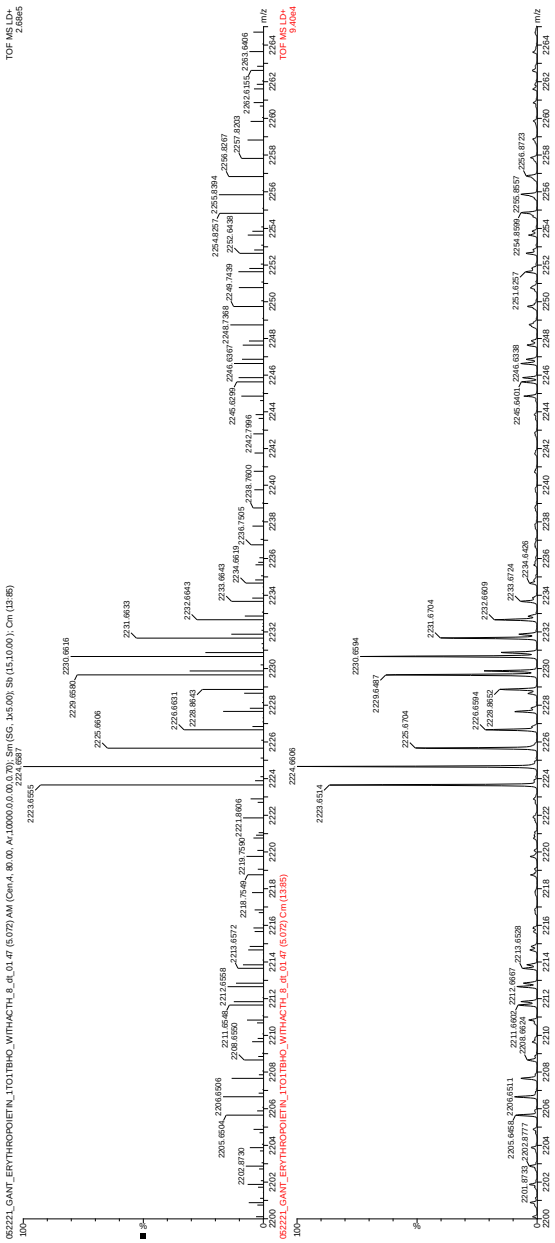

	m/z	peak area
Tb-labeled	2223.6555	2.483e5
Ho-labeled	2229.6580	2.075e5

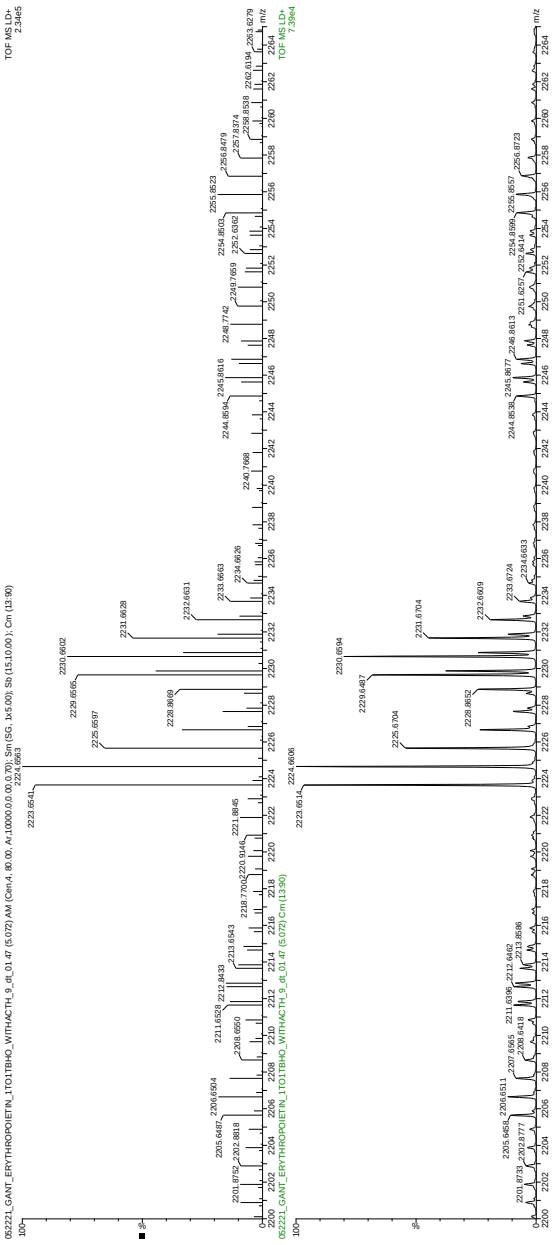

	m/z	peak area
Tb-labeled	2223.6541	2.210e5
Ho-labeled	2229.6565	1.796e5

APPENDIX N

References for the adaptation of chapters

Chapter 1:
Sections adapted from Randi L. Gant-Branum, Thomas J. Kerr, and John A. McLean, "Labeling Strategies in Mass Spectrometry-Based Protein Quantitation", *Analyst,* **2009**, *134*, 1525 – 1530.

Chapter 2:
Sections adapted from Randi L. Gant-Branum, Joshua A. Broussard, and John A. McLean, "Identification of Phosphorylation Sites within the Signaling Adaptor APPL1 by Mass Spectrometry." *J. Proteome Res.*, **2010**, *9* (3), 1541–1548.

Chapter 3:
Sections adapted from Relative Quantitation of Phosphorylated Peptides and Proteins using Phosphopeptide Element-Coded Affinity Tagging (PhECAT). In preparation for submission to *Bioconjugate Chemistry*.

Chapter 4:
Sections adapted from Relative Quantitation of Phosphorylated Peptides and Proteins using Phosphopeptide Element-Coded Affinity Tagging (PhECAT). In preparation for submission to *Bioconjugate Chemistry*.

(1) Floyd, R. A. *Exp. Biol. Med.* **1999**, *222*, 236-245.
(2) Kovacech, B.; Zilka, N.; Novak, M. *Cellular and Molecular Neurobiology* **2009**, *29*, 799-805.
(3) Liu, F.; Iqbal, K.; Grundke-Iqbal, I.; Hart, G. W.; Gong, C.-X. *Proceedings of the National Academy of Sciences of the United States of America* **2004**, *101*, 10804-10809.
(4) Shental-Bechor, D.; Levy, Y. *Proceedings of the National Academy of Sciences* **2008**, *105*, 8256-8261.
(5) Hitosugi, T.; Kang, S.; Vander Heiden, M. G.; Chung, T.-W.; Elf, S.; Lythgoe, K.; Dong, S.; Lonial, S.; Wang, X.; Chen, G. Z.; Xie, J.; Gu, T.-L.; Polakiewicz, R. D.; Roesel, J. L.; Boggon, T. J.; Khuri, F. R.; Gilliland, D. G.; Cantley, L. C.; Kaufman, J.; Chen, J. *Sci. Signal.* **2009**, *2*, ra73-.
(6) Savage, K.; Baur, P. *J Cell Sci* **1983**, *64*, 295-306.
(7) Mimura, Y.; Sondermann, P.; Ghirlando, R.; Lund, J.; Young, S. P.; Goodall, M.; Jefferis, R. *Journal of Biological Chemistry* **2001**, *276*, 45539-45547.
(8) Parekh, R. B.; Dwek, R. A.; Sutton, B. J.; Fernandes, D. L.; Leung, A.; Stanworth, D.; Rademacher, T. W.; Mizuochi, T.; Taniguchi, T.; Matsuta, K.; Takeuchi, F.; Nagano, Y.; Miyamoto, T.; Kobata, A. *Nature* **1985**, *316*, 452-457.
(9) Gant-Branum, R. L.; Kerr, T. J.; McLean, J. A. *The Analyst* **2009**, *134*, 1525-1530.
(10) Manning, G.; Whyte, D. B.; Martinez, R.; Hunter, T.; Sudarsanam, S. *Science* **2002**, *298*, 1912-1934.
(11) Thingholm, T. E.; Jensen, O. N.; Larsen, M. R.; WILEY-VCH Verlag, 2009; Vol. 9, pp 1451-1468.
(12) Reinders, J.; Sickmann, A.; WILEY-VCH Verlag, 2005; Vol. 5, pp 4052-4061.
(13) Chen, P.-L.; Scully, P.; Shew, J.-Y.; Wang, J. Y. J.; Lee, W.-H. *Cell* **1989**, *58*, 1193-1198.
(14) Webb, D. J.; Schroeder, M. J.; Brame, C. J.; Whitmore, L.; Shabanowitz, J.; Hunt, D. F.; Horwitz, A. R. *J Cell Sci* **2005**, *118*, 4925-4929.
(15) Webb, D. J.; Donais, K.; Whitmore, L. A.; Thomas, S. M.; Turner, C. E.; Parsons, J. T.; Horwitz, A. F. *Nat Cell Biol* **2004**, *6*, 154-161.
(16) Webb, D. J.; Kovalenko, M.; Whitmore, L.; Horwitz, A. F. *Biochemical and Biophysical Research Communications* **2006**, *346*, 1284-1288.
(17) Webb, D. J.; Mayhew, M. W.; Kovalenko, M.; Schroeder, M. J.; Jeffery, E. D.; Whitmore, L.; Shabanowitz, J.; Hunt, D. F.; Horwitz, A. F. *J Cell Sci* **2006**, *119*, 2847-2850.
(18) Gant-Branum, R. L.; Broussard, J. A.; Mahsut, A.; Webb, D. J.; McLean, J. A. *Journal of Proteome Research* **2010**, *9*, 1541-1548.
(19) Matsuoka, S.; Ballif, B. A.; Smogorzewska, A.; McDonald, E. R.; Hurov, K. E.; Luo, J.; Bakalarski, C. E.; Zhao, Z.; Solimini, N.; Lerenthal, Y.; Shiloh, Y.; Gygi, S. P.; Elledge, S. J. *Science* **2007**, *316*, 1160-1166.

(20) Graves, J. D.; Krebs, E. G. *Pharmacology & Therapeutics* **1999** *82*, 111-121.
(21) López, E. M., R.; López, I.; Ashman, K.; Mendieta, J.; Wesselink, J.; Gómez-Puertas, P.; Ferreir, A. *Journal of Integrated OMICS* **2010**, *accepted October 2010*.
(22) Hunter, T. *Cell* **2000**, *100*, 113-127.
(23) Mann, M.; Ong, S.-E.; Grønborg, M.; Steen, H.; Jensen, O. N.; Pandey, A. *Trends in Biotechnology* **2002**, *20*, 261-268.
(24) Palumbo, A. M.; Reid, G. E. *Analytical Chemistry* **2008**, *80*, 9735-9747.
(25) Palumbo, A. M.; Tepe, J. J.; Reid, G. E. *Journal of Proteome Research* **2008**, *7*, 771-779.
(26) Apweiler, R.; Hermjakob, H.; Sharon, N. *Biochimica et Biophysica Acta (BBA) - General Subjects* **1999**, *1473*, 4-8.
(27) Becker, K. L. *Principles and practice of endocrinology and metabolism*; Lippincott Williams & Wilkins, 2001.
(28) Taoka, K.-i.; Ham, B.-K.; Xoconostle-Cazares, B.; Rojas, M. R.; Lucas, W. J. *Plant Cell* **2007**, *19*, 1866-1884.
(29) Chen, D.; Juarez, S.; Hartweck, L.; Alamillo, J. M.; Simon-Mateo, C.; Perez, J. J.; Fernandez-Fernandez, M. R.; Olszewski, N. E.; Garcia, J. A. *J. Virol.* **2005**, *79*, 9381-9387.
(30) Haines, N.; Irvine, K. D. *Nat Rev Mol Cell Biol* **2003**, *4*, 786-797.
(31) Varki, A. C., R.D.; Esko, J.D.; Freeze, H.H.; Stanley, P.; Bertozzi, C.R.; Hart, G.W. and Etzler, M.E., Ed. *Essentials of Glycobiology*, 2nd ed.; Cold Spring Harbor Laboratory Press: Cold Spring Harbor 2009.
(32) Huhn, C.; Selman, M. H. J.; Ruhaak, L. R.; Deelder, A. M.; Wuhrer, M. *PROTEOMICS* **2009**, *9*, 882-913.
(33) Jacquemin, M.; Radcliffe, C. M.; Laven'homme, R.; Wormald, M. R.; Vanderelst, L.; Wallays, G.; Dewaele, J.; Colllen, D.; Vermylen, J.; Dwek, R. A.; Saint-Remy, J.-M.; Rudd, P. M.; Dewerchin, M. *Journal of Thrombosis and Haemostasis* **2006**, *4*, 1047-1055.
(34) Kaneko, Y.; Nimmerjahn, F.; Ravetch, J. V. *Science* **2006**, *313*, 670-673.
(35) Mori, K.; Iida, S.; Yamane-Ohnuki, N.; Kanda, Y.; Kuni-Kamochi, R.; Nakano, R.; Imai-Nishiya, H.; Okazaki, A.; Shinkawa, T.; Natsume, A.; Niwa, R.; Shitara, K.; Satoh, M. *Cytotechnology* **2007**, *55*, 109-114.
(36) Hartweck, L. M.; Scott, C. L.; Olszewski, N. E. *Genetics* **2002**, *161*, 1279-1291.
(37) Shafi, R.; Iyer, S. P. N.; Ellies, L. G.; O'Donnell, N.; Marek, K. W.; Chui, D.; Hart, G. W.; Marth, J. D. *Proceedings of the National Academy of Sciences of the United States of America* **2000**, *97*, 5735-5739.
(38) Vosseller, K.; Wells, L.; Lane, M. D.; Hart, G. W. *Proceedings of the National Academy of Sciences of the United States of America* **2002**, *99*, 5313-5318.
(39) Boyle, W. J.; van der Geer, P.; Hunter, T.; Tony, H.; Bartholomew, M. S. In *Methods in Enzymology*; Academic Press, 1991; Vol. Volume 201, pp 110-149.

(40) Loo, R. R. O.; Mitchell, C.; Stevenson, T. I.; Martin, S. A.; Hines, W. M.; Juhasz, P.; Patterson, D. H.; Peltier, J. M.; Loo, J. A.; Andrews, P. C. *ELECTROPHORESIS* **1997**, *18*, 382-390.
(41) Neville, D. C. A.; Townsend, R. R.; Rozanas, C. R.; Verkman, A. S.; Price, E. M.; Gruis, D. B. *Protein Science* **1997**, *6*, 2436-2445.
(42) Porath, J.; Carlsson, J. A. N.; Olsson, I.; Belfrage, G. *Nature* **1975**, *258*, 598-599.
(43) Zhong, J.; Molina, H.; Pandey, A. *Phosphoproteomics*; John Wiley & Sons, Inc., 2001.
(44) Marcus, K.; Immler, D.; Sternberger, J.; Meyer, H. E. *ELECTROPHORESIS* **2000**, *21*, 2622-2636.
(45) Sun, T.; Campbell, M.; Gordon, W.; Arlinghaus, R. B.; John Wiley & Sons, Inc., 2001; Vol. 60, pp 61-75.
(46) Desiderio, D. M.; Kai, M. *Biological Mass Spectrometry* **1983**, *10*, 471-479.
(47) Mirgorodskaya, O. A.; Kozmin, Y. P.; Titov, M. I.; Körner, R.; Sönksen, C. P.; Roepstorff, P.; John Wiley & Sons, Ltd., 2000; Vol. 14, pp 1226-1232.
(48) Yao, X.; Freas, A.; Ramirez, J.; Demirev, P. A.; Fenselau, C. *Analytical Chemistry* **2001**, *73*, 2836-2842.
(49) Ong, S.-E.; Blagoev, B.; Kratchmarova, I.; Kristensen, D. B.; Steen, H.; Pandey, A.; Mann, M. *Mol Cell Proteomics* **2002**, M200025-MCP200200.
(50) Ahrends, R.; Pieper, S.; Kuhn, A.; Weisshoff, H.; Hamester, M.; Lindemann, T.; Scheler, C.; Lehmann, K.; Taubner, K.; Linscheid, M. W. *Mol Cell Proteomics* **2007**, *6*, 1907-1916.
(51) Chen, M.; Su, X.; Yang, J.; Jenkins, C. M.; Cedars, A. M.; Gross, R. W. *Analytical Chemistry* **2009**, *82*, 163-171.
(52) Goshe, M. B.; Conrads, T. P.; Panisko, E. A.; Angell, N. H.; Veenstra, T. D.; Smith, R. D. *Analytical Chemistry* **2001**, *73*, 2578-2586.
(53) Gygi, S. P.; Rist, B.; Gerber, S. A.; Turecek, F.; Gelb, M. H.; Aebersold, R. *Nat Biotech* **1999**, *17*, 994-999.
(54) Kerr, T. J.; McLean, J. A. *Chemical Communications*, *46*, 5479-5481.
(55) Liu, H.; Zhang, Y.; Wang, J.; Wang, D.; Zhou, C.; Cai, Y.; Qian, X. *Analytical Chemistry* **2006**, *78*, 6614-6621.
(56) Oda, Y.; Huang, K.; Cross, F. R.; Cowburn, D.; Chait, B. T. *Proceedings of the National Academy of Sciences of the United States of America* **1999**, *96*, 6591-6596.
(57) Qian, W.-J.; Goshe, M. B.; Camp, D. G.; Yu, L.-R.; Tang, K.; Smith, R. D. *Analytical Chemistry* **2003**, *75*, 5441-5450.
(58) Whetstone, P. A.; Butlin, N. G.; Corneillie, T. M.; Meares, C. F. *Bioconjugate Chemistry* **2004**, *15*, 3-6.
(59) Ross, P. L.; Huang, Y. N.; Marchese, J. N.; Williamson, B.; Parker, K.; Hattan, S.; Khainovski, N.; Pillai, S.; Dey, S.; Daniels, S.; Purkayastha, S.; Juhasz, P.; Martin, S.; Bartlet-Jones, M.; He, F.; Jacobson, A.; Pappin, D. J. *Molecular & Cellular Proteomics* **2004**, *3*, 1154-1169.
(60) Zieske, L. R. *Journal of Experimental Botany* **2006**, *57*, 1501-1508.

(61) Shadforth, I.; Dunkley, T.; Lilley, K.; Bessant, C. *BMC Genomics* **2005**, *6*, 145.
(62) Zhou, H.; Watts, J. D.; Aebersold, R. *Nat Biotech* **2001**, *19*, 375-378.
(63) Wada, Y.; Azadi, P.; Costello, C. E.; Dell, A.; Dwek, R. A.; Geyer, H.; Geyer, R.; Kakehi, K.; Karlsson, N. G.; Kato, K.; Kawasaki, N.; Khoo, K.-H.; Kim, S.; Kondo, A.; Lattova, E.; Mechref, Y.; Miyoshi, E.; Nakamura, K.; Narimatsu, H.; Novotny, M. V.; Packer, N. H.; Perreault, H.; Peter-Katalinic, J.; Pohlentz, G.; Reinhold, V. N.; Rudd, P. M.; Suzuki, A.; Taniguchi, N. *Glycobiology* **2007**, *17*, 411-422.
(64) Harvey, D. J. *Expert Review of Proteomics* **2005**, *2*, 87-101.
(65) Tao, L.; McLean, J. R.; McLean, J. A.; Russell, D. H. *Journal of the American Society for Mass Spectrometry* **2007**, *18*, 1232-1238.
(66) Fenn, L.; Kliman, M.; Mahsut, A.; Zhao, S.; McLean, J. *Analytical and Bioanalytical Chemistry* **2009**, *394*, 235-244.
(67) Kliman, M.; Vijayakrishnan, N.; Wang, L.; Tapp, J. T.; Broadie, K.; McLean, J. A. *Molecular BioSystems* **2010**, *6*, 958-966.
(68) McLean, J. A.; Ruotolo, B. T.; Gillig, K. J.; Russell, D. H. *International Journal of Mass Spectrometry* **2005**, *240*, 301-315.
(69) Ruotolo, B. T.; Gillig, K. J.; Woods, A. S.; Egan, T. F.; Ugarov, M. V.; Schultz, J. A.; Russell, D. H. *Analytical Chemistry* **2004**, *76*, 6727-6733.
(70) Fenn, L. S.; McLean, J. A. *Molecular BioSystems* **2009**, *5*, 1298-1302.
(71) McLean, J. A., Russell, D. H *American Biotechnology Laboratory* **2005**, *23*, 18-21.
(72) Hilderbrand, A. E.; Myung, S.; Clemmer, D. E. *Analytical Chemistry* **2006**, *78*, 6792-6800.
(73) McLean, J. A.; Ridenour, W. B.; Caprioli, R. M.; John Wiley & Sons, Ltd., 2007; Vol. 42, pp 1099-1105.
(74) Howdle, M. D.; Eckers, C.; Laures, A. M. F.; Creaser, C. S. *Journal of the American Society for Mass Spectrometry* **2009**, *20*, 1-9.
(75) Corneillie, T. M.; Lee, K. C.; Whetstone, P. A.; Wong, J. P.; Meares, C. F. *Bioconjugate Chemistry* **2004**, *15*, 1392-1402.
(76) Clark, R. C.; Dijkstra, J. *International Journal of Biochemistry* **1980**, *11*, 577-585.
(77) Clark, R. C. *International Journal of Biochemistry* **1981**, *13*, 233-236.
(78) Annan, W. D.; Manson, W.; Nimmo, J. A. *Analytical Biochemistry* **1982**, *121*, 62-68.
(79) Meyer, H. E.; Hoffmann-Posorske, E.; Korte, H.; Heilmeyer jr, L. M. G. *FEBS Letters* **1986**, *204*, 61-66.
(80) Poot, A. J.; Ruijter, E.; Nuijens, T.; Dirksen, E. H. C.; Heck, A. J. R.; Slijper, M.; Rijkers, D. T. S.; Liskamp, R. M. J.; WILEY-VCH Verlag, 2006; Vol. 6, pp 6394-6399.
(81) Zheng, Y.; Guo, Z.; Cai, Z. *Talanta* **2009**, *78*, 358-363.
(82) Mitsuuchi, Y. J., Steven W.; Sonoda, Gonosuke; Tanno, Satoshi; Golemis,Erica A.; and Testa Joseph R. *Oncogene* **1999**, *18*, 8.
(83) Deepa, S. S.; Dong, L. Q. *American Journal of Physiology - Endocrinology And Metabolism* **2009**, *296*, E22-E36.

(84) Dephoure, N.; Zhou, C.; VillÃ©n, J.; Beausoleil, S. A.; Bakalarski, C. E.; Elledge, S. J.; Gygi, S. P. *Proceedings of the National Academy of Sciences* **2008**, *105*, 10762-10767.
(85) Sugiyama, N.; Masuda, T.; Shinoda, K.; Nakamura, A.; Tomita, M.; Ishihama, Y. *Molecular & Cellular Proteomics* **2007**, *6*, 1103-1109.
(86) Beausoleil, S. A.; Jedrychowski, M.; Schwartz, D.; Elias, J. E.; VillÃ©n, J.; Li, J.; Cohn, M. A.; Cantley, L. C.; Gygi, S. P. *Proceedings of the National Academy of Sciences of the United States of America* **2004**, *101*, 12130-12135.
(87) Ballif, B. A.; VillÃ©n, J.; Beausoleil, S. A.; Schwartz, D.; Gygi, S. P. *Molecular & Cellular Proteomics* **2004**, *3*, 1093-1101.
(88) Miaczynska, M.; Christoforidis, S.; Giner, A.; Shevchenko, A.; Uttenweiler-Joseph, S.; Habermann, B.; Wilm, M.; Parton, R. G.; Zerial, M. *Cell* **2004**, *116*, 445-456.
(89) Habermann, B. *EMBO reports* **2004**, *5*, 6.
(90) VÃ¡rnai, P. t.; Lin, X.; Lee, S. B.; Tuymetova, G.; Bondeva, T.; SpÃ¤t, A.; Rhee, S. G.; HajnÃ³czky, G. r.; Balla, T. *Journal of Biological Chemistry* **2002**, *277*, 27412-27422.
(91) Schenck, A.; Goto-Silva, L.; Collinet, C.; Rhinn, M.; Giner, A.; Habermann, B.; Brand, M.; Zerial, M. *Cell* **2008**, *133*, 486-497.
(92) Li, J.; Mao, X.; Dong, L. Q.; Liu, F.; Tong, L. *Structure* **2007**, *15*, 525-533.
(93) Zhu, G.; Chen, J.; Liu, J.; Brunzelle, J. S.; Huang, B.; Wakeham, N.; Terzyan, S.; Li, X.; Rao, Z.; Li, G.; Zhang, X. C. *EMBO J* **2007**, *26*, 3484-3493.
(94) Zerial, M.; McBride, H. *Nat Rev Mol Cell Biol* **2001**, *2*, 107-117.
(95) Lin, D. C.; Quevedo, C.; Brewer, N. E.; Bell, A.; Testa, J. R.; Grimes, M. L.; Miller, F. D.; Kaplan, D. R. *Mol. Cell. Biol.* **2006**, *26*, 8928-8941.
(96) Mao, X.; Kikani, C. K.; Riojas, R. A.; Langlais, P.; Wang, L.; Ramos, F. J.; Fang, Q.; Christ-Roberts, C. Y.; Hong, J. Y.; Kim, R.-Y.; Liu, F.; Dong, L. Q. *Nat Cell Biol* **2006**, *8*, 516-523.
(97) Nechamen, C. A.; Thomas, R. M.; Cohen, B. D.; Acevedo, G.; Poulikakos, P. I.; Testa, J. R.; Dias, J. A. *Biology of Reproduction* **2004**, *71*, 629-636.
(98) Liu, J.; Yao, F.; Wu, R.; Morgan, M.; Thorburn, A.; Finley, R. L.; Chen, Y. Q. *Journal of Biological Chemistry* **2002**, *277*, 26281-26285.
(99) Posner, B. I.; Faure, R.; Burgess, J. W.; Bevan, A. P.; Lachance, D.; Zhang-Sun, G.; Fantus, I. G.; Ng, J. B.; Hall, D. A.; Lum, B. S. *Journal of Biological Chemistry* **1994**, *269*, 4596-4604.
(100) Nichols, A. M. W., Forest M. *Methods in Molecular Biology - Springer Protocols* **2009**, *492*, 18.
(101) Taylor, C. F.; Paton, N. W.; Lilley, K. S.; Binz, P.-A.; Julian, R. K.; Jones, A. R.; Zhu, W.; Apweiler, R.; Aebersold, R.; Deutsch, E. W.; Dunn, M. J.; Heck, A. J. R.; Leitner, A.; Macht, M.; Mann, M.; Martens, L.; Neubert, T. A.; Patterson, S. D.; Ping, P.; Seymour, S. L.; Souda, P.; Tsugita, A.; Vandekerckhove, J.; Vondriska, T. M.; Whitelegge, J. P.; Wilkins, M. R.; Xenarios, I.; Yates, J. R.; Hermjakob, H. *Nat Biotech* **2007**, *25*, 887-893.
(102) Tanabe, H. H., T.; Murayama, K.; Terada, T.; Shirouzu, M.; Yokoyama, S.

(103) Mega, T.; Hamazume, Y.; Nong, Y.-M.; Ikenaka, T. *J Biochem* **1986**, *100*, 1109-1116.
(104) Fadden, P.; Haystead, T. A. J. *Analytical Biochemistry* **1995**, *225*, 81-88.
(105) Woods, A. S. *Journal of Proteome Research* **2004**, *3*, 478-484.
(106) Woods, A. S.; Moyer, S. C.; Jackson, S. N. *Journal of Proteome Research* **2008**, *7*, 3423-3427.
(107) Jackson, S. N.; Wang; Woods, A. S. *Journal of Proteome Research* **2005**, *4*, 2360-2363.
(108) Holland, M.; Yagi, H.; Takahashi, N.; Kato, K.; Savage, C. O. S.; Goodall, D. M.; Jefferis, R. *Biochimica et Biophysica Acta (BBA) - General Subjects* **2006**, *1760*, 669-677.
(109) Krapp, S.; Mimura, Y.; Jefferis, R.; Huber, R.; Sondermann, P. *Journal of Molecular Biology* **2003**, *325*, 979-989.
(110) Parekh, R.; Roitt, I.; Isenberg, D.; Dwek, R.; Rademacher, T. *The Journal of Experimental Medicine* **1988**, *167*, 1731-1736.

Randi L. Gant-Branum

Vanderbilt University
Department of Chemistry
7330 Stevenson Center
Nashville, TN 37235

C:(931) 206-5092
W:(615) 343-4563
randi.l.gant@vanderbilt.edu
randigant@yahoo.com

Education

Bachelor of Science - (2006) - University of Tennessee at Chattanooga
- Major- Chemistry (Biochemistry Concentration)
  Minor- Biology
- *Cum Laude* - 3.71 GPA
- Research Mentor: Manuel F. Santiago – (423) 425-5364
- University Honors for completion of Honors coursework and GPA above 3.5
- Departmental Honors for completion of a Departmental Honors Dissertation
  Thesis Title: "Degradation of Pyrimidines by *Pseudomonas syringae"*

Doctor of Philosophy in Chemistry– (August 2011) – Vanderbilt University
- Degree Focus – Analytical Chemistry, Mass Spectrometry, Ion Mobility-Mass Spectrometry, Proteomics, and Quantitative Proteomics and Glycomics
- 3.18 GPA
- Research Mentor: John A. McLean - (615) 322-1195
- Thesis Title: "Characterization of Post-Translationally Modified Peptides and Proteins Using Lanthanide-based Labeling Strategies."

Professional Experience

Instrumentation:

HPLC-ESI-MS/MS – High-Performance Liquid Chromatography- Electrospray Ionization-Tandem Mass Spectrometer
DE-MALDI-TOFMS – Delayed Extraction-Matrix-Assisted Laser Desorption Ionization-Time of Flight Mass Spectrometer
GC-MS – Gas Chromatography-Mass Spectrometer
DT-IM-MS – Drift Tube-Ion Mobility-Mass Spectrometer (custom)
TW-IM-MS/MS – Travelling Wave-Ion Mobility-Mass Spectrometer (Waters Synapt© G1 and G2 models)
UV-Visible Spectrophotometry (with automated scans for enzyme kinetics)
ICP-OES – Inductively Coupled Plasma-Optical Emission Spectrometry
NMR – Nuclear Magnetic Resonance
CV – Cyclic Voltammetry
ICP-MS – Inductively Coupled Plasma-Mass Spectrometry

Software:

Data Explorer – DE-MALDI-TOFMS software
Xcalibur – HPLC-ESI-MS/MS software
Mass Lynx – TW-IM-MS/MS software
Simion (LabView)- Instrument building software
SEQUEST – algorithm for searching tandem MS data
GPMAW – (a customized algorithm for searching tandem MS data)
ExPASy Proteomics Server and all related programs such as

Peptide Mass, Protein Prospector, Mascot, BLAST, GlycoMod, and GlycanMass.
P-mod - (a customized algorithm for searching tandem MS data)
ExPASy Proteomics Server
Adobe Professional
EndNote
CorelDraw
ChemDraw
Microsoft Word, Outlook, Powerpoint, Excel

Grant Writing:

NIH-RO1 Grants
NIH-R21 Grants
Independent Research Proposal – Prepared and presented an original NIH Research proposal unrelated to the graduate mentor's field as required by the Vanderbilt Chemistry PhD program.

Training:

Lab Safety and Fire Safety Training Course (VU Chemistry)
Responsible Conduct of Research though the Collaborative Institutional Training Initiative and the NIH.

- **Also possesses experience in critical peer review of scientific journals, undergraduate and graduate mentoring, and purchasing.**

Publications

Vanderbilt (Chronological Order)

R. L. Gant-Branum, T. J. Kerr, and J. A. McLean. Labeling Strategies in Mass Spectrometry-Based Protein Quantitation. *Analyst.* **2009**, *134*, 1525 – 1530.

R. L. Gant-Branum, J. A. Broussard, D. J. Webb, and J. A. McLean. Identification of Phosphorylation Sites within the Signaling Adaptor APPL1 by Mass Spectrometry. *Journal of Proteome Research*, **2010**, 9 (*3*), 1541–1548

R. L. Gant-Branum, T. J. Kerr, and J. A. McLean. Phosphoproteomic Selection, Relative Quantitation, and Localization using Phosphopeptide Element-Coded Affinity Tagging (PhECAT). Submitted to *Analytical Chemistry*. **2011**.

T. J. Kerr, **R. L. Gant-Branum**, and J. A. McLean. Multiplexed Relative Quantitation of Peptide Functionality Using Lanthanide-based Structural Shift Reagents. *International Journal of Mass Spectrometry*. in press. **2011**.

R. L. Gant-Branum and J. A. McLean. Targeted Selection of Glycoproteins and Phosphoproteins Using Mobility Shift Strategies and Ion Mobility-Mass Spectrometry. In preparation.

University of Tennessee at Chattanooga (Chronological Order)

E. B. Burnette, **R. L. Gant**, G. M. Meyer, and M. F. Santiago. Regulation of Pyrimidine Catabolism in *Pseudomonas lemonnieri* ATCC 12983. *Journal of Undergraduate Chemistry Research.* **2006**, *5*, 9-13.

R. L. Gant, M. L. Hacker, G. M. Meyer, and M. F. Santiago. Degradation of Pyrimidines by *Pseudomonas syringae*. *Research Journal of Microbiology*. **2007**, *2*(*11*), 851-855.

Presentations (Primary Presenter)

Vanderbilt (Chronological Order)

Phosphoproteomic Tagging Strategies for Ion Mobility-Mass Spectrometry. **R. L. Gant,** T. J. Kerr, and J. A. McLean. Presented at the annual meeting of the Tennessee Academy of Sciences (TAS), **2007** in Nashville, TN.

Structural Separation of Phosphorylated Peptides Using Chemical Derivatization and Ion-Mobility Mass Spectrometry. **R. L. Gant**, T. J. Kerr, and J. A. McLean. Presented at the annual Vanderbilt Institute for Chemical Biology (VICB) retreat, **2008** in Florence, AL.

Phosphoproteomics using selective derivatization and structural separations by ion mobility-mass spectrometry. **R. L. Gant**, T. J. Kerr, and J. A. McLean. Presented at the annual meeting of the American Society for Mass Spectrometry (ASMS), **2008** in Denver, CO.

Phosphoproteomic Mapping with Two-dimensional Structural Separations by Ion Mobility-Mass Spectrometry. **R. L. Gant** and J. A. McLean. Presented at the annual meeting of the Federation of Analytical Chemistry and Spectroscopy Societies (FACSS) meeting, **2008** in Reno, NV.

Multiplexed Quantitiative Phosphoproteomics using a Lanthanide Based Tagging Strategy with MALDI-TOFMS. **R. L. Gant** and J. A. McLean. Presented at the South Eastern Regional Meeting of the American Chemical Society (SERMACS), **2009** in Nashville, TN.

Identification of protein phosphorylation sites of human APPL1 using MS, MS/MS, and IM-MS. **R. L. Gant-Branum** and J. A. McLean. Presented at the annual meeting of the American Society for Mass Spectrometry (ASMS), **2009** in Philadelphia, PA.

Quantitative Proteomic Strategies using Ion Mobility Shift Labels. **R. L. Gant-Branum**, T. J. Kerr, J. A. McLean. Invited talk at the annual meeting of the Federation of Analytical Chemistry and Spectroscopy Societies (FACSS) meeting, **2009** in Louisville, KY.

University of Tennessee at Chattanooga (Chronological Order)

Degradation of Pyrimidines by *Pseudomonas syringae*. **R. L**. **Gant**, G. M. Meyer, and M. F. Santiago. Presented at the 56th Southeast Regional Meeting of the American Chemical Society, **2004** in Research Triangle Park, NC.

Pyridine Nucleotide Transhydrogenase Activity in *Pseudomonas syringe*. **R. L. Gant,** M. F. Santiago. Abstracts of Papers, 61st Southwest and the 57th Southeast Joint Regional Meeting of the ACS, **2005** in Memphis, TN.

Reducing Agent of Dihydropyrimidine Dehydrogenase. **R. L. Gant,** G. M. Meyer, and M. F. Santiago. Presented at the 229th American Chemical Society National Meeting, **2005** in San Diego, CA.

Reductive pathway of penicillin-resistant *Pseudomonas syringae*. **R. L. Gant,** S. Prince, M. F. Santiago, G. M. Meyer. 229th American Chemical Society National Meeting, **2005**. in San Diego, CA.

Professional Organizations and Societies

American Chemical Society Student Affiliates, UTC Chapter (2003-2006) – Vice President
American Chemical Society
American Society for Mass Spectrometry
Federation of Analytical Chemistry and Spectroscopy Societies